

**INDUSTRIAL PNEUMATIC VALVE STICTION
COMPENSATION**

BY

Mohamed Abdeen Mohamed Hassan

A Thesis Presented to the
DEANSHIP OF GRADUATE STUDIES

KING FAHD UNIVERSITY OF PETROLEUM & MINERALS

DHAHRAN, SAUDI ARABIA

In Partial Fulfillment of the
Requirements for the Degree of

MASTER OF SCIENCE

In

SYSTEMS ENGINEERING

MAY 2015

KING FAHD UNIVERSITY OF PETROLEUM & MINERALS
DHAHRAN- 31261, SAUDI ARABIA
DEANSHIP OF GRADUATE STUDIES

This thesis, written by **Mohamed Abdeen Mohamed Hassan** under the direction of his thesis advisor and approved by his thesis committee, has been presented and accepted by the Dean of Graduate Studies, in partial fulfillment of the requirements for the degree of **MASTER OF SCIENCE IN SYSTEMS ENGINEERING.**



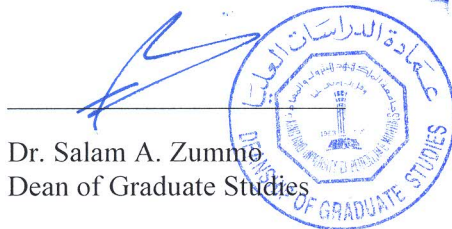
Dr. Sami El Ferik
(Advisor)



Dr. Adel Ahmed
For Department Chairman



Dr. Moustafa Elshafei
(Member)



Dr. Salam A. Zummo
Dean of Graduate Studies



Dr. Samir Al-Amer
(Member)

16/6/15

Date

©Mohamed Abdeen Mohamed Hassan

2015

*Dedicated to my
Father's soul, mother, siblings and their sacrifices
And to my small family
Walaa Hussein*

ACKNOWLEDGMENTS

All praise is to Allah, the Almighty alone. May the Peace and Blessings of Allah be upon the Messenger of Allah (salallahualewasalam), his family, and his companions (radhiallahoanhum).

I am grateful to the King Fahd University of Petroleum & Minerals for providing a great environment for research and academics. I wish to extend my gratitude to my thesis adviser Dr. Sami El-Ferik for his continuous support, patience, and much needed encouragement. I am also thankful to my thesis committee Dr. Moustafa El-Shafei and Dr. Samir Al-Amer for their time and useful comments.

My mother (Tata) is always with me in my thoughts and I live with her encouragement and kindness. All good I do goes to my mother. For all my studies. I am also thankful to my brothers and sisters for their encouragement and support. I am thankful to my fiancée for her patience and help during long hours of studies and research, she equally shares this work.

I am very thankful to my friends at KFUPM for making my master full of enjoyment. I am indebted to all the people I meet here at KFUPM.

TABLE OF CONTENTS

ACKNOWLEDGMENTS	III
TABLE OF CONTENTS	IV
LIST OF TABLES	VIII
LIST OF FIGURES	IX
LIST OF ABBREVIATIONS	XI
ABSTRACT	XII
ABSTRACT (ARABIC)	XII
CHAPTER 1 INTRODUCTION AND MOTIVATION	1
1.1. Background	1
1.2. Work Justification and objectives	3
1.3. Research Methodology:	5
1.3.1. Matlab Simulation:	5
1.3.2. Experimental Setup:	5
CHAPTER 2 LITERATURE REVIEW	7
2.1. Knocker Based Methods	7
2.2. Two-Move Based Methods	9
2.3. Adaptive & Nonlinear Based Methods	13
2.4. Dynamic Inversion Methods	14
2.5. PID Retuning Methods	15
CHAPTER 3 VALVE STICTION MODELING	17

3.1.	Physical Models.....	17
3.1.1.	Karnopp Model	17
3.2.	Data-Driven Models	19
3.2.1.	Choudhury Model.....	19
3.2.2.	Kano Model	23
3.2.3.	He Model.....	26
3.2.4.	Two-Layer Binary Tree Model.....	27
CHAPTER 4 STICTION COMPENSATION METHODS		30
4.1.	Knocker Method.....	30
4.2.	Dithering Method.....	31
4.3.	Constant Reinforcement Method	31
4.4.	Approximate Inverse Method.....	32
4.5.	Adaptive Inverse Control (LMS-FIR Method)	35
4.5.1.	Finite Impulse Response Filter	36
4.5.2.	Least Mean Square Algorithm	37
4.5.3.	Adaptive Inverse Control by using LMS-FIR Filter	38
4.6.	Adaptive Inverse Control (DE-FIR Method) (Proposed Method)	39
CHAPTER 5 DIFFERENTIAL EVOLUTION ALGORITHM.....		40
5.1.	Overview	40
5.2.	Optimization Procedure in DE for Single Objective Optimization Problem	41
5.2.1.	Initialization	42
5.2.2.	Evaluation and Finding the Best Solution	43
5.2.3.	Mutation	43
5.2.4.	Crossover	44

5.2.5.	Selection.....	45
5.2.6.	Stopping Criteria.....	45
5.3.	Objective Function Optimization	45
5.3.1.	Control Elements Range	46
5.3.2.	Optimization Parameters	46
CHAPTER 6 RESULTS AND DISCUSSION.....		47
6.1.	Overview	47
6.2.	PI retuning with DE Algorithm	47
6.2.1.	PI retuning with DE algorithm (Choudhury Model).....	48
6.2.2.	PI tuning with DE algorithm (karnopp Model):	51
6.3.	FIR filter optimized with DE algorithm (Proposed method)	52
6.4.	Study of Compensation methods (Simulation)	56
6.4.1.	Knocker Method.....	57
6.4.2.	Dithering Method.....	60
6.4.3.	Constant Reinforcement Method (CR).....	63
6.4.4.	Approximate Inverse Method.....	64
6.4.5.	Adaptive Inverse Control Method (LMS-FIR)	68
6.4.6.	Adaptive Inverse Control Method (DE-FIR).....	72
6.4.7.	Numerical analysis and discussion.....	77
CHAPTER 7 EXPERIMENTAL VALIDATION.....		79
7.1.	Introduction	79
7.2.	Experimental Setup	79
7.2.1.	Setup Calibration.....	82
7.2.2.	Knocker Method.....	86

7.2.3.	Dithering Method.....	87
7.2.4.	Constant Reinforcement Method (CR).....	89
7.2.5.	Approximate Inverse Method.....	91
7.2.6.	Adaptive Inverse Control Method (LMS-FIR)	92
7.2.7.	Adaptive Inverse Control Method (DE-FIR).....	94
7.2.8.	Numerical analysis and discussion.....	99
CHAPTER 8 SUMMARY AND FUTURE WORK.....		102
8.1.	Summary.....	102
8.2.	Contribution of this Thesis.....	102
8.3.	Future Work.....	103
REFERENCES.....		105
VITAE.....		105

LIST OF TABLES

Table 6.1: PI Parameters Tuning Range (Choudhury Model).....	49
Table 6.2: Effects of Optimization Parameters on PI Parameters (Choudhury Model) ...	49
Table 6.3:PI Parameters Tuning Range (Karnopp Model).....	51
Table 6.4:Effects of Optimization Parameters on PI Parameters (Karnopp Model)..	51
Table 6.5:FIR Filter Weights with Different Optimization Parameters.	54
Table 6.6: Equivalent Stiction Scenario's in the Three Models.	56
Table 6.7: Knocker Optimization Range.	59
Table 6.8:Knocker Optimized Parameters.....	60
Table 6.9: Dithering Optimization Range.....	51
Table 6.10: Dithering Optimized Parameters.	62
Table 6.11: CR Optimized Parameters.	63
Table 6.12: Approximate Inverse Optimized Parameters.....	51
Table 6.13: DE-FIR Filter Weights.	751
Table 6.14: ISE and Variance as percentage for all Compensators.....	78
Table 7.1:Level Transmitterr Calibration Measurements.....	84
Table 7.2: Equivalent Stiction Scenario's in the Two Models.	84
Table 7.3: Knocker Compensator Parameters.	87
Table 7.4: Dither Compensator Parameters.	87
Table 7.5: CR Compensator Parameters.	89
Table 7.6:Approximate Inverse Compensator Parameters.	91
Table 7.7: LMS-FIR Filter Weights.....	94
Table 7.8: DE-FIR Filter Weights	94
Table 7.9: ISE,Var,Max_e and E as Percentage for All Compensators.	100
Table 7.10: Compensators Ranking by Kano Model.....	101

LIST OF FIGURES

Figure 1.1: Pneumatic Valve Components.	2
Figure 1.2: MATLAB Simulink Blocks.	6
Figure 2.1: Knocker Signal.	8
Figure 2.2 : Three movements Signal.	10
Figure 2.3: Process Control Loop With Two-Move Stiction Compensator.	11
Figure 3.1: Signal and Logic Flow Chart for the Choudhury Stiction Model.	22
Figure 3.2: Stiction Parameters Relation to Stiction Behavior.	23
Figure 3.3: Flow Chart of Kano Stiction Model.	26
Figure 3.4: Flow Chart of He Stiction Model.	27
Figure 3.5: Two layer Binary Tree Stiction Model.	28
Figure 4.1: Block Diagram illustrating the Knocker used in a feedback loop.	31
Figure 4.2: Control Signal using the knocker Compensator.	31
Figure 4.3: CR compensator structure.	32
Figure 4.4: Valve input-output pattern in case of stiction.	33
Figure 4.5: Inverse pattern of valve stiction.	34
Figure 4.6: Backlash Inverse pattern.	34
Figure 4.7: Block diagram of stiction and stiction inverse.	35
Figure 4.8: FIR Filter withan adaptive algorithmm for weightstuning.	37
Figure 4.9: Structure of single loop with AIC.	39
Figure 5.1: DE flowchart.	42
Figure 5.2: Crossover Proceudres.	42
Figure 6.1: Simulink configurations for PID retuning.	48
Figure 6.2: PV for PI tuning with DE algorithm and Choudhury Stiction Model.	50
Figure 6.3: OP for PI tuning with DE algorithm and Choudhury stiction Model.	50
Figure 6.4: PV for PI tuning with DE algorithm and Karnopp stiction model.	52
Figure 6.5: OP for PI tuning with DE algorithm and Karnopp stiction model.	52
Figure 6.6: PV for FIR filter tuned with DE algorithm.	54
Figure 6.7: OP for FIR filter tuned with DE algorithm.	55
Figure 6.8: Simulink blocks for Knocker Compensator.	58
Figure 6.9: Knocker Compensator with Choudhury Model.	58
Figure 6.10: Knocker Compensator with Kano Model.	59
Figure 6.11: Knocker Compensator with Two Layer Model.	59
Figure 6.12: Dither Compensator with Choudhury Model.	61
Figure 6.13: Dither Compensator with Kano Model.	61
Figure 6.14: Dither Compensator with Two Layer Model.	62
Figure 6.15: CR Compensator with Choudhury Model.	63
Figure 6.16: CR Compensator with Kano Model.	64
Figure 6.17: CR Compensator with Two Layer Model.	64
Figure 6.18: Simulink Blocks for Approximate Inverse Compensator.	65

Figure 6.19: Approximate Inverse Compensator with Choudhury Model.	66
Figure 6.20: Approximate Inverse Compensator with Kano Model.....	67
Figure 6.21: Approximate Inverse Compensator with Two Layer Model.....	67
Figure 6.22: Simulink Blocks for LMS-FIR Compensator.	68
Figure 6.23: LMS-FIR Compensator with Choudhury Model.	69
Figure 6.24: LMS-FIR Compensator with Kano Model.....	69
Figure 6.25: LMS-FIR Compensator with Two Layer Model.....	70
Figure 6.26: LMS-FIR Weights with Choudhury Model.	71
Figure 6.27: LMS-FIR Weights with Kano Model.....	71
Figure 6.28: LMS-FIR Weights with Two Lasyer Model.	71
Figure 6.29: DE-FIR Compensator with Choudhury Model.	73
Figure 6.30: DE-FIR Compensator with Kano Model.....	73
Figure 6.31: DE-FIR Compensator with Two Layer Model.....	74
Figure 6.32: Optimization Iterations with Choudhury Model.	75
Figure 6.33: Optimization Iterations with Kano Model.....	75
Figure 6.34: Optimization Iterations with Two Layer Model.....	76
Figure 7.1: Tank level control Loop.	80
Figure 7.2: Experimental Setup (Full picture).	81
Figure 7.3: Experimental Setup (Components).	81
Figure 7.4: Experimental Setup (Human Machine Interface).....	82
Figure 7.5: Tank Level and Transmitter current relation.....	83
Figure 7.6: The four stiction scenarios with Kano Model.	84
Figure 7.7: The four stiction scenarios with He Model.	85
Figure 7.8: Knocker Compensator with Kano Model.....	86
Figure 7.9: Knocker Compensator with He Model.....	86
Figure 7.10: Dither Compensator with Kano Model.	88
Figure 7.11: Dither Compensator with He Model.	88
Figure 7.12: CR Compensator with Kano Model.	90
Figure 7.13: CR Compensator with He Model.	90
Figure 7.14: Approximate Inverse Compensator with Kano Model.....	91
Figure 7.15: Approximate Inverse Compensator with He Model.....	92
Figure 7.16: LMS-FIR Compensator with Kano Model.....	93
Figure 7.17: LMS-FIR Compensator with He Model.....	93
Figure 7.18: DE-FIR Compensator with Kano Model.....	95
Figure 7.19: DE-FIR Compensator with He Model.....	95
Figure 7.20: Optimization Iterations with Kano Model.....	96
Figure 7.21: SP change for dead band of Kano model with DE-FIR.	97
Figure 7.22: SP change for undershoot of Kano model with DEFIR.	98

LIST OF ABBREVIATIONS

Stiction	Static Friction
FIR	Finite Impulse Response Filter
DE	Differential Evolution Algorithm
PID	Proportional Integral Derivative
PV	Process Variable
OP	Control Signal
MV	Valve Stem Position
SP	Set-point
CR	Constant Reinforcement
AIC	Adaptive Inverse Control
LMS	Least Mean Square
HMI	Human Machine Interface
E/P	Electrical to Pressure Converter
LMS-FIR	Finite ImpulseResponse Filter tuned by LMS
DE-FIR	Finite Impulse Response Filter tuned by DE

ABSTRACT

Full Name : Mohamed Abdeen Mohamed Hassan
Thesis Title : Industrial Pneumatic Valve Stiction Compensation
Major Field : Systems Engineering
Date of Degree : May 2015

Increasing the reliability and performance of control systems is one of the crucial fields of studies in the process industries. Since typical control system is hierarchical in their control strategy, where the high level is responsible for determining the set-point that must be performed and tracked by the low level elements in the control loop such as actuator (valve), any unsatisfactory performance of one element in any level may distract the entire system. One type of this distraction appears as oscillatory response where the final output (process variable) is going up and down the set point in periodical basis. This why a remarkable number of researchers are interesting in how to identify the source of the oscillatory behavior in the control system and how to compensate for it.

This work will focus on compensation of one of this oscillatory source that mainly occurs in pneumatic valves commonly used in industrial process today, it is called stiction (abbreviation for static friction) and it is categorized as type of nonlinearity much resemble to backlash.

In This work, a new stiction compensation method in the spirit of adaptive filtering and intelligence control theories was introduced, the new compensation method was proposed for a process containing sticky valve to reduce the stiction effect to minimum without aggressive movements to the valve stem. In order to ensure stability, the method uses FIR

filter (Finite Impulse Response) with weights optimized by DE algorithm (Differential Evolution).The performance of this method is validated by simulation using (Matlab / Simulink) as well as experimentally using a test-bench water tank level control loop. The proposed method demonstrated an excellent performance in reducing the oscillation,minimizing the energy supply to the control signal and reducing valve stem movements when compared with the known compensation techniques in the literature, such as the knocker method.

ملخص الرسالة

الاسم الكامل: محمد عابدين محمد حسن

عنوان الرسالة: تعويضات تأثير الاحتكاك السكوني في الصمامات الصناعية التي تعمل بالهواء

التخصص: هندسة النظم

تاريخ الدرجة العلمية: مايو ٢٠١٥

زيادة الإجماعية وكفاءة الاداء في أنظمة التحكم يعتبر من أهم مجالات الأبحاث في تحكم العمليات. فمعظم أنظمة التحكم ذات استراتيجية هرمية، يحدد المستوى الأعلى فيها القيم المطلوبة لمتغيرات العملية والتي يتم تنفيذها ومتابعتها بواسطة عناصر المستويات الدنيا مثل الصمامات، لذلك الاستجابة الخاطئة لاجد عناصر هذه المستويات ينتج عنها تشويش لاستجابة المنظومة بأكملها. أحد نواتج هذا التشويش يظهر في صورة تذبذب دائم في قيمة متغير العملية النهائي، وبالتأكيد هي من النواتج الغير مرغوب فيها، لذلك نجد أغلب الباحثون مهتمون بتحديد مصدر هذا التذبذب.

يتمركز محور هذه الأطروحة حول تقليل التذبذب الناتج من الاحتكاك السكوني في الصمامات الصناعية التي تعمل بالهواء. تم اقتراح طريقة جديدة باستخدام نظريات المرشحات التكيفية والتحكم الذكي لتعويض التذبذب في عملية ذات استجابة من الدرجة الأولى وتحتوي على صمام معتل كجزء منها. الطريقة المستحدثة تتكون من مرشح ذو استجابة نبضية محدودة يتم تدريبه وتكييفه بواسطة خوارزمية التطور التفاضلي.

تم قياس كفاءة الطريقة المستحدثة باستخدام برنامج محاكاة وعلما باستخدام منظومة تحكم في خزان مياه. الطريقة المستحدثة أظهرت كفاءة عالية في تقليل التذبذب الناتج من الاحتكاك السكوني باقل طاقة مستهلكة من قبل إشارة التحكم وباقل حركة لعمود الصمام عندما تمت مقارنتها بطرق تعويضية أخرى موجودة في الدراسات السابقة مثل طريقة المطرقة.

CHAPTER 1

INTRODUCTION AND MOTIVATION

1.1. Background

The PID controller is the most common controller in the industry nowadays, because it is simple, easy to tune, well known, and performs well in most of processes. Typical control loop consists of a controller, actuators, sensors and the process to be controlled. A typical petrochemical plant consists of hundreds or thousands of such control loop, these loops are integrating together to form a huge control system network, thus any fault or failure in single loop may propagate through this network to disturb the entire system or major part of it[1]. Thus the importance of improving the performance of each individual control loop. Recent study[2], shows that only about thirty percent of the control loops are working within the desired response ranges. There are many reasons behind the degradation of these loops response, such as oscillations, poor disturbance rejection, poor set-point tracking and bad controller tuning. Static friction nonlinearity, or stiction as a short, is one of the main causes of periodical oscillations in control loops. Surveys reported in [3] show that stiction is the root cause behind around 20% to 30% of all control loops oscillation. Other typical and similar nonlinearities common in practice are backlashes, dead zones, and saturations. Each of these nonlinearities has specific

structure. Taking these nonlinear structures into account may improve the controller performance. This in turn will improve the product quality, economy, and safety.

Typical control valve, as shown in Figure 1.1, has three major components: the valve body, the actuator and accessories. The valve body consists of the valve casing and the valve seat. The actuator consists of a valve stem attached with the valve plug in the lower end and with diaphragm in the upper end. The gap between the seat ring and valve plug determines the amount of flow of the fluid. The actuating units consists of the diaphragm and a spring to balance and push back the pneumatic control force, and ensures fail open and fail close safety modes. Accessories include several components such as positioners, Electrical to Pressure (E/P) transducers, position sensors and limit switches. Position of the diaphragm changes according to the input signal. In practice, the signal is usually generated by a PID controller, and then it is transformed to proper pneumatic signal by E/P converter.

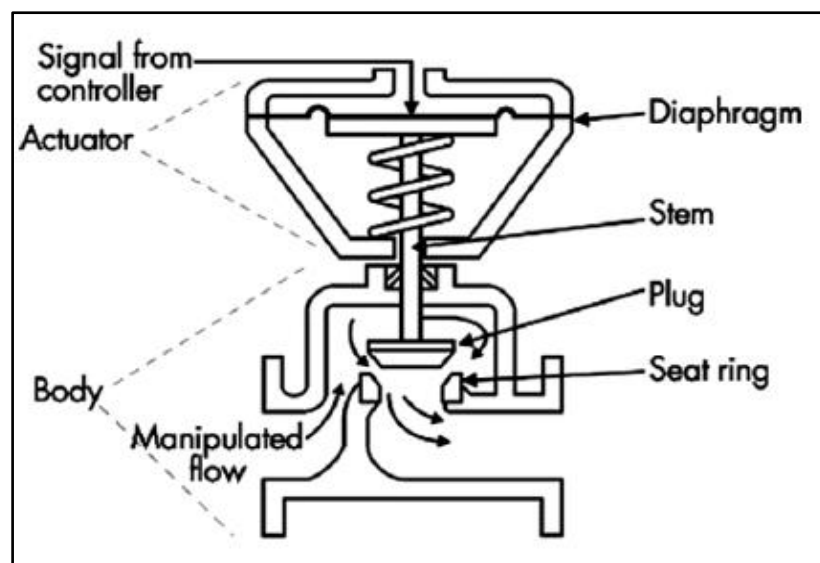


Figure 1.1: Pneumatic Valve Components.

Instrument Society of America (ISA) defines the stiction as: “Stiction is the resistance to the start of the motion, usually measured as the difference between the driving values required to overcome static friction upscale and downscale” (ISA Subcommittee SP75.05, 1979) [45].

Valve stiction is inherently a physical problem and the way to resolve it has been through valve maintenance. However, the valve maintenance usually is done in normal periodical maintenance, which is typically between 6 months to 3 years. Inherently valve maintenance needs the production line to be shut down, which is not appreciated in most cases, especially when there is no bypass line. The loss of energy and product quality prior to and during the maintenance period can be quite high. For these reasons, identification, quantification and compensation algorithms (Soft Solutions) for stiction are needed to ensure improved asset management, high quality product, better energy management, cost reduction and higher savings.

1.2. Work Justification and objectives

Stiction is abbreviation of two words “*Static Friction*”. Friction is known as a natural resistance to relative motion between two contacting bodies.

There are many things that can cause stiction, the valve design inherently has high friction e.g. a high temperature tight leak packing design, or a tight leakage seal. Sometimes thermal expansion of the internals can cause friction.

Despite of the availability of many compensation methods in the literature, almost all of them have one or two disadvantages. Some of the methods compensate the stiction at the cost of aggressive movement of valve stem, which in turn will reduce the valve life time.

Other methods don't have immunity against disturbance such as set-point change, other need previous knowledge of stem position such as original two move method.

The main objective of this work is to introduce simple and robust stiction compensation method that doesn't have the flaws of the methods proposed in literature.

The specific objective of this research contains:-

1. Apparently, to study the effect of *PID* controller retuning with intelligent method (DE optimization technique) on stiction, and intentionally the performance and efficiency of DE algorithm will be tested on this type of nonlinear problem.
2. Using the intelligent method to tune an adaptive Finite Impulse Filter (FIR) in order to invert the stiction dynamic. Also to investigate the possibility if the method can be implemented off-line and/or on-line.
3. Implementing and testing of the proposed method in objective two above in Matlab Simulink environment and conduct further validation through experiment.
4. For comparison purpose, different type of compensation methods stated in literature, will be simulated and implemented experimentally. The methods that will be tested in both simulation and experiments are :
 - a. Klocker method.
 - b. Constant Reinforcement (CR).
 - c. Dithering (pulses).
 - d. Approximate Inverse Compensation.
 - e. Adaptive Inverse Control (AIC) :

1. FIR Filter optimized with LMS.
2. FIR Filter optimized with DE algorithm (proposed method).

1.3. Research Methodology:

The work is divided into two parts; first all the work steps will be carried out in simulation environments (MATLAB/Simulink), and if the results are found to be satisfactory further validation will be carried out using experimental test-bench water tank level control loop.

1.3.1. Matlab Simulation:

Configuration such as shown in Figure 1.2 below will be created by Simulink control Toolbox, the parameters values for PID controller and transfer function will be taken from literature, all the previous mentioned methods will be tested with different valve stiction models to insure the consistence of obtained results.

1.3.2. Experimental Setup:

The experimental validation of the simulation will be carried out here. A single closed level loop control will be used as pilot plant. The water level in tank will be the process variable, the level is measured by level transmitter and fed back to a digital controller which has the ability to communicate with HMI in Personal Computer. The control signal will actuate a pneumatic valve through E/P converter. It is worth to mention that the valve is at good condition and not suffering from stiction, actually the stiction will be created or programmed in the controller (soft element) by using stiction model from literature.

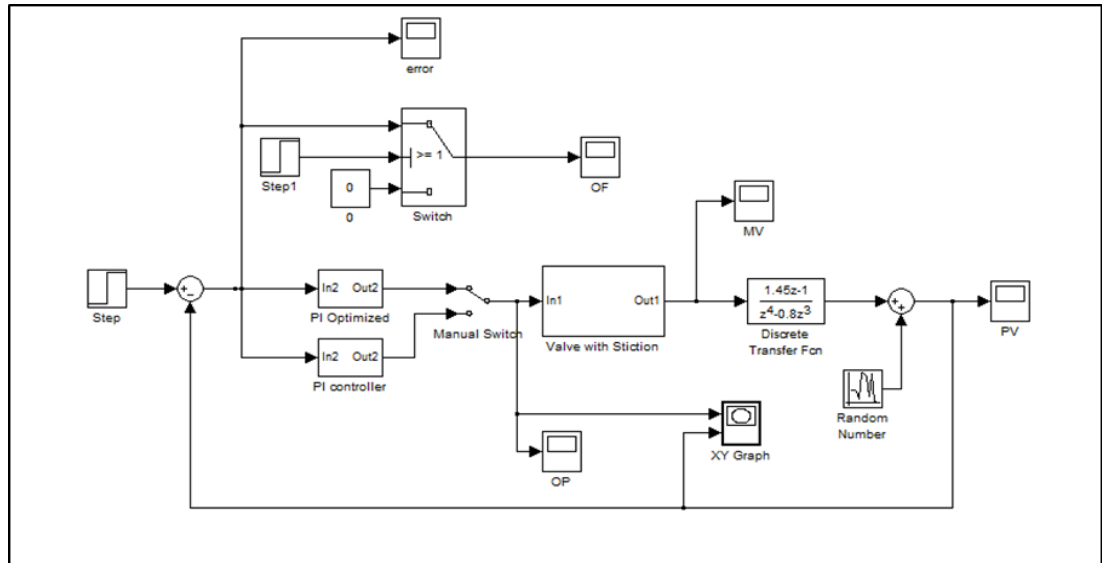


Figure 1.2: MATLAB Simulink Blocks.

CHAPTER 2

LITERATURE REVIEW

There are several methods and approaches in literature for nonlinear dynamic compensation in general and valve stiction in particular. Since most of them have the same operation principle, we can categorize them based on these principles into knocker based methods, two-move based methods, adaptive and nonlinear based methods, dynamic inversion based methods and PID retuning methods.

2.1. Knocker Based Methods

Tore Haggund[4], introduced the knocker approach to compensate the valve stiction. In knocker approach short pulses of equal amplitude and duration (sequence of pulses with relatively small energy content) are added in the direction of the rate of change of the control signal to the original control signal. This explains the reasons behind calling it knocker. The method has the ability to overcome friction by “knocking” on the valve. In his work, Haggund set constraints on the pulse parameters (pulse amplitude a , width τ and sampling interval h) as shown in Figure 2.1. He also validated his theoretical concept experimentally. The major disadvantage of his proposed method is the cost related to the aggressive movement of the valve stem.

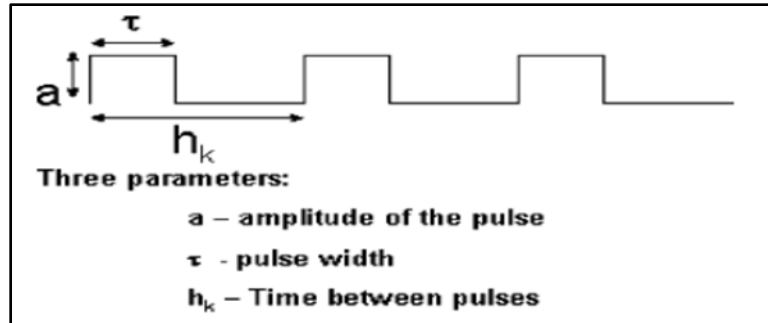


Figure 2.1: Klocker Signal.

In Srinivasan & Rengaswamy [5], showed that the performance of the friction compensation proposed by Hagglund depends mainly on the selection of the amplitude 'a' and it cannot be left fixed to any arbitrary value as stated in [4]. They proposed another stage prior to the compensation block to detect and estimate the valve stiction using a Shape-Based Technique and Model-Based Technique. Then, klocker parameters are tuned based on the estimated stiction. However, this method may influence excessive wearing due to the extreme movement of the valve stem. To overcome these limitations, Srinivasan and Rengaswamy in [6], formulated an optimization problem with three objectives to be minimized: aggressive stem movement, energy and output variability. They used the 'fmincon' algorithm of the MATLAB optimization toolbox as optimizer but due to non-smoothness of one of the three terms, the optimizer failed to find the global minimum instead stuck on local one. Also due to real-time issues, the Simulink interface could not solve the optimization formulation between each iteration. Alternate non-gradient based optimization techniques that use function evaluation such as DIRECT (DIVERRECTangle method) was proposed to overcome the real-time issues.

Lee Ivan and S. Lakshminarayanan[7], introduced a new compensation method called constant reinforcement (CR), approach which is similar to knocker method but the added signal is now constant. However, this approach can be useful only during the period in which the valve does not respond to the changes in controller output and it does not consider any extra movements.

Karthiga and Kalaivani[8], introduced a new approach based on Farenzena and Trierweiler Method [9] and Tore Haggglundwork[4].Their approach involves three movements and each one is obtained and calculated depends on the desired closed loop performances.These movements are generated by any signal generator continuously. This signal is added to the controller signal.

Sivagamasundari and Sivakumar[10],proposed another knocker based method using positive and negative amplitudes selected according to the stiction model. The experimental results showed that the proposed method has an improved valve stem response than the original knocker method, but still displaying aggressive movement.

2.2. Two-Move Based Methods

Srinivasan and Rengaswamy in [11], introduced the two-move method for first time.They used the same objectives as in their previous work in designing the friction compensator. The main idea of this approach is to keep the valve at its steady state position and it was born from the following observations:

- Stiction always prevents the valve stem from reaching its final steady state position, instead makes the stem jump around it.
- This jumping behavior continues between two positions, one above and another below the steady state position.

- If stiction does not occur and after an enough time for the transient behavior to die out, the process variable, control signal and valve stem position will reach their final steady state values.

From these observations Srinivasan concluded that if a compensation signal can be added to force the valve stem to reach its steady state and remains at this position, then the controller can achieve the desired process variable value, provided no further set-point change or disturbance occurs during this period. To accomplish this, he found that at least he needs two moves, the first move to push the stem to a steady state position and the second move to force the stem to remain at steady state position. Srinivasan proved his new method mathematically and demonstrated it experimentally using liquid level setup. However, the use of simple stiction model (Stenman's Model) with one parameter only and assumption of no set-point change and disturbance during this period may reduce the accuracy of this method.

Farenzena and Trierweiler[9], introduced the three movements method. In their work they focused mainly to overcome the limitations of the two move introduced by Srinivasan and Rengaswamy before. They claimed that the new approach can achieve better set-point tracking and disturbance rejection, depending on the tuning parameters.

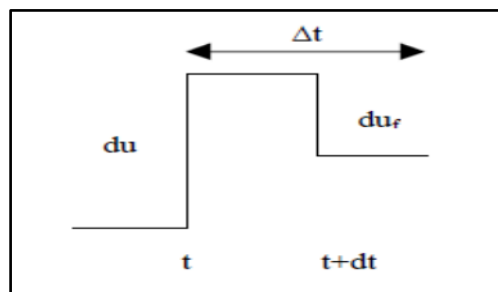


Figure 2.2: Three Movements Signal.

$$du = 0.95 \frac{dy}{k} \left(1 - \exp\left(-\frac{ft}{\tau}\right)\right) \quad (2.1)$$

$$dt = rt \quad (2.2)$$

Where τ and K the time constant and process gain respectively, dy and rt are the set-point change and the desired closed loop rise-time. To avoid continues valve movement a small offset between process variable and set-point (OFS) is allowed and tuned based on the desired offset in the process variable. The Δt is the distance between each pair of moves parameter and has been set based on the desired closed loop rise time.

Antonio et al [12], improved the two-move compensation method by proposing two approaches. The first consists of four moves and the second is of two moves. Antonio et al used Karnopp model for implementing the valve stiction. The effectiveness of their proposed compensators is demonstrated using simulation examples and a flow control loop in a pilot plant. However, both approaches require the process to be a self-regulating process and the second two moves method requires also that both valve and process have similar dynamics.

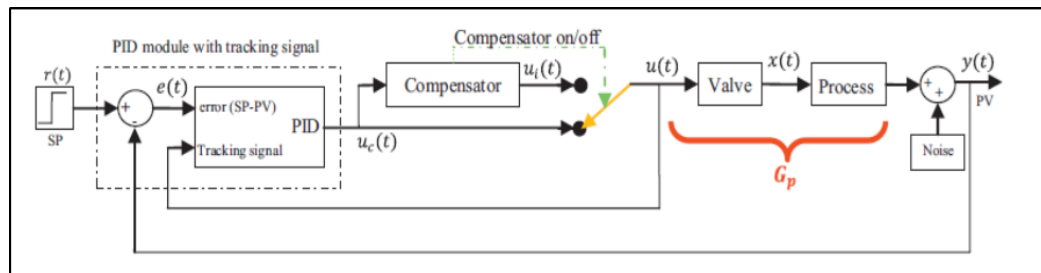


Figure 2.3: Process Control Loop With Two-Move Stiction Compensator.

The compensating signal for the first method is given by

$$u_i(t) = \begin{cases} \alpha_1: & t_1 < t \leq t_1 + T_m \\ u_i(t_1) - \text{sign}(\alpha_1)\alpha_2: & t_1 + T_m < t \leq t_1 + 2T_m \\ u_i(t_1 + T_m) - \text{sign}(\alpha_1)\alpha_3: & t_1 + 2T_m < t \leq t_1 + 3T_m \\ u_i(t_1 + 2T_m) + \text{sign}(\alpha_1) \frac{SP - y_t}{k_p}: & t > t_1 + 3T_m \end{cases} \quad (2.3)$$

In the first step, at $t = t_1$, moves PV from its stuck position far enough from SP , requiring:

$$\alpha_1 = \text{sign}(du_{cf}(t_1)/dt)(S + 2J + uc(t_1)) \quad (2.4)$$

where $u_{cf}(t)$ is the filtered signal from controller output. The second step, at $t = t_1 + T_m$, requires $S < \alpha_2 < \alpha_1$ to change the direction of valve movement. T_m is the time interval required for the stabilization of the PV . The third step at $t = t_1 + 2T_m$ aims to estimate the joint process and valve gain $k_p = \Delta y / \alpha_3$, and to calculate OP_{ss} , requiring $\alpha_3 > J$. The fourth step at $t = t_1 + 3T_m$ applies OP_{ss} for PV to reach SP . During compensation steps PI controller is switched to output tracking and $uc(t)$ is not added to $u(t)$. Therefore,

$$u(t) = \begin{cases} u_i(t), & t_1 < t < t_1 + 3T_m \\ u_c(t), & t < t_1 \text{ and } t > t_1 + 3T_m \end{cases} \quad (2.5)$$

The compensating signal for the second method is given by

$$u_i(t) = \begin{cases} u_c(t_1) + \alpha S \left(1 - \frac{t-t_1}{kT_p}\right) \text{sign}\left(\frac{du_{cf}}{dt}\right), & t_1 \leq t < t_2 \\ u_c(t_1) + \frac{\alpha S}{2} \text{sign}\left(\frac{du_{cf}}{dt}\right), & t > t_2 \end{cases} \quad (2.6)$$

where uc is the controller output, u_{cf} is the filtered controller output, T_p is the period of oscillation, α is a real number greater than one, S is the stick band plus the dead band and t_1, t_2 , and k are parameters tuned with specific conditions.

In [13], by imitating the two moves approach, Wang introduced a closed-loop compensation method by adding a rectangular wave to the set-point for a short period of time. The author provided illustrative analysis to tune the rectangle height and period and proved the method by simulation and experimentally validated the approach using a water tank setup.

2.3. Adaptive & Nonlinear Based Methods

Canudas [14], proposed adaptive technique to compensate for the friction that occurs in robot manipulators at velocity close to zero. Similar work was done by Bernard and Park [15], they used observer to estimate and update the friction parameters continuously.

Keller and Isermann [16], presented work on nonlinear adaptive position control of a standard pneumatic cylinder. They used state controller as outer control loop for the whole system and adaptive feed forward compensator for friction compensation in what is called "friction compensation supervision and adjustment" (FCSA). The work was validated experimentally.

Yazdizadeh and Khorasani [17], proposed a simple adaptive feedback linearization control law based on Lyapunov scheme for friction compensation. The weak point in their method is the need to know the friction parameters in advance by using Recursive least squares (RLS) or least mean squares (LMS) estimator. They presented two examples of mechanical systems to validate their approach.

Huang et al [18], presented a work using neural network. He used an adaptive identification method to estimate friction force and then used Proportional Derivative (PD) controller in order to compensate for the estimated friction. Analytically, he

showed that his proposed compensator is able to achieve regional stability of the closed-loop system and he supported the theoretical analysis by dynamic simulations.

Kayihan and Doyle [19], presented a Nonlinear local control strategy, where a nonlinear locally intelligent actuator design is developed to control a valve independently of the distributed control system. Nonlinear control is implemented through the direct synthesis of a sliding-stem valve model within a nonlinear structure Input output linearization IOL with internal model control, referred to as NLIMC, was used to improve tracking performance over the linear controller currently used by smart valves.

Alamir[20] presented adaptive methodology to compensate friction without knowing the friction model (mass sliding on surface).He used Fourier series for friction term approximation.The adaptive updating for coefficient's was done by a Lyapunov approach.

Mei et al [21], presented a novel compensation method, based on Kang's method, for nonlinear friction in mechatronic servo systems,which is considered as modified Southward's traditional compensation method for nonlinear friction.The stability of the proposed method was proved with Lyapunov's stability theorem and enhanced tracking performance is verified experimentally using the SCARA robot.

2.4. Dynamic Inversion Methods

Selmic and Lewis [22], introduced a dynamic inversion compensation scheme for backlash nonlinearity.They used two layer neural network with back-stepping technique as compensator to invert the backlash dynamic in the feed forward path.

In [23],Widrow illustrated the idea of adaptive inverse.He stated that "the adaptive control is seen as a two part problem: control of plant dynamics and control of plant

noise. The parts are treated separately” .It is clear that the plant will always track the input if the controller dynamic is exactly the inverse of plant dynamic, the second part is control of plant internal noise is done with an optimal adaptive noise canceller. In [24],Widrow discussed the adaptive inverse control based on the linear and nonlinear filter, which gave more insight into the topic for the linear and nonlinear SISO and MIMO plants.

The first work related to actuator was presented in [25], where Tao used a gradient projection optimization technique to tune the weight of the adaptive inverse filter to cancel the actuator uncertainty like dead band, hysteresis etc.

Thethi[26], developed AIC based on Bacterial Foraging Optimization (BFO).the performance of this method is tested via three different models against standard squared norm based models and it showed competent performance.

2.5. PID Retuning Methods

Kionget al.[27], addressed the friction modeling in servomechanisms by dual relay feedback approach., The friction model components that was targeting were Coulomb and viscous friction., A PID was used as feedback motion controller and in the compensation part, a feed forward friction compensator was tuned adaptively based on the dual relay friction components identification.

Mohammad andHuang [28],presented a new framework for stiction compensation by retuning the PID controller based on trajectories plotting “root locus”. They determined the conditions in order to avoid oscillations or a limit cycle to take place in the process. It must be noted that the parameters tuning should be in the allowable parameter ranges.

Which are set based on process needs and limitations. Prior knowledge of these ranges are essential for the tuning procedures. He proved the idea experimentally.

Mishra et al.[29],used stiction combating intelligent controller (SCIC) to curb stiction. SCIC replaces the linear PI controller in the control loop, it can be considered as variable gain PI controller based on fuzzy logic that use Takagi-Sugeno (TS) scheme. Mishra tested the performance of his proposed controller using a laboratory scale flow process. His controller outperformed the normal linear PI controller in stiction reduction with lesser aggressive stem movement.

Chen Li and Choudhury group [30], proposed a mechanism to compensate the oscillation in cascade controllers, through the tuning of the outer and the inner controller. They supported there method with detailed frequency analysis, finally they validated it through simulation examples and a pilot-scale flow-level cascade control experiment.

CHAPTER 3

Valve Stiction Modeling

Generally, the areas of valve stiction study can be categorized into three. The first is the research on how to detect the stiction and quantify it. The second is how to model the stiction, and finally, how to compensate it. Many studies have been conducted on the three areas, but lately the last area tends to attract the researchers more than the two other areas. This may be due to the satisfactory results that have been achieved in the first two areas and unlike the third area.

In this work, the focus will be on the compensation area, even though, some valve stiction models from literature will be covered in this chapter. The existing valve models can be divided into two main groups, either physical models or data driven models.

3.1. Physical Models

Physical models describe the friction phenomenon using balance of forces and Newton's Second law of motion. These types of models require previous knowledge of various parameters and features of the valve such as spring coefficient, moving part mass, and friction coefficients (static, viscous and Coulomb), which may be considered as a disadvantage, since it is not easy to get these parameters.

3.1.1. Karnopp Model

Karnopp model is the most popular physical models introduced by Karnopp[31], aiming to solve the problems with null speed detection and avoiding the switching between the model equations that describe the sticking or sliding body.

The model defines an interval around $v=0$, creating a dead zone for $|v|<DV$. Depending on $|v|<DV$ or not, the friction force is a saturated version of the external force or a static function of velocity, as presented in equation (3.2). DV is a parameter to be defined.

From Newtons laws, we have:

$$m \frac{d^2x}{dt^2} = \sum Forces = F_{pressure} - F_{spring} - F_{friction} \quad (3.1)$$

Where:

m : the mass of valve moving part.

$F_{pressure}=S_aP$, is the actuator force, S_a is the diaphragm area and P is air pressure.

$F_{spring}=K_mx$, is the spring force, K_m is spring constant and x stem position.

$F_{friction}$ is the friction force given by:

$$F_{friction}(v) = \left[F_c + (F_s - F_c) e^{-\left(\frac{v}{v_s}\right)^2} \right] sgn(v) + F_v v \quad (3.2)$$

F_c : coulomb friction coefficient.

F_s : static friction coefficient.

v : stem velocity.

v_s : stribek velocity.

F_v : viscous friction coefficient.

3.2. Data-Driven Models

A detailed physical model that has many unknown parameters, is often difficult to estimate. Besides, complex models are much slower to run in a computer. Data driven models or empirical models simplify the stiction simulation based on real data. They are simple, directly formulated from stiction behavior logic and have few parameters to tune. Many models of this type exist in the literature. Below, we discussed some models that will be used in simulation later on. These models are: Choudhury model, Kano model, He model and Two-layer binary tree model.

3.2.1. Choudhury Model

Introduced by Shoukat Choudhury [32]. The model consists of two parameters, namely the size of dead band plus stick band S (specified in the input axis) and slip jump J (specified on the output axis). Note that the term ' S ' contains both the dead band and stick band.

The model algorithm can be described as:

- The controller output in (mA) is converted into percentage of valve travel (position signal) by using a look-up table
- The valve travel has boundary between 0% and 100% resemble the fully closed and fully open cases.
- For the signal in range between 0–100%, the slope of the position signal is calculated by specific algorithm.

- In two consecutive instants ,the slope direction may change or remain in its original direction.If the slope change its direction or remain constant with slope sign equal zero the valve is assumed to be stuck.,To monitor these possibilities the sign function is used as indicator and it can be one of the following cases:
 - Slope sign is equal '+1' for positive slope of the position signal.
 - Slope sign is equal '-1' for negative slope of the position signal.
 - Slope sign is equal '0' for zero slope of the position signal.

Therefore, when sign (slope) changes from '+1' to '-1' or vice versa, it means the direction of the input signal has been changed and the valve is in the beginning of its stick position. Now, the valve may stick again while traveling in the same direction (opening or closing direction) only if the input-signal to the valve does not change or remains constant for two consecutive instants, which is usually uncommon in practice. For this situation, the sign (slope) changes to '0' from '+1' or '-1' and vice versa. The algorithm again detects here the stick position of the valve in the moving phase and this stuck condition is denoted with the indicator variable $I=1$. The value of the input signal when the valve gets stuck is denoted as x_{ss} . This value of x_{ss} is kept in memory and does not change until the valve gets stuck again. The cumulative change of input signal to the model is calculated from the deviation of the input signal from x_{ss} .

- For the case when the input signal changes its direction (i.e., the sign(slope) changes from '+1' to '-1' or vice versa), if the cumulative change of the input signal is more than the amount of the dead band plus stick band (S), the valve slips and starts moving.

- For the case when the input signal does not change direction (i.e., the $\text{sign}(\text{slope})$ changes from '+1' or '-1' to zero, or vice versa). If the cumulative changes of the input signal is more than the amount of the stick band (J), the valve slips and starts moving. Note that this takes care of the case when the valve sticks again while travelling in the same direction [33].
- The output is calculated using the equation:

$$\text{output} = \text{input} - \text{sign}(\text{slope})(S - J)/2 \quad (3.3)$$

Depending on the type of stiction present in the valve. It can be described as follows:

- Dead band: If $J = 0$, it represents pure dead band case without any slip jump.
- Stiction (undershoot): If $J < S$, the valve output can never reach the valve input. There is always some offset. This represents the undershoot case of stiction.
- Stiction (no offset): If $J = S$, the algorithm produces pure stick-slip behavior. There is no offset between the input and output. Once the valve overcomes stiction, valve output tracks the valve input exactly. This is the well-known “stick slip case”.
- Stiction (overshoot): If $J > S$, the valve output overshoots the valve input due to excessive stiction, This is termed as overshoot case of stiction.

Recall that J is an output (y-axis) quantity. Also, the magnitude of the slope between input and output is 1.

- The parameter J signifies the slip jump start of the control valve immediately after it overcomes the dead band plus stick band. It accounts for the offset between the valve input and output signals.
- Finally, the output is again converted back to a mA signal using a look-up table based on the valve characteristics such as linear, equal percentage or square root, and the new valve position is reported.

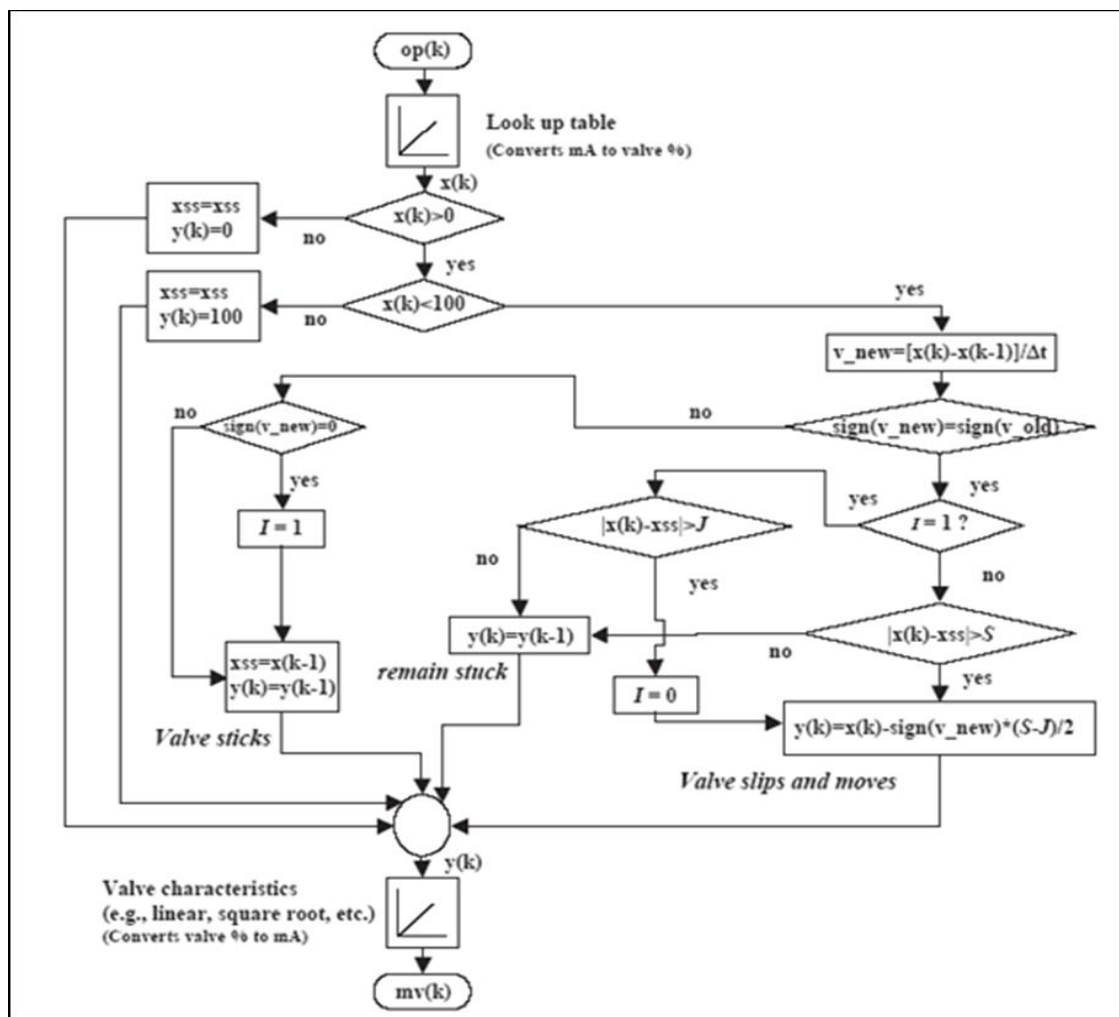


Figure 3.1: Signal and Logic Flow Chart for the ChoudhuryStiction Model.

3.2.2. Kano Model

This is improved version of Choudhury model. The model was introduced to deal with both deterministic and stochastic signals, which is lacking in Choudhury model, as claimed by Kano [33]. To model the relationship between the controller output and the valve position of a pneumatic control valve, the balance among elastic force, air pressure, and frictional force needs to be taken into account. The relationship can be described as shown in the Figure 3.2 below.

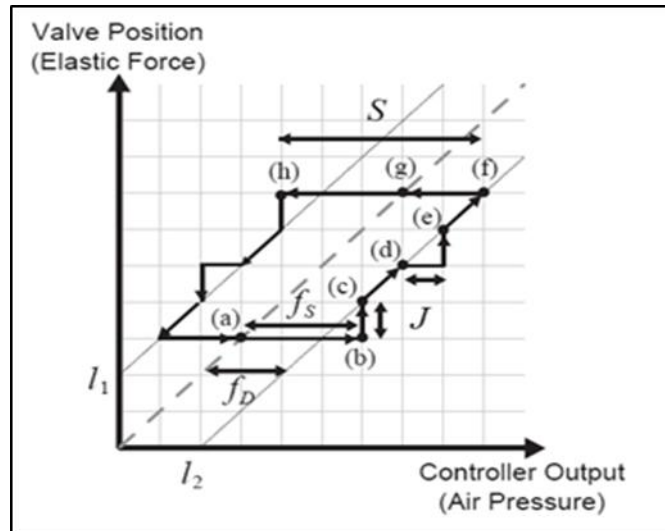


Figure 3.2: Stiction Parameters Relation to Stiction Behavior.

The dashed line denotes the states where elastic force and air pressure are balanced. The controller output and the valve position change along this line in an ideal situation without any friction. The ideal relationship is disturbed when friction arises. For example, the valve is resting at (a), where elastic force and air pressure are balanced. The valve position cannot be changed due to static friction even if the controller output, i.e., air pressure, is increased. The valve begins to open at (b), where the difference between air pressure and elastic force exceeds the maximum static frictional force. Since the

frictional force changes from static f_s to kinetic f_D when the valve starts to move at (b), a slip-jump of size ($J = f_s - f_D$) happens and the valve state changes from (b) to (c). Thereafter, the valve state changes along the line l_2 which deviates from the ideal line by f_D because the difference between air pressure and elastic force is equal to f_D . When the valve stops at (d), the difference between air pressure and elastic force needs to exceed f_s again for the valve to open further. Since the difference between them is f_D at (d), air pressure must increase by J to open the valve. Once air pressure exceeds elastic force by f_D , the valve state changes to (e) and then follows l_2 . Air pressure begins to decrease when the controller orders the valve to close at (f). At this moment, the valve changes its direction and comes to rest momentarily. The valve position does not change until the difference between elastic force and air pressure exceeds the maximum static frictional force f_s . The valve state (h) is just point-symmetric to (b). The difference of air pressure between (f) and (h) is given by ($S = f_s + f_D$) the valve state follows the line l_1 while the valve position decreases. The abovementioned phenomena can be modeled as a flowchart shown in Figure 3.3. The input and output of this valve stiction model are the controller output u and the valve position y , respectively. Here, the controller output is transformed to the range corresponding to the valve position in advance. The first two branches check if the upper and the lower bounds of the controller output are satisfied. In this model, two states of the valve are explicitly distinguished: 1) a moving state ($stp = 0$), and 2) a resting state ($stp = 1$). In addition, the controller output at the moment the valve state changes from moving to resting is defined as u_s . u_s is updated and the state is changed to the resting state ($stp = 1$) only when the valve stops or changes its direction ($\Delta u(t)\Delta u(t-1) \leq 0$) while its state is moving ($stp = 0$). Then, the following two conditions

concerning the difference between $u(t)$ and u_S are checked unless the valve is in a moving state. The first condition judges whether the valve changes its direction and overcomes the maximum static friction (corresponding to (b) and (h) in Figure 3.2). Here, $d = \pm 1$ denotes the direction of frictional force. The second condition judges whether the valve moves in the same direction and overcomes friction. If one of these two conditions is satisfied or the valve is in a moving state, the valve position is updated via the following equation.

$$y(t) = u(t) - df_D = u(t) - \frac{d(S-J)}{2} \quad (3.4)$$

On the other hand, the valve position is unchanged if the valve remains in a resting state. The valve stiction model developed here has several advantages compared with the model proposed by [32]. First, it can cope with stochastic input as well as deterministic input. Second, u_S can be updated at appropriate timings by introducing the valve state stp . Third, it can change the degree of stiction according to the direction of the valve movement.

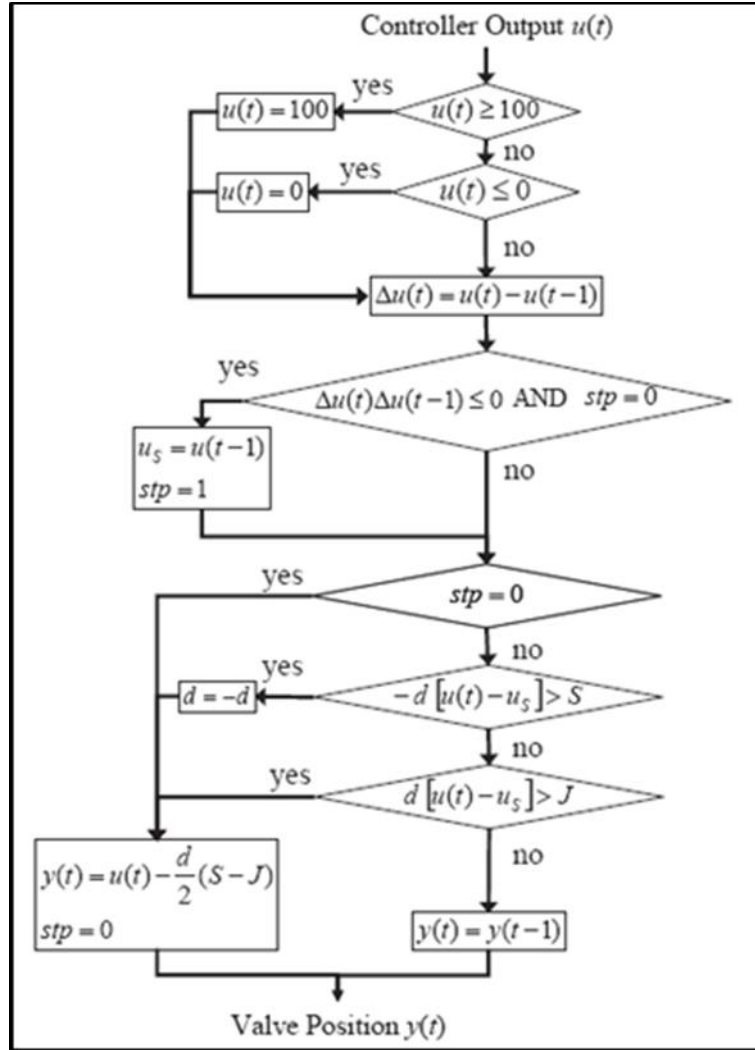


Figure 3.3: Flow Chart of Kano Stiction Model.

3.2.3. He Model

Based on the sticky-valve behavior, Q.He et al.[34]proposed a new valve stiction model.It uses the static friction f_s and dynamic friction f_D as model parameters, which brings the model closer to the physical model, rather thanthe stick band S and slip jump J used in previous two models. Figure 3.4 shows the flowchart of the proposed model. The variable u_r is the residual force acting on the valve which has not materialized a valve move. The variable cum_u is a temporary variable, which is the current net force acting

on the valve. If cum_u is large enough in magnitude to overcome the static friction f_s , the valve position $u_v(t)$ will be the controller output $u(t)$ offset by the dynamic stiction f_D . Otherwise, the valve position will not change and cum_u is the residual force on the valve to be used in the next control instant.

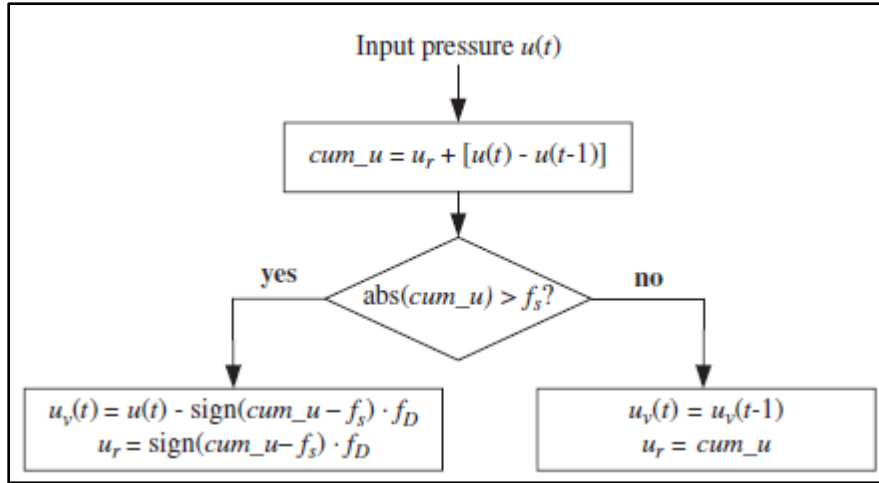


Figure 3.4: Flow Chart of He Stiction Model.

3.2.4. Two-Layer Binary Tree Model

Introduced in [35] asexentionto the model proposed by *He*, to addresses all possible state transitions, as well as different stiction patterns. Logically, because the valve has two states, stick and slips, there are four possible state transitions: stick to slip, keep sticking, slip to stick, and keep slipping. The main drawback of the *He* model is that it only covers the first two possible state transitions. In the *He* model, it is assumed that the static friction affects every valve movement, so that the model is applicable. However, when the valve keeps slipping, the model becomes inadequate.

According to Figure 3.5, the model first updates the value of $cum_u(k)$, and, in addition, the direction of movement $d(k)$ is obtained via $sgn(cum_u(k))$; then, if the valve status

flag (*Stop*) is equal to 1, the logic flows to the left branch, which determines the position of the valve if it is stuck in the previous interval.

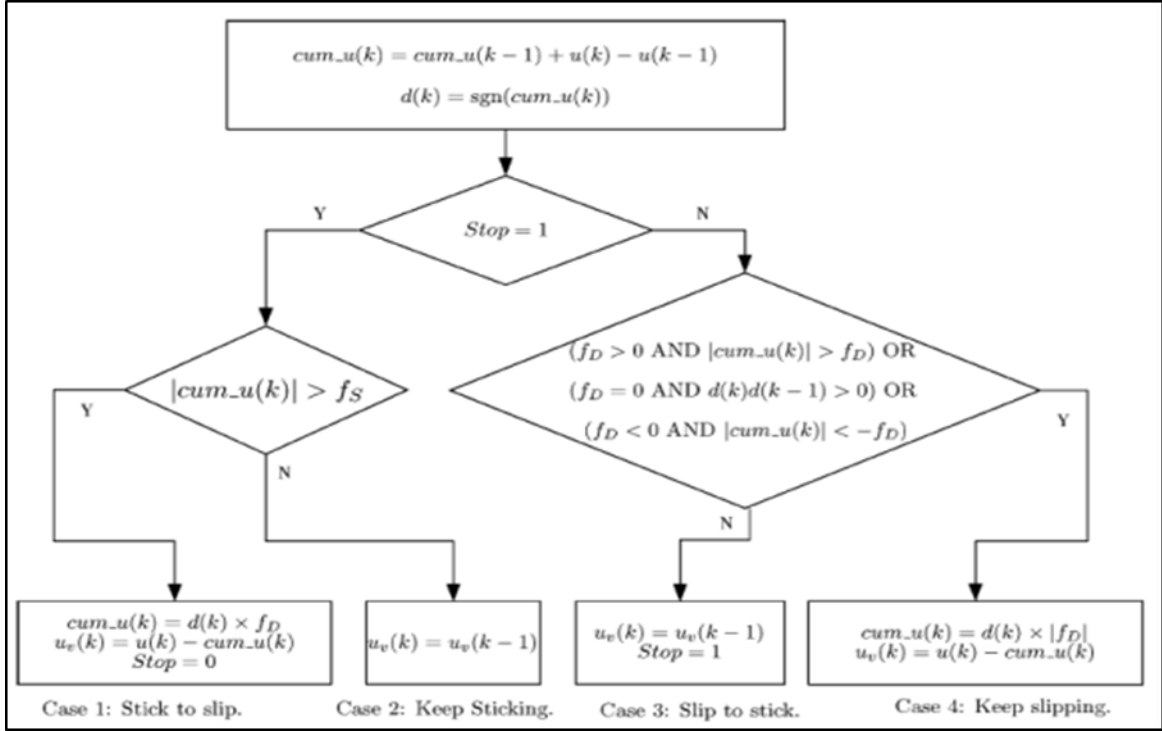


Figure 3.5: Two layer Binary Tree Stiction Model.

The algorithm contained in the left branch is identical to the *He* model. In other words, the *He* model is part of the complete model that is being proposed. If $cum_u(k)$ is large enough to overcome the static friction f_S , the valve position $u_v(k)$ will be the controller output $u(k)$ minus the dynamic friction f_D . The term $cum_u(k)$ is updated to be equal to $\pm f_D$, because, when the valve starts slipping, the force being counteracted by friction is equal to $\pm f_D$ (the sign is dependent on the direction of movement $d(k)$). In addition, the valve status flag *Stop* is updated to be zero, to indicate that the valve switches to a slipping mode. Otherwise, the valve remains in the previous position. When the valve is

in a slipping state, the condition to determine the status in the next instant is dependent on the sign of f_D , because the two pairs f_s, f_D and S, J have the following relationships:

$$f_s = \frac{S + J}{2} ; \quad f_D = \frac{S - J}{2}$$

The various stiction patterns corresponding to S and J are discussed by Choudhury et al.

Note that $f_s > 0$, because $S > 0$ and $J > 0$. The MV-OP pattern that corresponds to f_D can

be summarized as follows:

(1) $f_D > 0$ (or $S > J$), which indicates stiction with undershoot or pure deadzone.

(2) $f_D = 0$ (or $S = J$), which indicates stiction with no offset or linear.

(3) $f_D < 0$ (or $S < J$), which indicates stiction with overshoot.

Pure deadzone and linear patterns can be seen as special cases of a stiction pattern with

$f_s = f_D > 0$ accordingly.

CHAPTER 4

Stiction Compensation Methods

4.1. Knocker Method

Introduced by Tore Hagglund[4] in 2002, the main idea is adding short pulses of equal amplitude and duration (sequence of pulses with a relatively small energy content) in the direction of the rate of change of the control signal to the control signal. Then, the knocker signal parameters (pulse amplitude, width and sampling interval) shown in Figure 2.1, should be tuned to get the optimal compensation.

$$u_k(t) = \begin{cases} a \operatorname{sign}(u_c(t) - u_c(t_p)) & t \leq t_p + h_k + \tau \\ 0 & t > t_p + h_k + \tau \end{cases} \quad (4.1)$$

Where t_p is the time of onset of the previous pulse. Hence, the sign of each pulse is determined by the rate of change of control signal $u_c(t)$.

Physically the knocker is inserted between the controller and the valve, illustrated in the following figure.

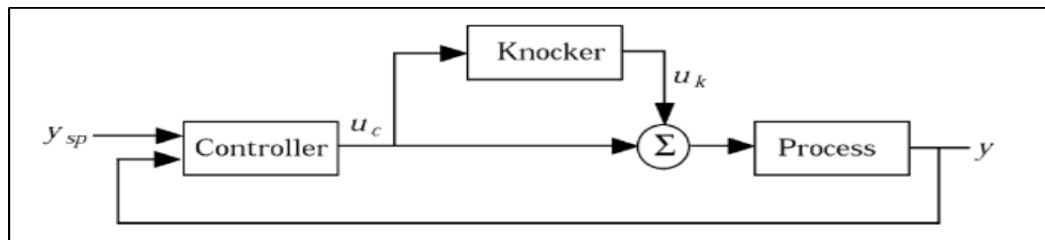


Figure 4.1: Block Diagram illustrating the Knocker used in a feedback loop.

The final control signal shape will have the original shape but with pulses imposed on it, the major disadvantage of this method is that it comes at the cost of aggressive movement of valve stem.

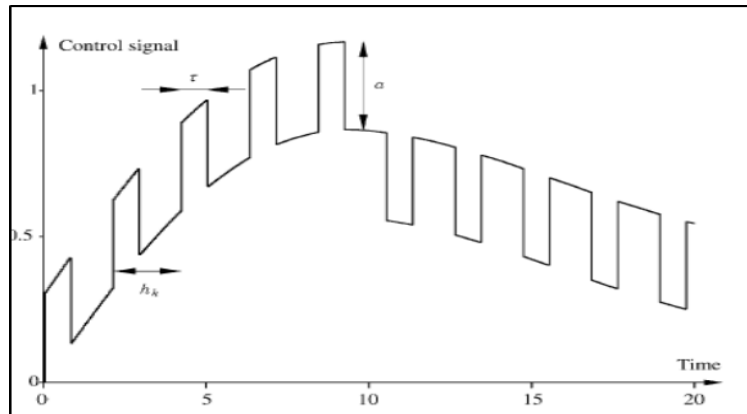


Figure 4.2: Control Signal using the knocker Compensator.

4.2. Dithering Method

Dithering is a high frequency signal with zero mean, in fact, it has positive and negative equal amplitude with equal duty cycle. However, the shape of the signal could pulse shape, triangular shape, or sinusoidal shape. The structure of dither compensator is similar to the knocker compensator, actually knocker can be considered as a special case of dither.

4.3. Constant Reinforcement Method

Introduced by Lee Ivan and S. Lakshminarayanan[5], this method curbs stiction by adding constant amplitude to the control signal with the same sign as its rate of change. If controller output is constant; there is no addition to its signal. The structure of Constant Reinforcement (CR) compensator is similar to knocker, actually CR can be considered as a special case of Knocker.

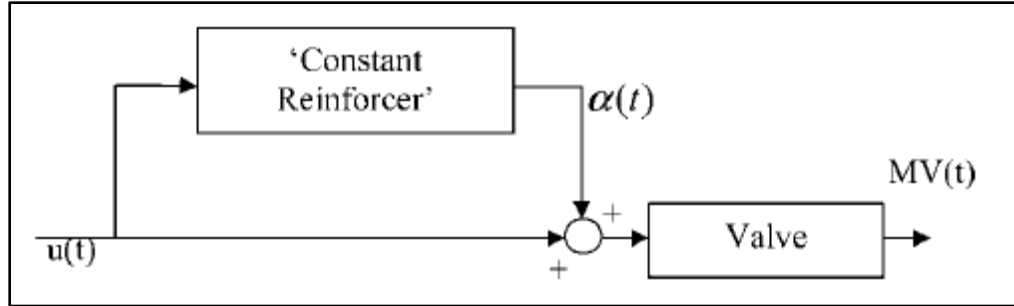


Figure 4.3: CR compensator structure.

$$\alpha(t) = a \times \text{sign}(\Delta u) \quad (4.2)$$

Where $\alpha(t)$ is added to u . The new compensator thus provides constant reinforcement of the OP signal, and the technique is referred to as the “constant reinforcement” (CR) approach. If the controller output u is constant, there will be no addition to its signal. This approach has a sensitivity problem, sometimes the noise changes the sign of the added signal, although the control signal doesn’t change its direction, and this problem can be reduced by adequate filtering.

4.4. Approximate Inverse Method

If by some mean an exact inverse dynamic of the stiction is inserted before the sticky valve, the stiction will be eliminated theoretically. However, the stiction is a kind of static nonlinearities that doesn’t change in its pattern easily or changes very slowly with small amount which can be neglected.

Figures 4.5 & 4.6 shows the stiction behavior and its inverse, since it is not possible to generate such kind of inverse behavior, a backlash inverse approximation is used. An approximated inverse of Stiction (i.e., the backlash inverse) is used to compensate for stiction severity. Clearly, variance is reduced more in case of smaller value of J . Stiction

can be represented as composed of other nonlinearities like deadband and backlash. With simulations, it has been figured out that the backlash is the dominating nonlinearity in the stiction phenomenon. Therefore, it is inferred to use backlash inverse as approximate inverse when stiction inverse is not available. The inverse for different nonlinearities including backlash can be found in Gang et al[36] as seen in figure 4.7.

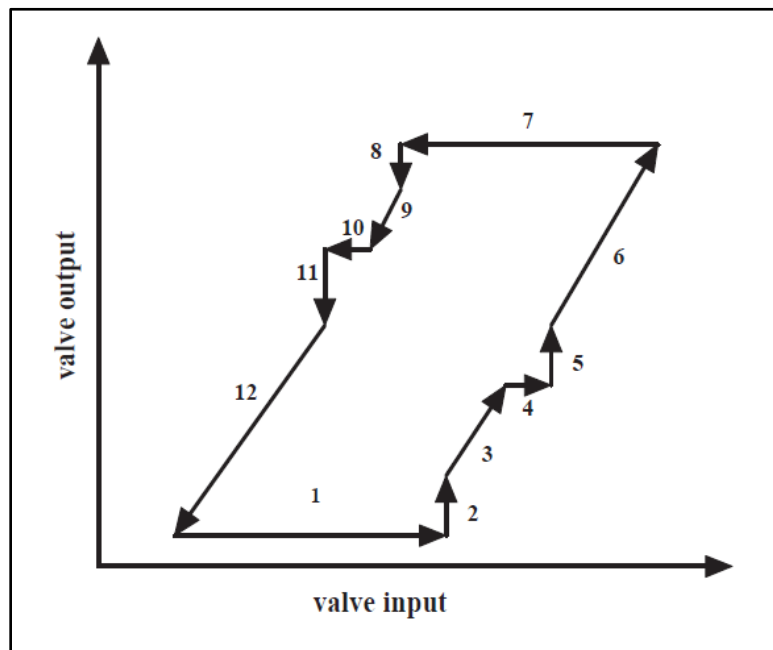


Figure 4.4: Valve input-output pattern in case of stiction.

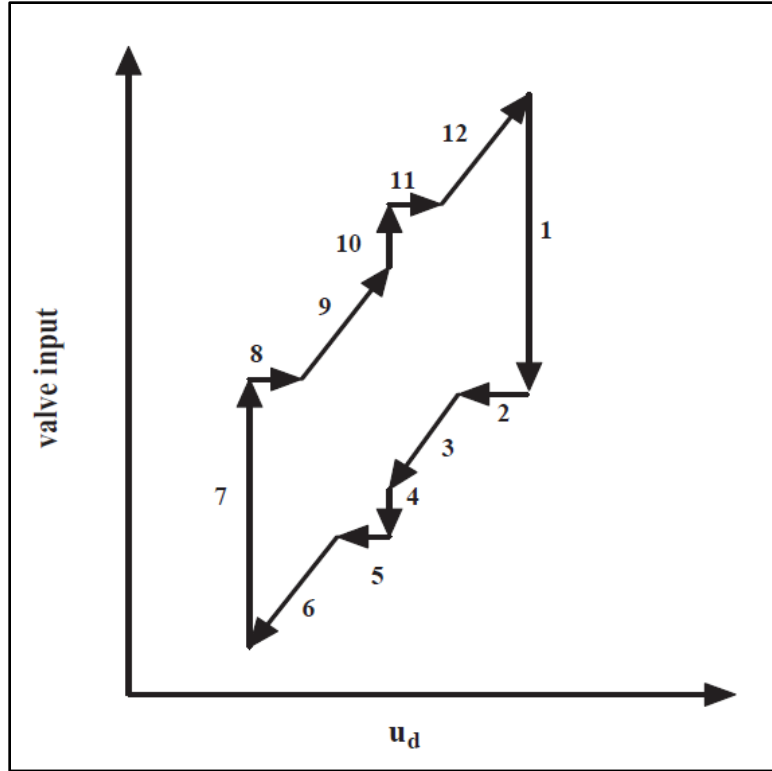


Figure 4.5: Inverse pattern of valve stiction.

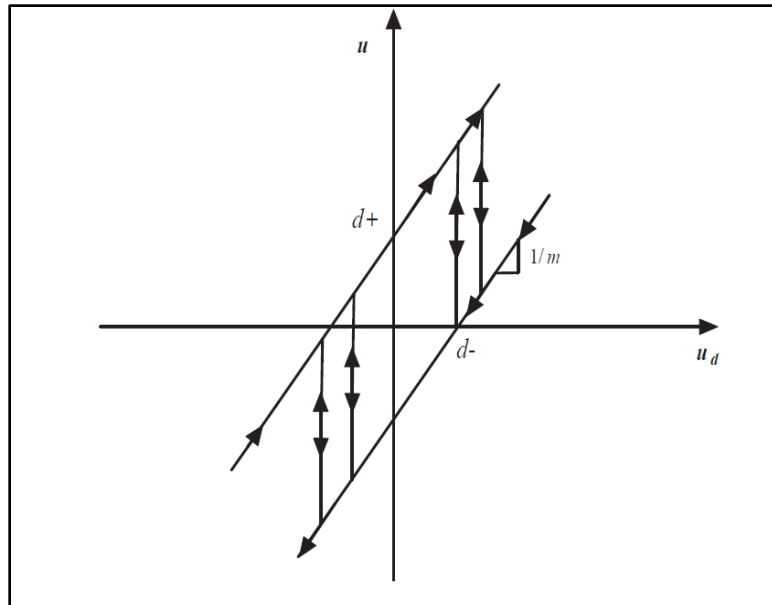


Figure 4.6: Backlash Inverse pattern.

$$u_t = \begin{cases} u(t-1) & \text{if } u_d(t) = u(t-1) \\ \frac{u(t)}{m} + d_- & \text{if } u_d(t) < u(t-1) \\ \frac{u(t)}{m} + d_+ & \text{if } u_d(t) > u(t-1) \end{cases} \quad (4.3)$$

Where $\frac{1}{m}$ is the slope of the parallel lines, d_- and d_+ are the crossings on the vertical axis.

Here $d_+ = S/2$ and $d_- = -S/2$, where S is the stickband plus deadband.

Stiction nonlinearity with inverse is represented in a block diagram as shown in Figure 4.8. Assume $S(\cdot)$ is the nonlinear function representing stiction nonlinearity and $SI(\cdot)$ represents the inverse of stiction. Then the stiction nonlinearity can be represented as.

$$x(t) = S(u(t)) \quad (4.4)$$

And the stiction inverse can be written as.

$$u(t) = SI(u_d(t)) \quad (4.5)$$

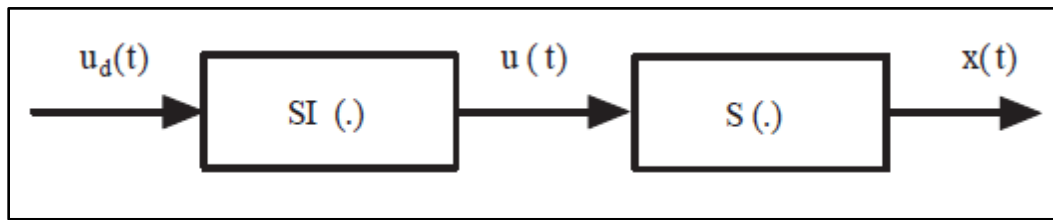


Figure 4.7: Block diagram of stiction and stiction inverse.

4.5. Adaptive Inverse Control (LMS-FIR Method)

Adaptive Inverse control (AIC) is one of the important applications for adaptive filtering theory [37], as explained by Bernard Widrow. In this section adaptive filtering theory is used to propose the adaptive inverse model of valve stiction nonlinearity. An introduction

to adaptive technique and the Least Mean Square adaptive algorithm is given. Then an adaptive inverse scheme is given to the model inverse of the valve nonlinearity.

N.B: this method is modified version from method introduced by M.Sabih[38].

4.5.1. Finite Impulse Response Filter

An adaptive digital filter is shown in Figure 4.9, has an input, an output, and other special input called the “desired response”, the adaptive filter contains adjustable parameters that control its impulse response, normally an adaptive algorithm such as the Least mean square is responsible for tuning these parameters “weight” to achieve the minimum error or difference between the plant output and the desired response. The most important filter used in adaptive inverse control is the FIR filter which has only zeros and no poles.

The FIR filter used for compensation is preferred to have a few number of possible weights to reduce the computation time and processing load needed for the optimization process.

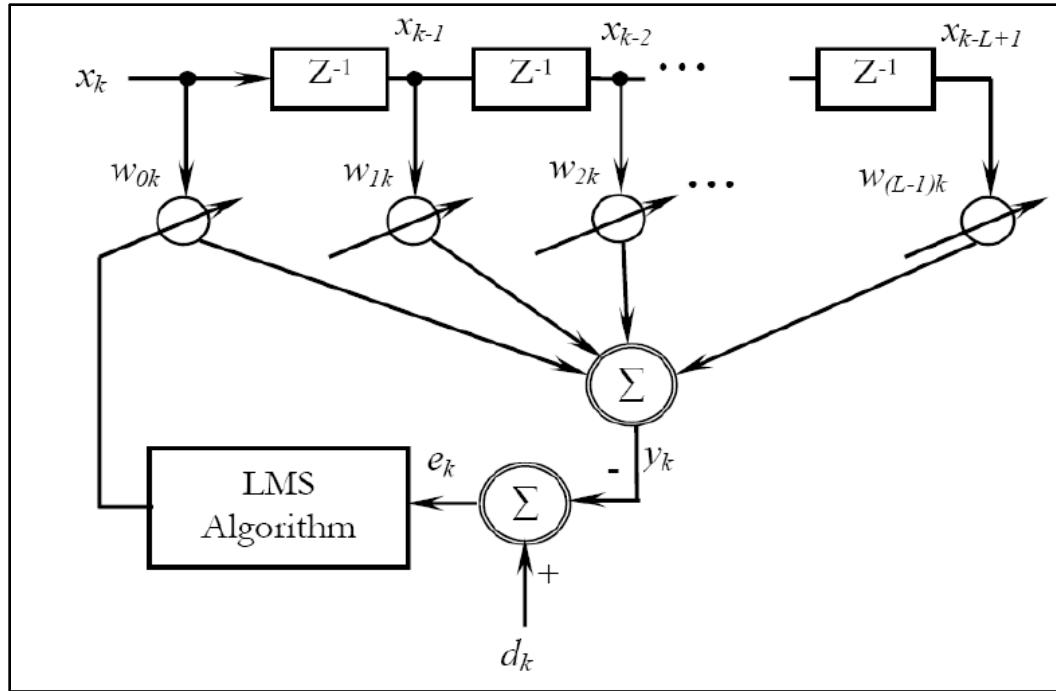


Figure 4.8: Finite Impulse Response Filter with adaptive algorithm for weights tuning.

4.5.2. Least Mean Square Algorithm

A Basic adaptive filter is depicted in Figure 4.9. The X is N^{th} input pattern having one Unit delay in each instant. This process is called as an adaptive linear combiner, Let $X_k = [x_k x_{k-1} x_{k-L+1}]^T$ form of the L-by-1 tap input vector. Where $L-1$ is the number of delay elements; this input span a multidimensional space denoted by N_k . Correspondingly, the tap weights $W_k = [w_{0k} w_{1k} w_{(L-1)k}]^T$ form the elements of the L-by-1 tap weight vector. The output samples are written as:

$$y_k = \sum_{l=0}^{L-1} w_{lk} x_{k-l} \quad (4.6)$$

The output can be represented in vector notation as

$$y_k = X_k^T W_k = W_k^T X_k \quad (4.7)$$

In addition to the Xinput, the adaptive filter also needs other data include a "desired response" or "training signal", *deck* for weight training. This is accomplished by comparing the output with the desired response to obtain an "error signal" e_k and then adjusting the weight vector to minimize this signal. The error signal is given by:

$$e_k = d_k - y_k \quad (4.8)$$

The weights associated with the network are then updated using the LMS algorithm. The weights update equation for n^{th} instant is given by:

$$w_k(n+1) = w_k(n) + \Delta w_k(n) \quad (4.9)$$

It can be further derived as:

$$w_k(n+1) = w_k(n) + 2 \cdot \eta \cdot e_k(n) \cdot X_k^T \quad (4.10)$$

Where η is the learning rate parameter ($0 < \eta < 1$). This procedure is repeated till the Mean Square Error (MSE) approaches a minimum value. The MSE at the time index k may be defined as, $\xi = E[e_k^2]$, where $E[.]$ is the expectation value of the signal.

4.5.3. Adaptive Inverse Control by using LMS-FIR Filter

A scheme to find the adaptive inverse model of the control valve is given in Figure 4.10. Since valve position MV is not available in most cases, the loop error (difference between set-point and the process variable) can be used as an objective function for the adaptive algorithm. Since the process variable oscillates around the set-point due to the valve stiction, the error also oscillates around zero. In other words, if the filter success to eliminate or minimize the oscillation amplitude in the loop error, the same thing will

occur in the process variable automatically, here and instead of OP and MV , SP and PV are required.

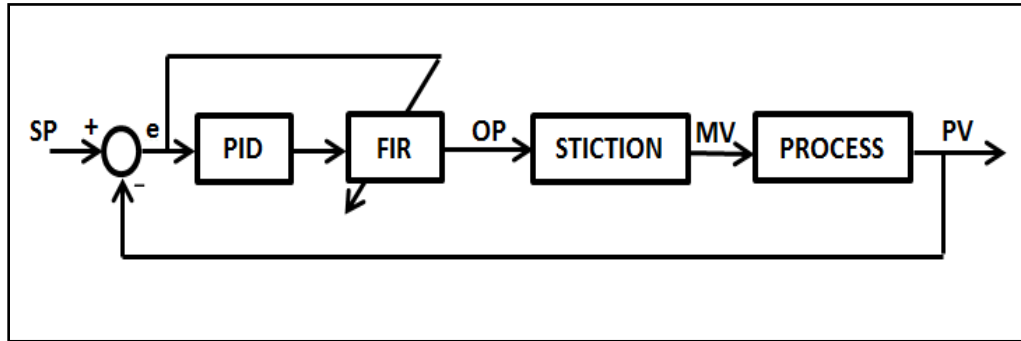


Figure 4.9: Structure of single loop with AIC.

4.6. Adaptive Inverse Control (DE-FIR Method) (Proposed Method)

The proposed method is an evolution of the LMS-FIR method, mentioned in section 4.5. proposed method gets benefits and resolves the weakness of the LMS-FIR method. In fact the proposed method uses intelligence control theory as well as an adaptive filtering theory to compensate valve stiction.

The only difference is the replacement of LMS optimization algorithm with intelligent one to guarantee that the optimization process will achieve the best or global minima. The classical methods such as least mean square have high possibility to be trapped in local minima especially when it is used in high nonlinearity problems. Differential Evolution Algorithm (*DE*) is one of these intelligent techniques that belong to an evolutionary algorithms family. Its main features are simplicity, robustness and fast convergence.

CHAPTER 5

Differential Evolution Algorithm

5.1. Overview

The differential evolution algorithm was introduced by Rainer Storn and Kenneth Price between 1994 to 1996 [39], [40], during their work to solve a problem called "Chebyshev Polynomial fitting problem", Kenneth came up with an idea to use vector differences for perturbing the vector population. Then, both authors worked out this idea and made several improvements, until the DE was successfully formulated and introduced.

The DE is a population based optimization technique and it is characterized by its simplicity, robustness, few control variables and fast convergence. Being an evolutionary algorithm, the DE technique is well-suited for solving non-linear and non-differentiable optimization problems. DE is a searching technique that requires a number of population (N_P) solutions (X_n^i) to form the population G_i , where each solution consists of a certain number of parameters X_{nj} depending on the problem dimension.

$G^i = [X_1^i, X_2^i, \dots, X_{NP}^i]$: generation, NP: population size

$X_n^i = [x_{n1}, x_{n2}, \dots, x_{nj}]$: problem dimension

The essential idea in any search technique depends on how to produce a variant (offspring) vector solution on which the decision will be made. In order to choose the best (parent or variant). The strategy applied in this technique is to use the difference between randomly selected vectors to generate a new solution. For each solution in the original population, a trial solution is generated by performing the process of mutation, recombination, and selection operators. The old and new solutions are compared and the best solutions are moved to the next generation.

Initially the DE was developed to solve single objective optimization problem. The DE was compared against the well-known Particle Swarm Optimization technique[41], and the author has concluded that DE has better performance.

5.2. Optimization Procedure in DE for Single Objective Optimization

Problem

The DE, as in any evolutionary technique, generally performs three steps: initialization, creating a new trial generation and selection, these steps are illustrated in Figure 5.1.

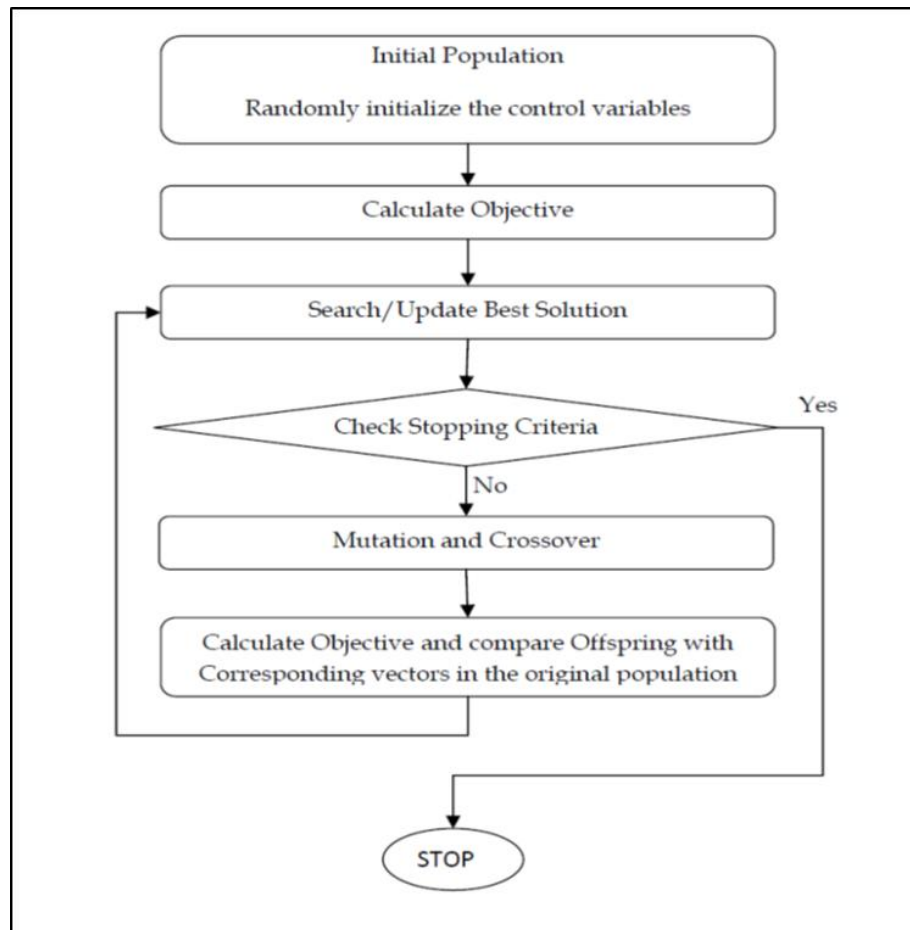


Figure 5.1: DE flowchart.

5.2.1. Initialization

As a preparation for the optimization process, the following requirements should be specified:

- Problem dimension which defines the number of control variables. Also, the range of each control element should be defined. This range is required during the process.
- N_P : population size.
- Number of generation or iterations.
- F : mutation factor.

- *CR*: Crossover factor, which determine the probability of offspring parameters for each control vector.

Optimization using DE requires many steps, the first one is to generate an initial population consisting of N_p solutions or vectors, as given by equation (5.1), where each vector contains the values of the various control variables which represent a candidate solution to the problem. This is done by assigning random values for each parameter of the solution \vec{X}_j within the range of the corresponding control variable.

$$X_{i,j} = X_{i,min} + random (X_{i,max} - X_{i,min}) \quad i = 1, D, j = 1, N_p \quad (5.1)$$

5.2.2. Evaluation and Finding the Best Solution

Once the initial population is created, the objective value for each vector is calculated and then compared to get the best solution that satisfies the optimal objective function. This value is stored externally and updated by comparison with all solutions in every generation.

5.2.3. Mutation

The mutation process is considered as the first step in the generation of new solutions. At this stage, for every single solution in the population in generation- i : $X_i^{(G)}$ $i = 1, N_p$, a mutant vector $V_i^{(G+1)}$ is generated using one of the following formulas:

$$V_i^{(G+1)} = X_{r1}^{(G)} + F(X_{r2}^{(G)} - X_{r3}^{(G)}) \quad (5.2)$$

$$V_i^{(G+1)} = X_{best}^{(G)} + F(X_{r1}^{(G)} - X_{r2}^{(G)}) \quad (5.3)$$

$$V_i^{(G+1)} = X_i^{(G)} + F(X_{best}^{(G)} - X_i^{(G)}) + F(X_{r1}^{(G)} - X_{r2}^{(G)}) \quad (5.4)$$

$$V_i^{(G+1)} = X_{r1}^{(G)} + F(X_{r2}^{(G)} - X_{r3}^{(G)}) + F(X_{r4}^{(G)} - X_{r5}^{(G)}) \quad (5.5)$$

where: $X_{r1}^{(G)}$, $X_{r2}^{(G)}$, $X_{r3}^{(G)}$, $X_{r4}^{(G)}$, $X_{r5}^{(G)}$ are randomly selected solution vectors from the current generation (different from each other and the corresponding X_i and $X_{best}^{(G)}$). $X_{best}^{(G)}$ is the solution to achieving best value. The mutation factor (F) takes values between 0 and 1 and plays a key role in controlling the speed of convergence.

5.2.4. Crossover

For better perturbation and enhancement in the diversity of the generated solutions, a crossover process is performed by DE. In this step, the parameters of the generated mutant vector and the corresponding solution vector i in the original population are copied to a trial solution according to a certain crossover factor $CR \in [0,1]$. For each parameter, a random number in the range $[0, 1]$ is generated and compared with CR , and if its value is less than or equal to CR , the parameter value is taken from the mutant vector, otherwise, it will be taken from the parent. Crossover process is shown in Figure 5.2. However, in case CR was defined to be zero, then all the parameters of the trial vector are copied from the parent vector X_i , except one value (randomly chosen) of the trial vector is set equal to the corresponding parameter in the mutant vector. On the other hand, if CR is set equal to one, then, all parameters will be copied from the mutant vector except one value (randomly chosen) of the trial vector is set equal to the corresponding parameter in the parent vector. The factor (CR) plays an important role in controlling the smoothness of the convergence. As CR becomes very small, it becomes very probable that the trial solutions would have characteristic of their parent vectors and consequently slowing down the solution convergence.

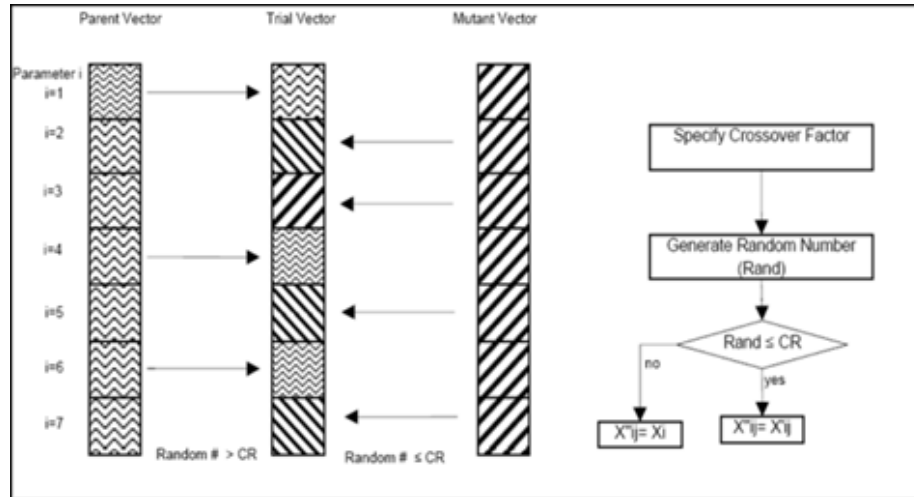


Figure 5.2: Crossover Procedures.

5.2.5. Selection

The final step toward generation of a new population is to compare the solutions in old population and their corresponding trial solutions and then select the best one. To accomplish this, the objective function value corresponding to each trial solution is calculated and compared with the value of the parent. If the new solution performs better, it will replace the parent, otherwise the old solution is retained.

5.2.6. Stopping Criteria

Once, a new generation is produced, the problem updates the global bestminmia. The user defined criteria would also be checked. In most of the cases, a maximum number of iterations is defined and selected as stopping criteria. In practice, the user can check the results and verify the change and can determine when to stop. Figure 5.2 shows a flow chart summarizing the procedure of DE as explained above.

5.3. Objective Function Optimization

As mentioned in Chapter 4, this method will replace the Least Mean Square method as an optimizer in the new proposed method, whereas the loop error will be used as the

objective function. Since the process variable is oscillating the error will oscillate too, so if the optimizer succeeds in minimization of this oscillation amplitude in the error that mean the process variable already has reduced its amplitude.

From above discussion we noticed that the maximum amplitude can be used as an objective function. However, due to noise in real industry this objective function may lead to wrong result. Thus, more robust and smooth objective function such as Integral square Error is used.

$$ISE = \frac{1}{T_2 - T_1} \int_{T_1}^{T_2} e(t)^2 dt \quad (5.6)$$

5.3.1. Control Elements Range

The lower and upper bound for each parameter should be defined, for example for the proposed method with four (4) length FIR filter, all weights were optimized between [-2,2].

5.3.2. Optimization Parameters

For all optimization processes carried out in this thesis, the following optimization parameters are adopted.

- Population size(Np=20)
- Generation Size(Ng=10)
- Crossover Factor(CR=0.5)
- Mutation Factor(F=0.5)

CHAPTER 6

Results and Discussion

6.1. Overview

In this chapter the PID controller was tuned by DE algorithm, then a new proposed method was designed and tested with various scenarios, finally a comparison with the other methods was held based on simulation and experimental results.

6.2. PI retuning with DE Algorithm

Firstly, as a step toward the design of the adaptive inverse control filter (DEFIR), the performance of the DE algorithm is questioned by studying the effect of PID retuning by using different stiction models. The result depend mainly on the stiction patterns and the range in which PID controller parameters can be changed.

Choudhury[42]recommended to retune the controller to compact stiction,his recommendations include increasing the proportional gain, reducing the integral gain and

using some of the derivative gain if required. Thus, from these recommendations the final result for the retuning process can be expected and if the DE algorithm succeeds to reach this result, it can be concluded that the DE is suitable for such nonlinear optimization.

A configuration, shown in Figure 6.1, was implemented in Matlab, Simulink to simulate a closed loop with a sticky valve. Choudhury and Karnopp models were used to create the stiction behavior.

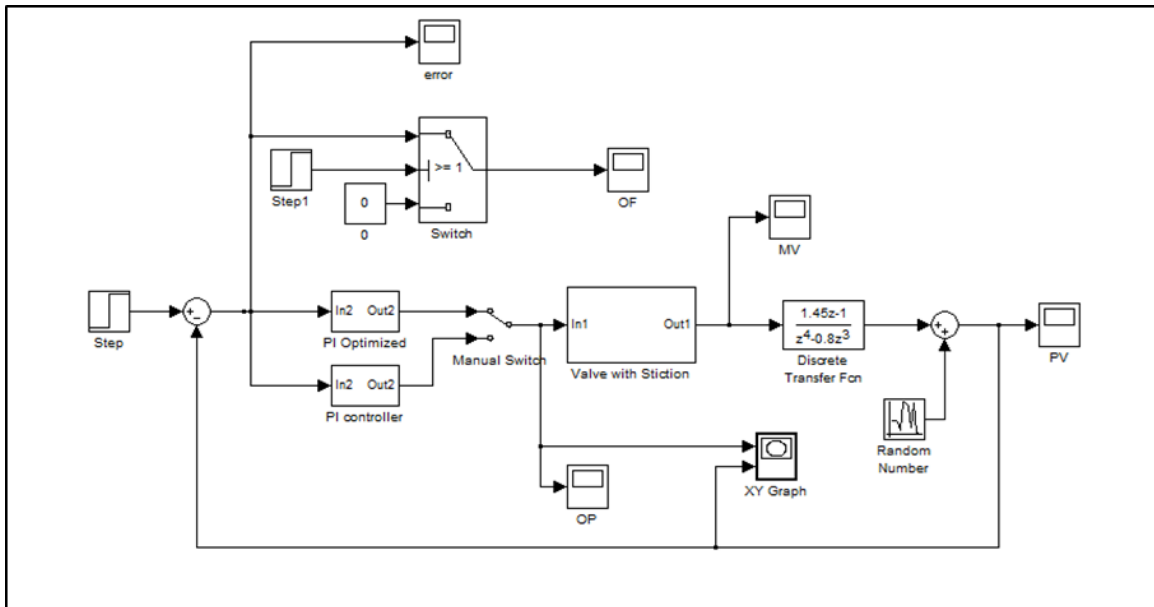


Figure 6.1: Simulink configurations for PID retuning.

6.2.1. PI retuning with DE algorithm (Choudhury Model)

In this section Choudhury model was used with the following stiction patterns: $S=10$ $J=5$, which is an undershoot case. The plant transfer function and original PID parameters were taken from [43].

The following tables and figures show the optimization range, original, and optimized PID parameters with different DE algorithm settings and their associated process variables and control signal, respectively.

PI parameter	Optimizations range Minimum value	Optimizations range Maximum value
K_p	0.001	0.3
K_I	0.05	0.1

Table 6.1: PI parameters tuning range (Choudhury Model).

PI parameters	K_p	K_I
Original	0.15	0.1
Optimized with DE Algorithm		
Population size=10 Generation number=0	0.1899	0.0639
Population size=20 Generation number=5	0.2448	0.05
Population size=20 Generation number=10	0.3	0.05

Table 6.2: Effects of optimization parameters on tuning PI parameters (Choudhury Model).

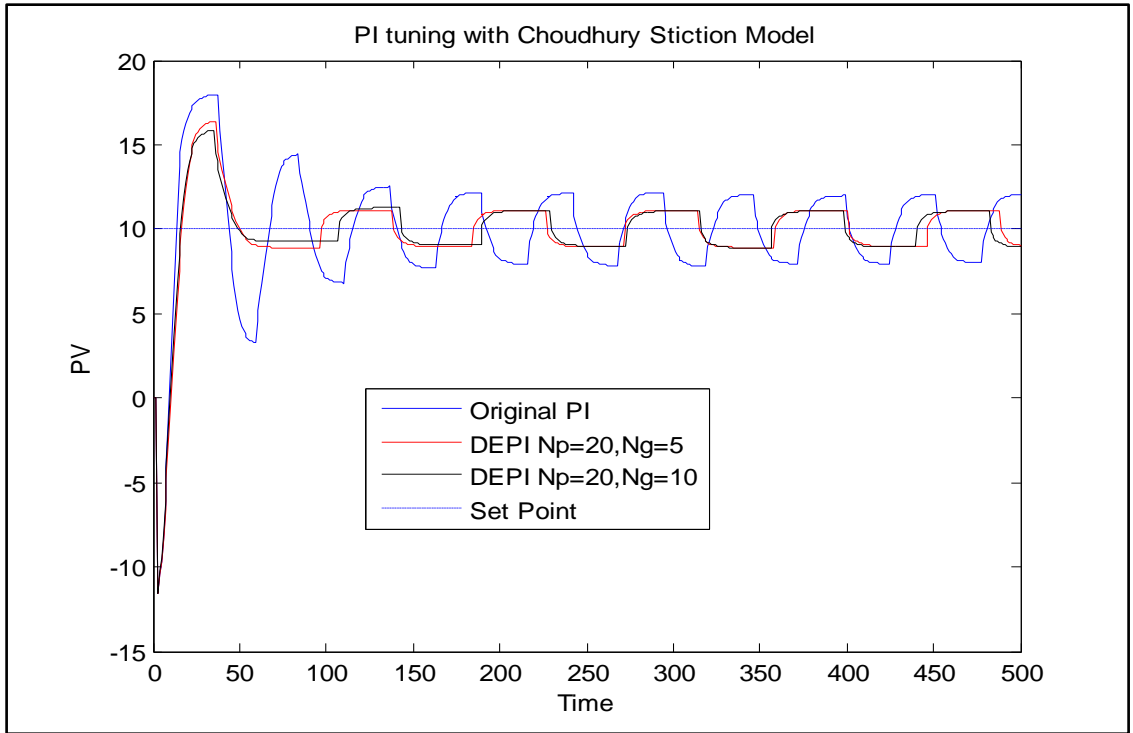


Figure 6.2: Process variable for PI tuning with DE algorithm and Choudhury stiction Model.

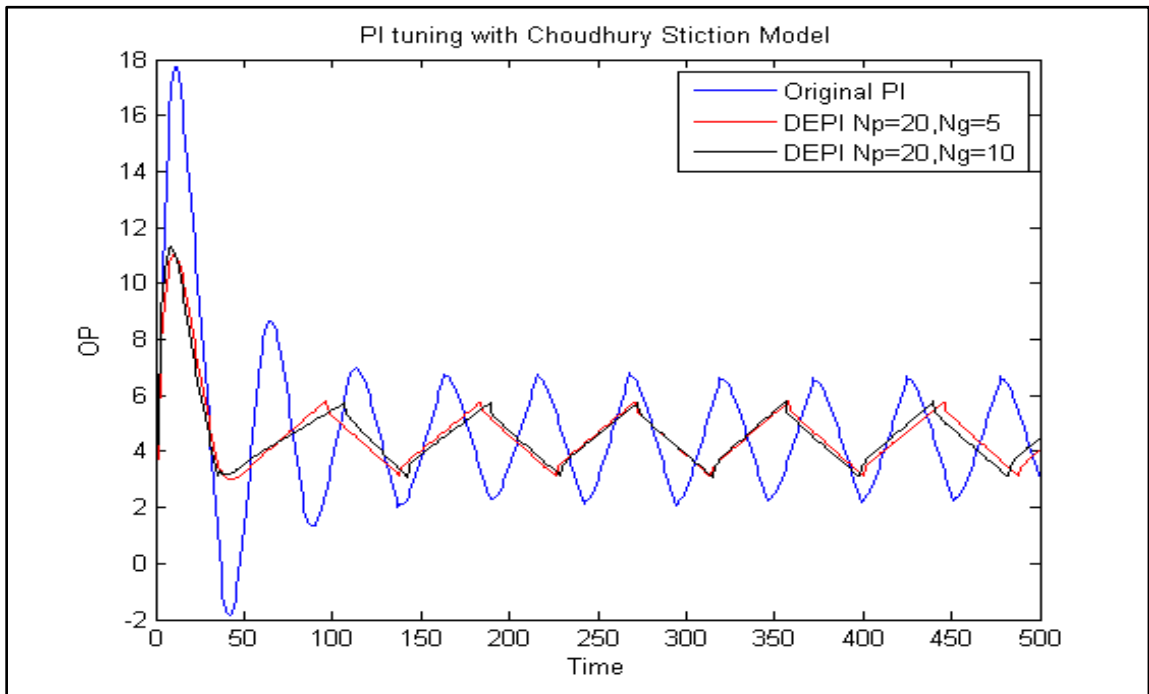


Figure 6.3: Control signal for PI tuning with DE algorithm and Choudhury stiction Model.

As seen from Figure 6.2, the optimized PID controller reduced stiction oscillation amplitude, and the new obtained gains for the controller are consistence with Choudhury recommendation [42].

6.2.2. PI tuning with DE algorithm (Karnopp Model):

Karnopp model is used here and all the valve parameters were taken from [44] except $F_c=300$ and $F_s=200$, which are arbitrarily tuned to get suitable stiction.

As in above section the following tables and figures summarize these results.

PI parameter	Optimizations range Minimum value	Optimizations range Maximum value
K_p	0	10
K_I	0.1	5

Table 6.3:PI parameters tuning range (Karnopp Model).

PI parameters	K_p	K_I
Original	1	0.6
Optimized with DE Algorithm		
Population size=10 generation number=0	8.27	1.76
Population size=20 generation number=10	10	0.7

Table 6.4: Effects of optimization parameters on tuning PI tparameters (Karnopp Model).

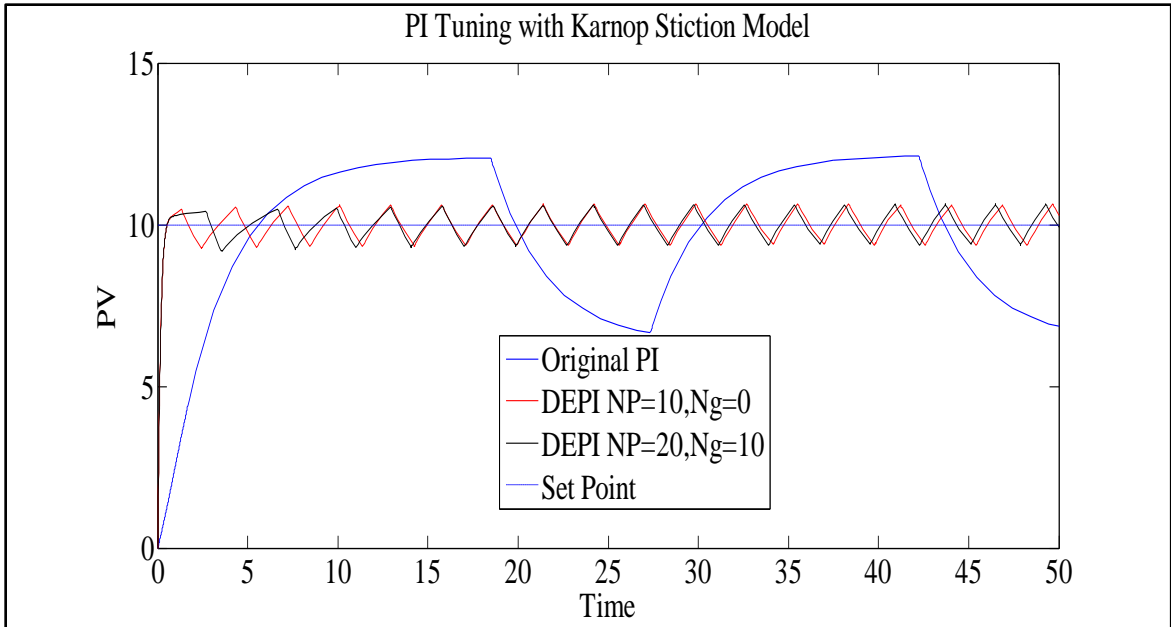


Figure 6.4: Process variable for PI tuning with DE algorithm and Karnopp stiction model.

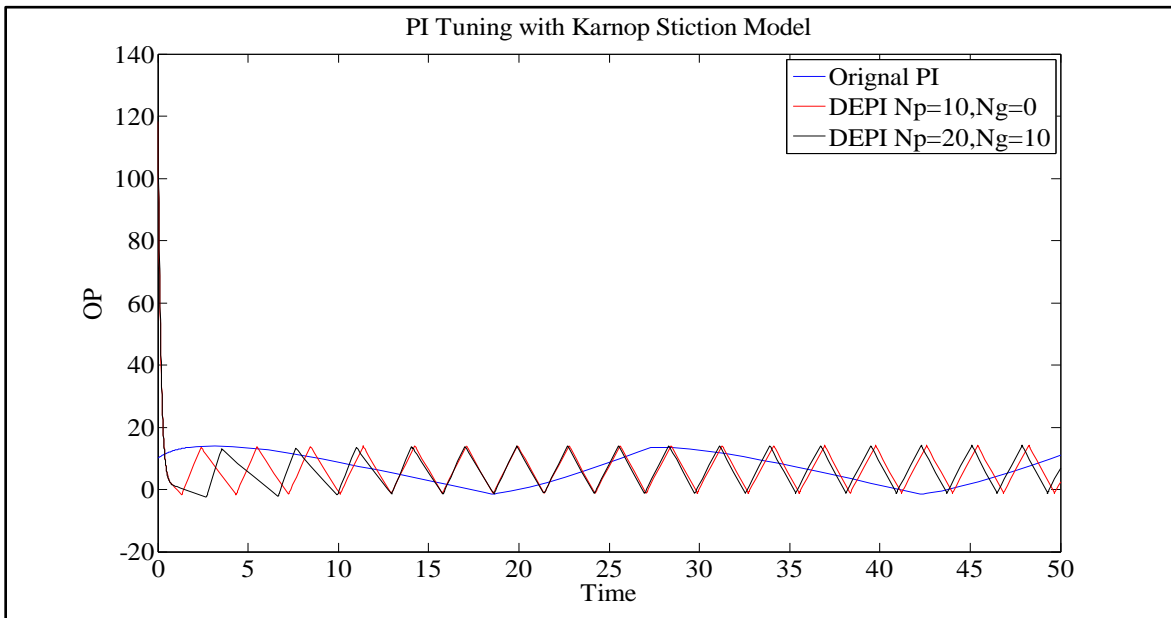


Figure 6.5: Control signal for PI tuning with DE algorithm and Karnopp stiction model.

6.3. FIR filter optimized with DE algorithm (Proposed method)

The optimized FIR filter with DE or DEFIR as short that introduced in Section 4.6 was tested here with various DE settings and scenarios, these settings are:

Stiction Behavior:

Model:Choudhury Model

Stiction patterns: $S=5, J=2$ (Undershoot case)

Filter parameters:

Filter length=4

Filter weights optimization range: [+5,-5], [+2,-2].

DE algorithm settings:

Population Size=20, 30

Generation number=10, 20

Objective function: ISE of ($OP-MV$) and ($SP-PV$)

The following table and figures demonstrate the final results for these scenarios.

DE optimization Settings	FIR weights			
	W_1	W_2	W_3	W_4
Population size=20 Generation number=10 Objective function =ISE ($OP-MV$) Weights range [+5, -5]	1.826	1.789	1.257	-3.976
Population size=30 Generation number=20 Objective function = ISE ($OP-MV$) Weights range [+5, -5]	2.136	3.6377	-2.726	-2.054
Population size=20 Generation number=10 Objective function = ISE ($OP-MV$) Weights range [+2, -2]	1.9728	1.3133	-1.528	-0.7359

Population size=20				
Generation number=10				
Objective function = ISE (<i>SP-MV</i>)	1.9782	-1.985	-0.0318	0.1645
Weights range [+2, -2]				

Table 6.5: FIR filter weights with different optimization parameters.

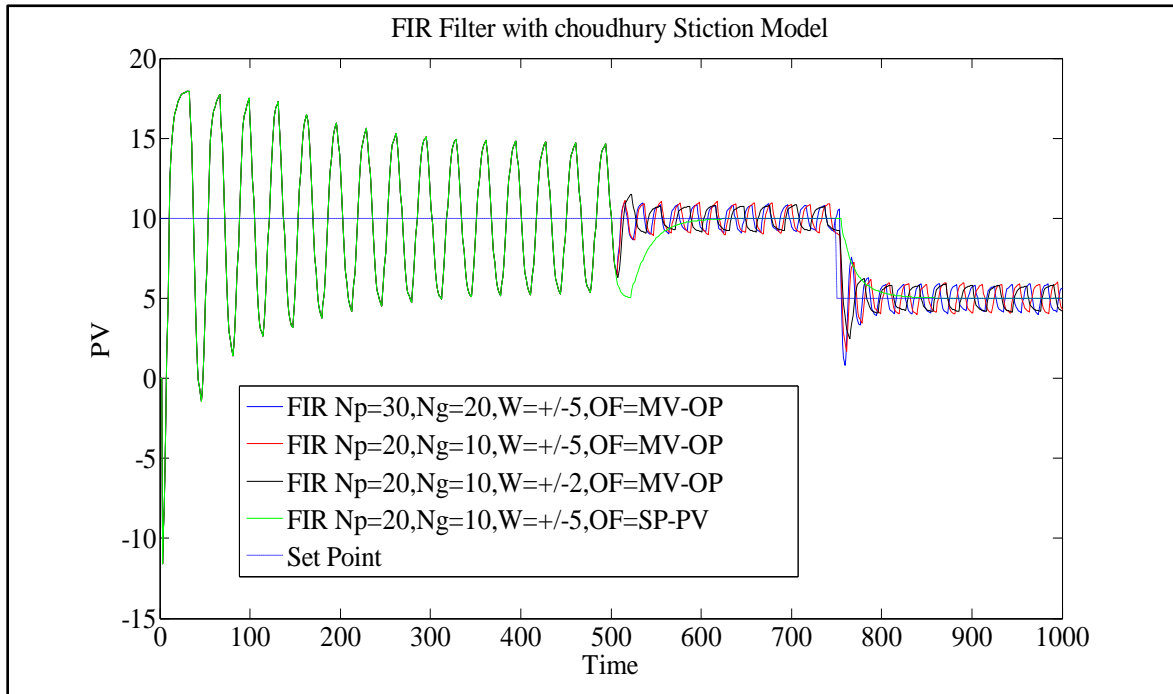


Figure 6.6: Process variable for FIR filter tuned with DE algorithm.

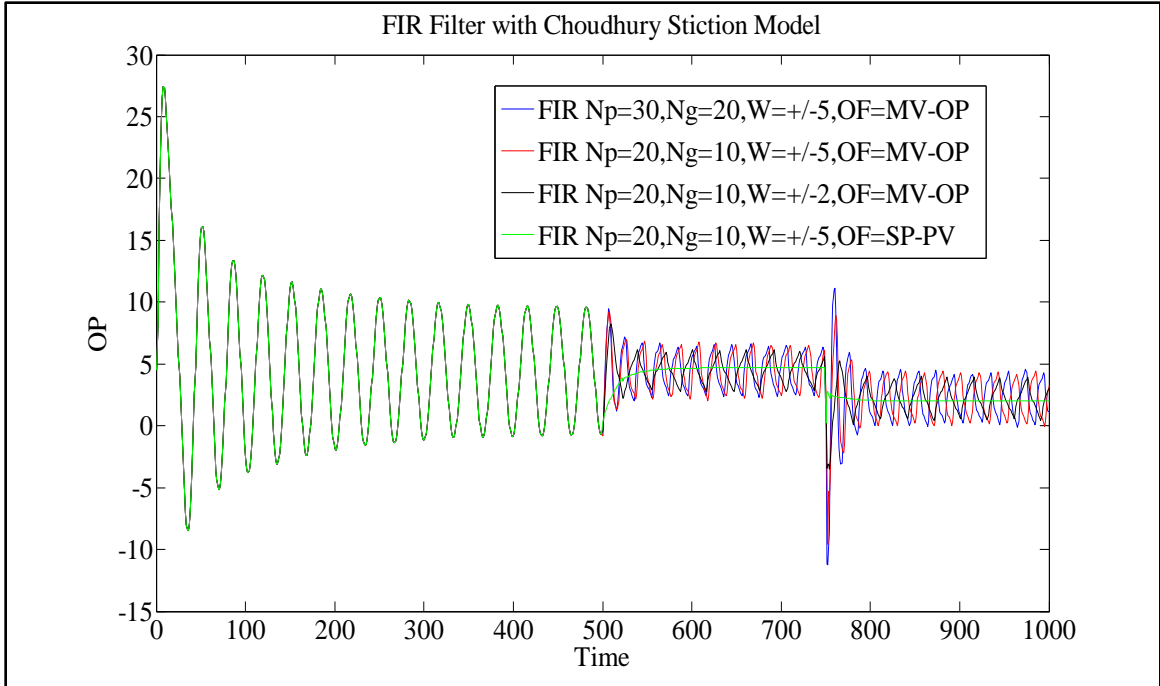


Figure 6.7: Control signal for FIR filter tuned with DE algorithm.

The proposed method was switched at 500 seconds and set-point change was applied at 750 seconds, the method succeeded in reducing the process output variability, especially when the loop error (SP-PV) was taken as objective function (green line), it has the ability to remove all the stiction behavior from the process output, this is due to the smoothness of the objective function which is not the case with the (MV-OP) fitness function. However the valve stem position (MV) information is not available in most cases. The thing that makes the choice of loop error (SP-PV) as fitness function is more preferable.

Also the ability of the proposed method was tested against disturbance such as set-point changes and it showed outstanding disturbance tracking ability.

6.4. Study of Compensation Methods(Simulation)

In this section six compensation methods including Sabih modified version and the proposed method were studied with different stiction models and different stiction scenarios.

The study is divided into two parts, simulation part using Matlab/Simulink and experimental part using level control loop prepared especially for this study. The simulation part was carried out using three various stiction models: Two layer model, Kano model and Choudhury model. Each model was tested in the four stiction cases or scenarios, pure deadband,undershoot,no offset, and overshoot. Table 6.6 shows these cases.

Stiction Scenario	Kano & Choudhury Models		Two Layer Model	
	S	J	f_s	f_D
Dead band	3	0	1.5	1.5
Undershoot	3	1.5	2.25	0.75
No offset	3	3	3	0
Overshoot	3	4.5	3.75	-0.75

Table 6.6: Equivalent stiction scenario's in the three models.

Note that all the scenarios were equivalent since $S=f_s+f_D$ and $J=f_s-f_D$.

The methods were covered in this study were:

- a. Knocker method.
- b. Dithering (pulses).
- c. Constant Reinforcement (CR).
- d. Approximate Inverse Compensation.
- e. Adaptive Inverse Control (AIC) :
 1. FIR Filter optimized with LMS.
 2. FIR Filter optimized with a DE algorithm (proposed method).

Note that all the first four compensation methods were optimized by DE too, although they should have been tuned manually or integrated with stiction severity quantification as in case of the approximate inverse method. This optimization process was done to reduce the process output variability to a minimum so that the results obtained from these methods would be on their optimum cases, thus resulting in fair comparison conditions among them. The DE optimization algorithm was run with the following parameters: Population size=20, Generation Number=10, Mutation factor=0.5, Crossover factor=0.5.

6.4.1. Knocker Method

The Knocker compensator given in Section 4.1 with configuration in Figure 6.8 was implemented in Matlab/Simulink with knocker compensator was activated at 200seconds, with knocker optimized parameters given in Table 6.8. The process variables, control signals, and stem positions for the three models are illustrated in Figures 6.9, 6.10 and 6.11, respectively.

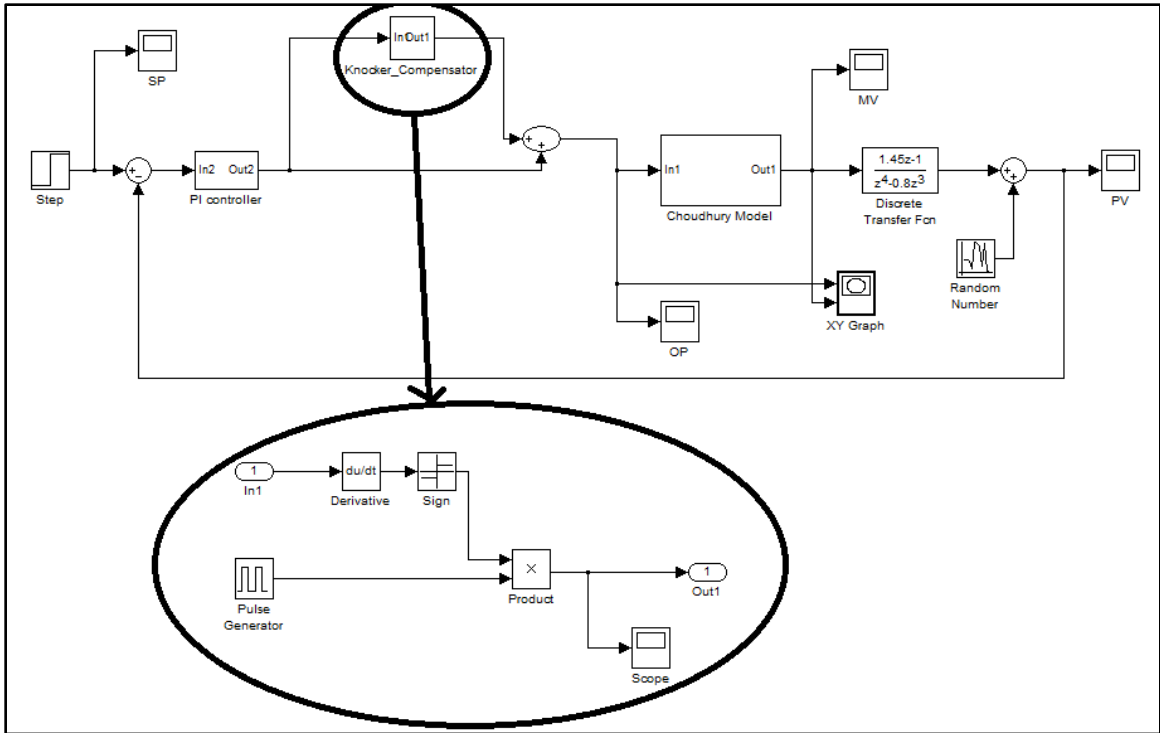


Figure 6.8: Simulink blocks for Knocker Compensator.

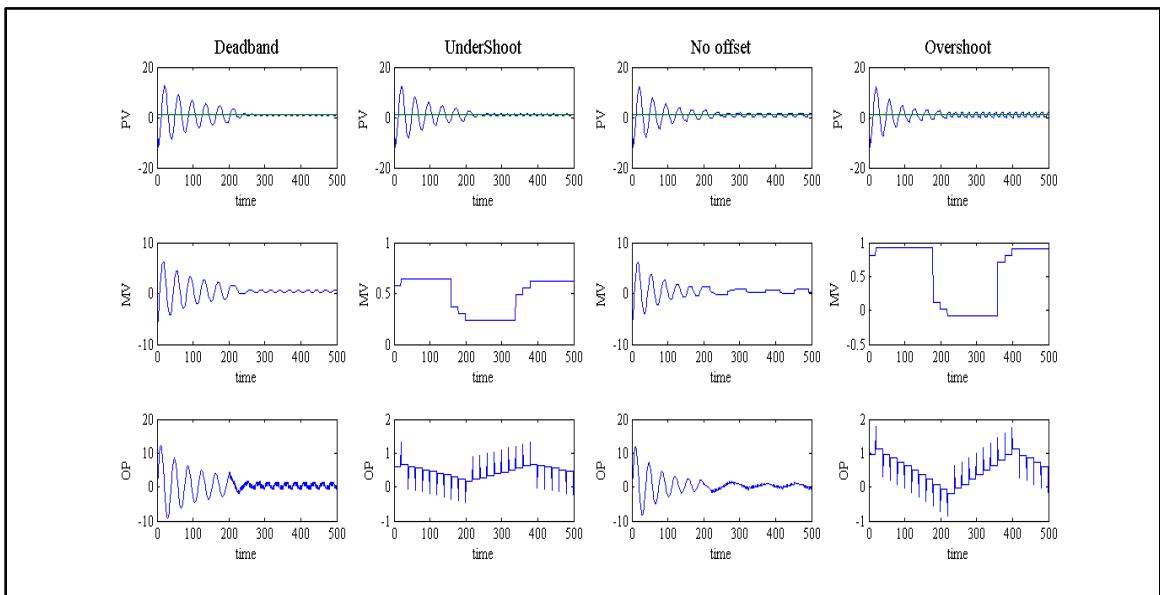


Figure 6.9: Knocker Compensator with Choudhury Model.

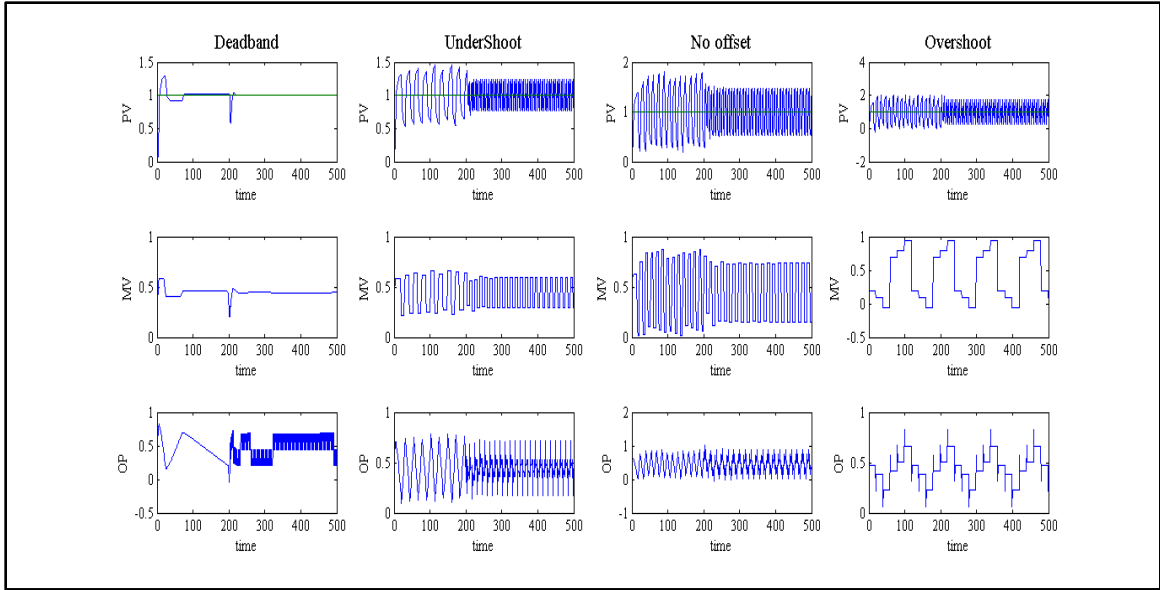


Figure 6.10: Knocker Compensator with Kano Model.

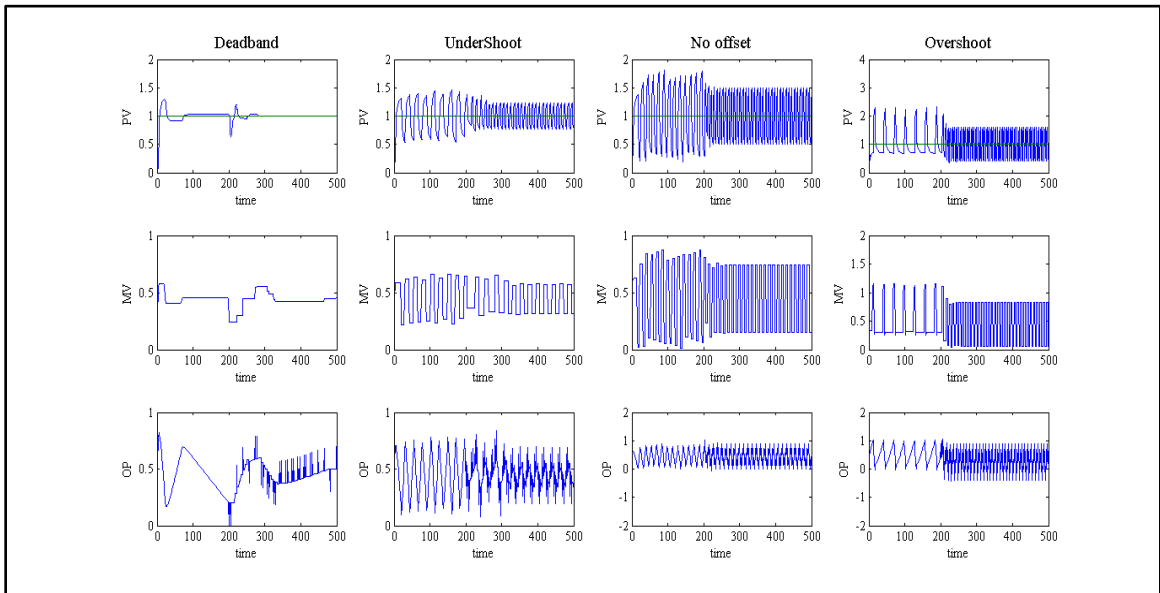


Figure 6.11: Knocker Compensator with Two Layer Model.

<i>Knocker Parameters</i>	Optimization Range	
	Min	Max
a	0	1
T	$25\%h_K$	$75\%h_K$
$h_k(sec)$	0.1	2

Table 6.7: Knocker Optimization Range.

<i>Knocker Parameters</i>	Choudhury Model			
	Dead band	Undershoot	No offset	Overshoot
<i>a</i>	0.89	0.65	0.4	0.65
<i>T</i>	1.34	0.075	0.75	0.075
<i>h_k(sec)</i>	2	0.1	1	0.1
	Kano Model			
<i>a</i>	0.24	0.26	0.25	0.16
<i>T</i>	1.12	0.62	0.7	0.052
<i>h_k(sec)</i>	2	1.5	2	0.1
	Two Layer Model			
<i>a</i>	0.2	0.22	0.25	0.49
<i>T</i>	0.24	0.87	0.63	0.96
<i>h_k(sec)</i>	0.43	1.67	2	2

Table 6.8:Knocker Optimized Parameters.

6.4.2. Dithering Method

The original dithering signal is a high frequency signal with zero mean. The dither signal can be generated with any signal generator. In this section pulse shape signal with amplitude A_m and frequency f is used.

A configuration similar to knocker was implemented with pulse signal generator replacing the knocker compensator. Tables 6.9 and 6.10 illustrated the optimization part and Figures 6.12, 6.13 and 6.14 illustrated the simulation responses to the optimized dithering signal.

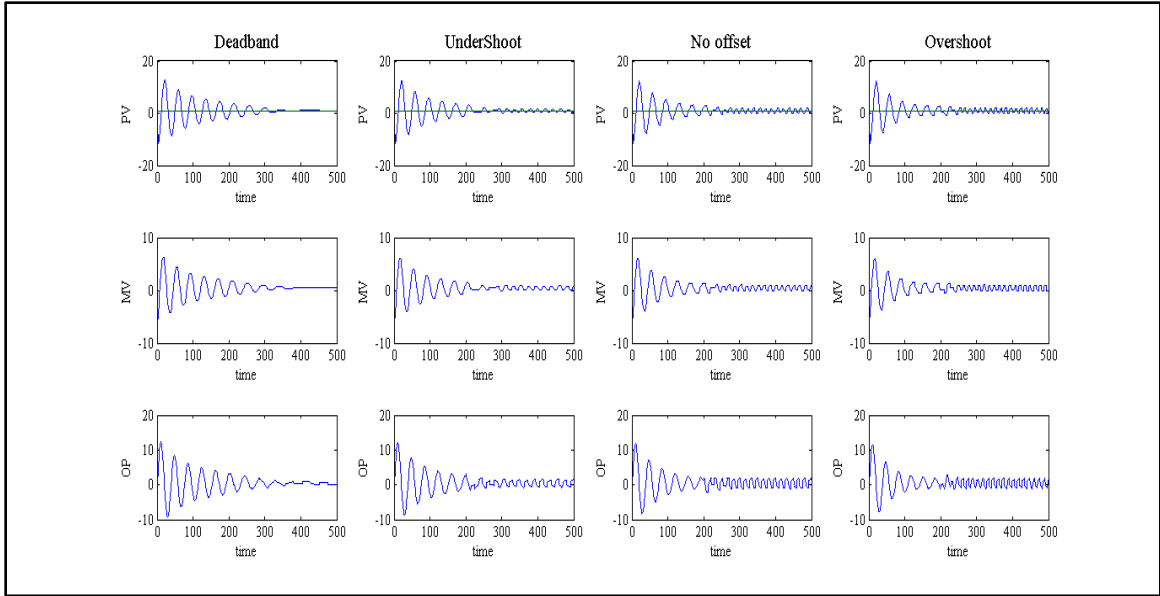


Figure 6.12: Dither Compensator with Choudhury Model.

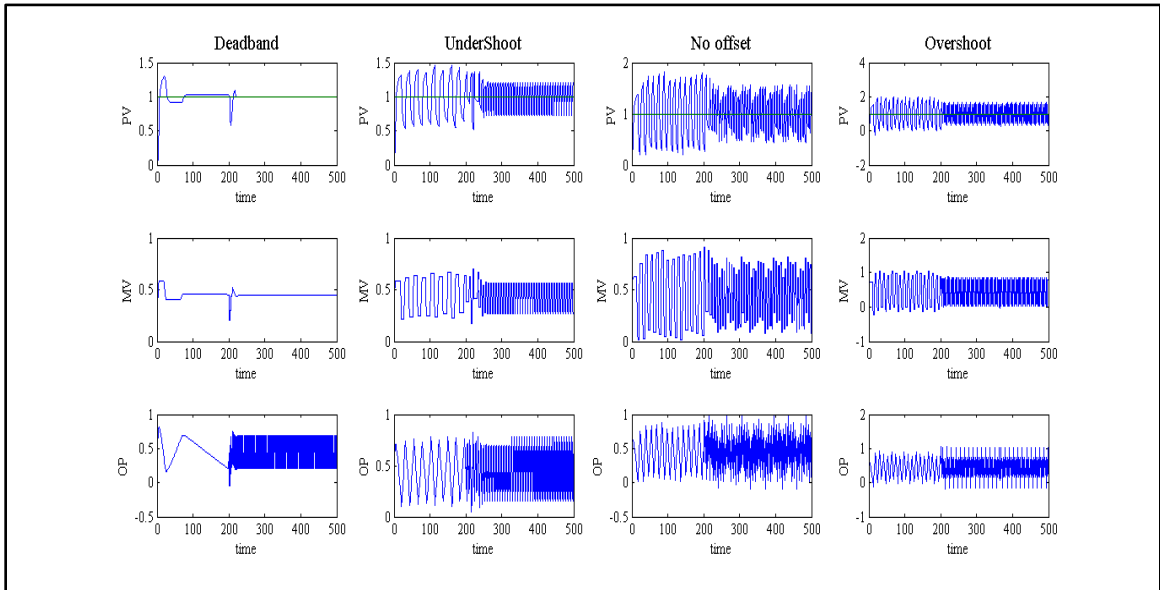


Figure 6.13: Dither Compensator with Kano Model.

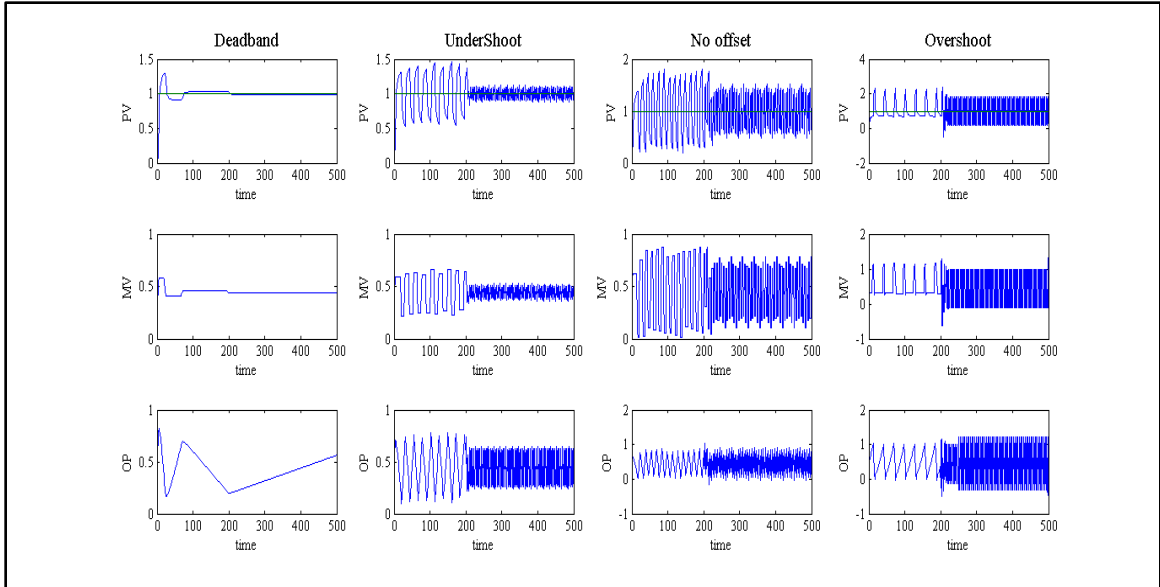


Figure 6.14: Dither Compensator with Two Layer Model.

Dither Parameters	Optimization Range	
	Min	Max
A_m	0	1
$f sec^{-1}$	0.01	1

Table 6.9: Dithering Optimization Range.

Dither Parameters	Choudhury Model			
	Dead band	Undershoot	No offset	Overshoot
A_m	0.28	0.674	0.976	0.944
$f sec^{-1}$	0.021	0.953	0.94	0.93
	Kano Model			
A_m	0.24	0.245	0.25	0.33
$f sec^{-1}$	0.45	0.29	0.56	0.42
	Two Layer Model			
A_m	0	0.178	0.257	0.67
$f sec^{-1}$	0.378	0.765	0.47	0.75

Table 6.10: Dithering Optimized Parameters.

6.4.3. Constant Reinforcement Method (CR)

The CR compensator is the simplest compensator from a structural point of view. It consists of constant signal with only one parameter to adjust which is the amplitude of the signal; this amplitude was optimized between 0 and 1, and the associated results are shown in Figures 6.15, 6.16 and 6.17

<i>CR Parameter</i>	Choudhury Model			
	Dead band	Undershoot	No offset	Overshoot
A_m	0.456	0.41	0.696	0.889
	Kano Model			
A_m	0.23	0.21	0.196	0.157
	Two Layer Model			
A_m	0.24	0.12	0.15	0.029

Table 6.11:CR Optimized Parameters.

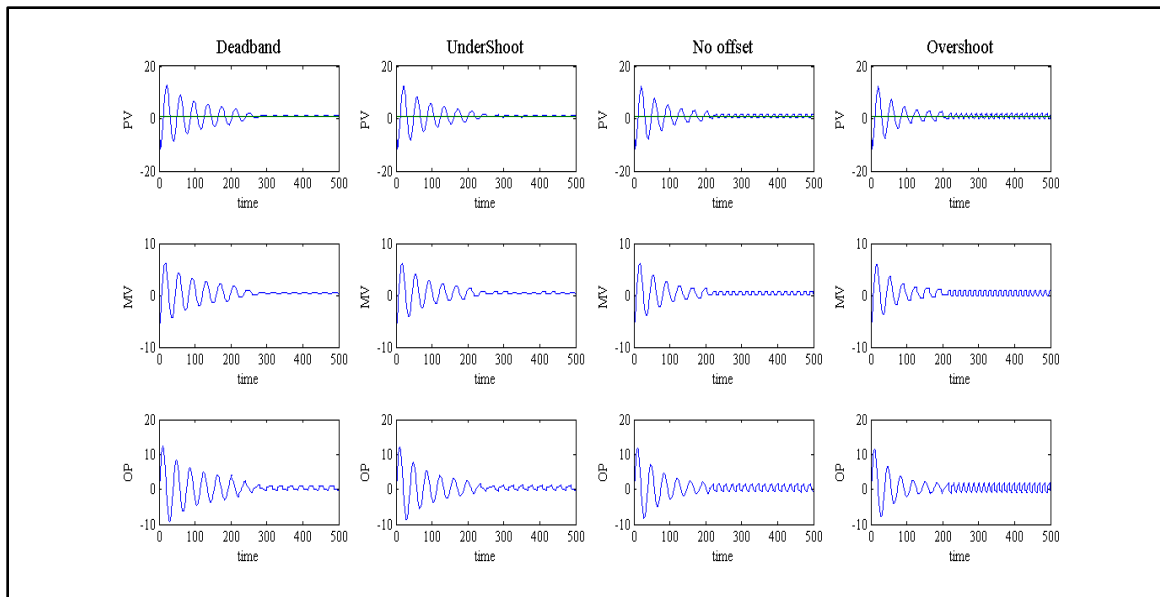


Figure 6.15: CR Compensator with Choudhury Model.

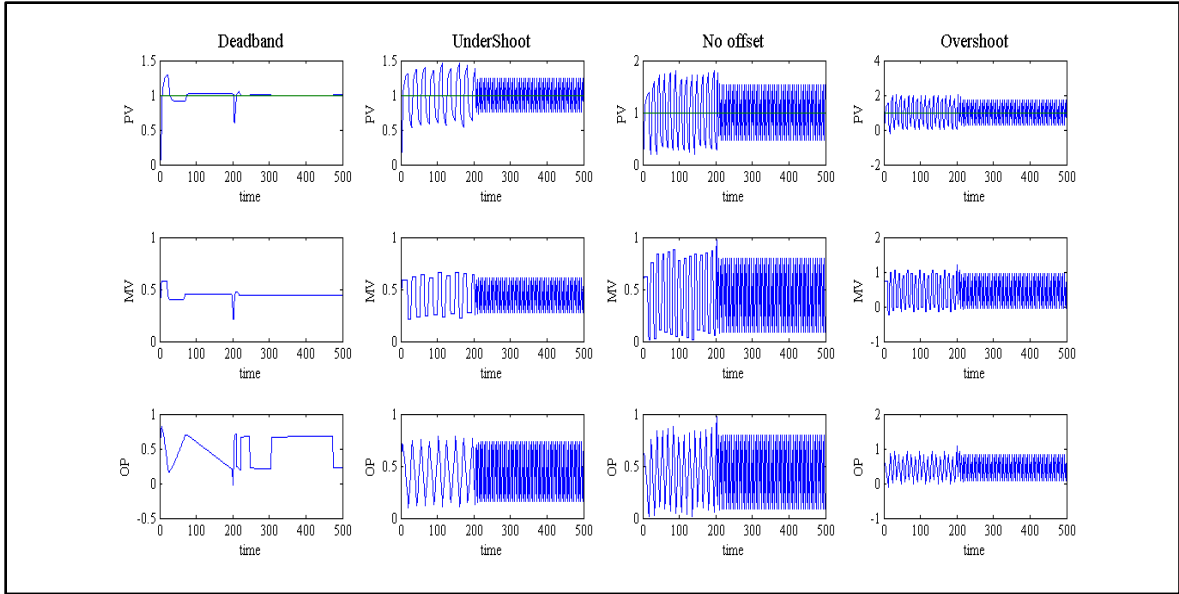


Figure 6.16: CR Compensator with Kano Model.

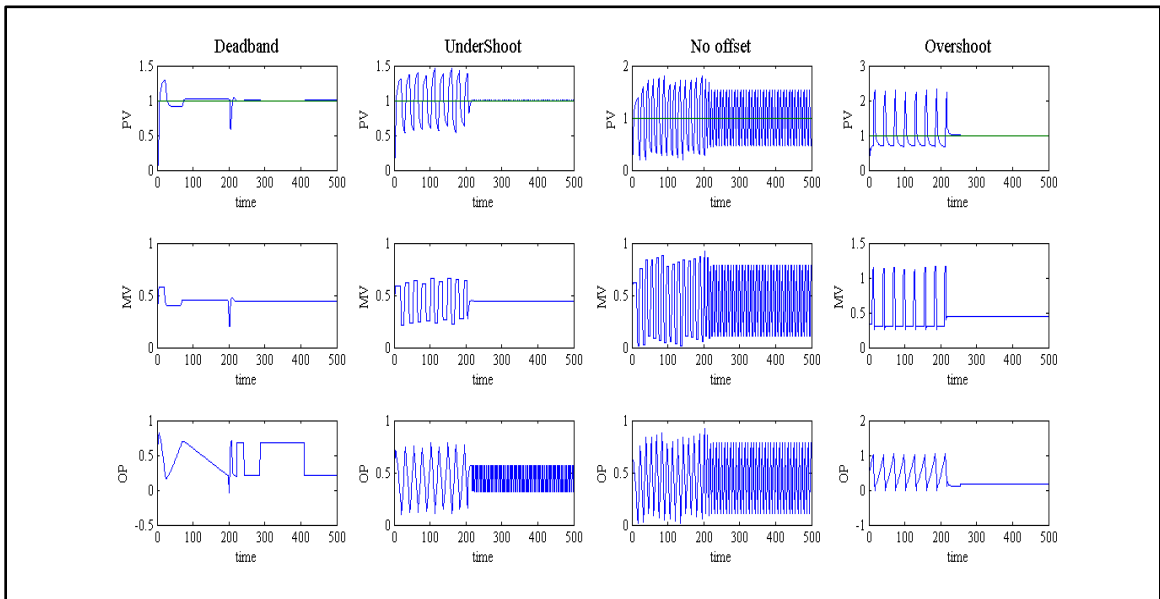


Figure 6.17: CR Compensator with Two Layer Model.

6.4.4. Approximate Inverse Method

Approximate inverse compensator was discussed in Section 4.4. The backlash inverse model was used to compact stiction since there is no exact inverse for stiction model. As

illustrated in Figure 6.18 the inverse model is inserted between the controller and the valve stiction block.

The slope of the inverse model was fixed at 1 and the backlash is symmetric. In fact, the positive and negative crossing edge were equal in magnitude ($d+ = -d-$), thus only one parameter needs to be optimized ($d+$), which was done by DE in the range between 0 and 1. The compensator was activated at 200 seconds, the results are shown in Figures 6.19, 6.20 and 6.21.

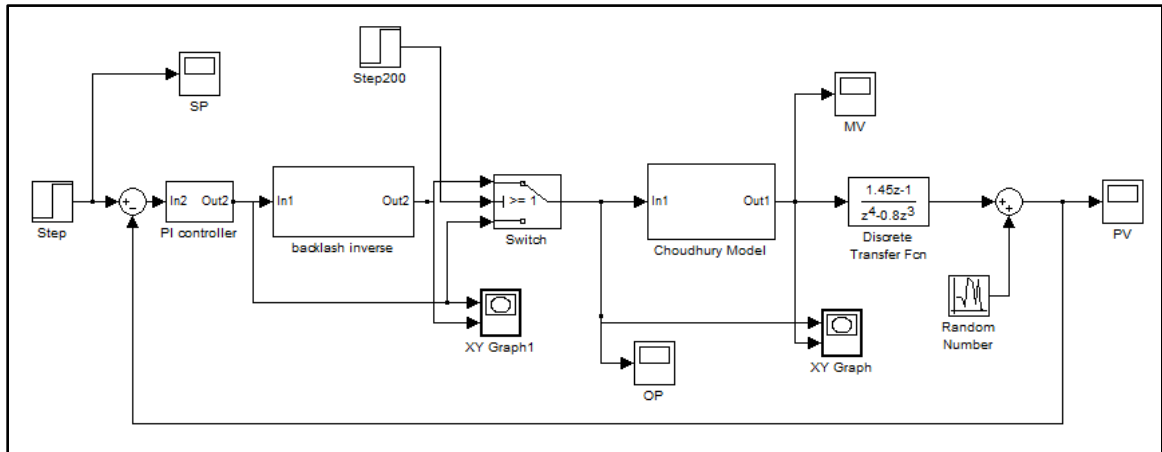


Figure 6.18: Simulink Blocks for Approximate Inverse Compensator.

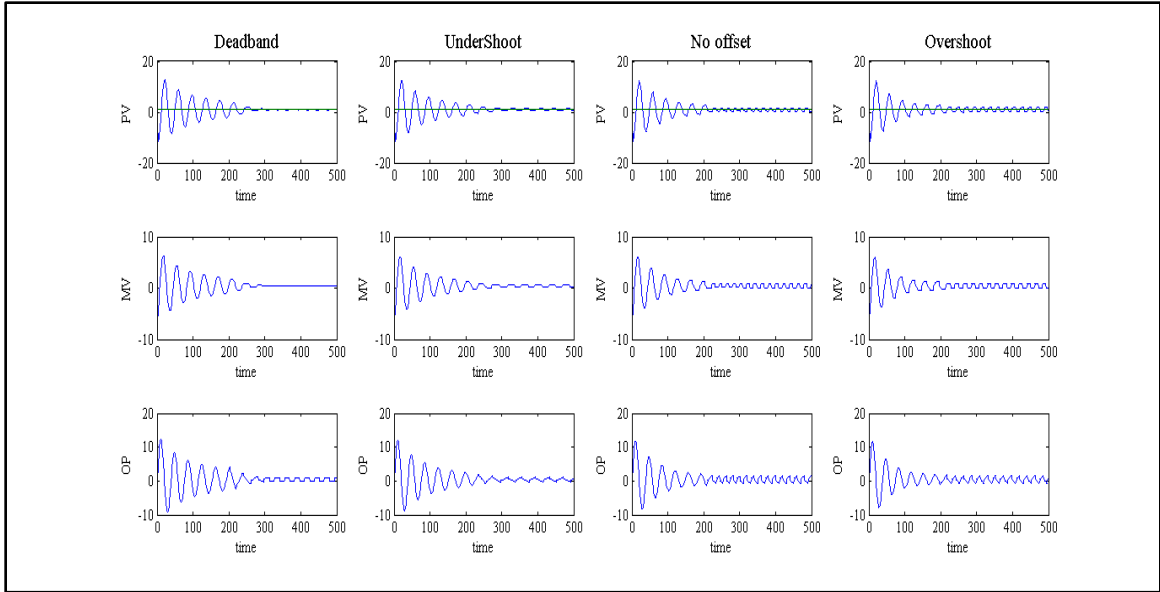


Figure 6.19: Approximate Inverse Compensator with Choudhury Model.

<i>Backlash inverse Parameter</i>	Choudhury Model			
	Dead band	Undershoot	No offset	Overshoot
d_+	2.94	1.45	3.82	2.9
#	Kano Model			
d_+	1.5	1.32	1.19	0.991
#	Two Layer Model			
d_+	1.49	0.773	0.92	1.39

Table 6.12: Approximate inverse Optimized Parameters.

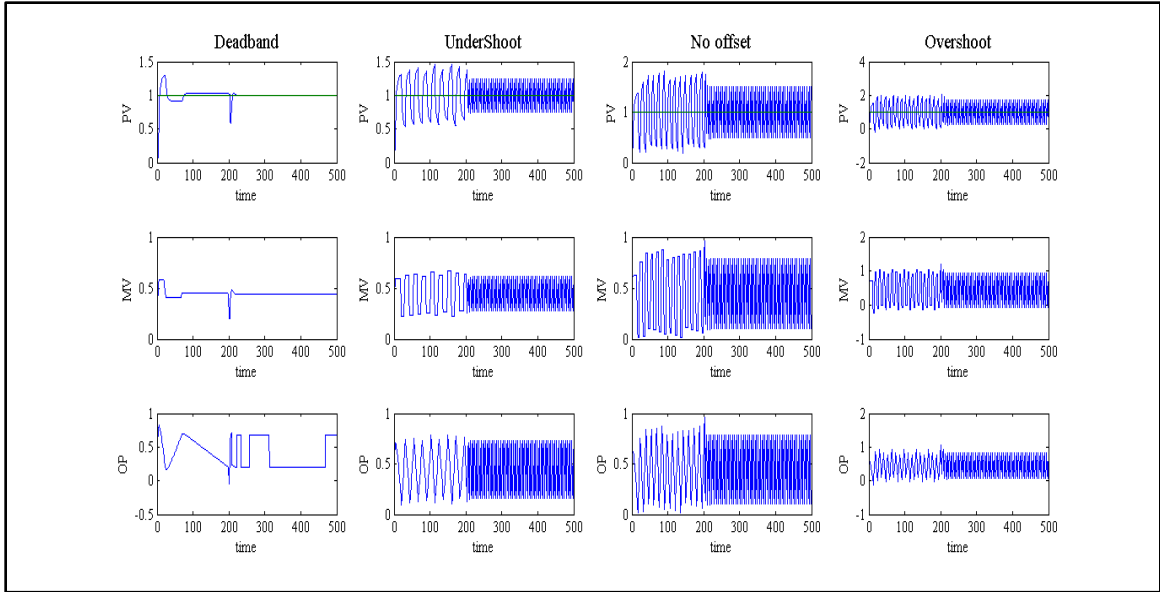


Figure 6.20: Approximate Inverse Compensator with Kano Model.

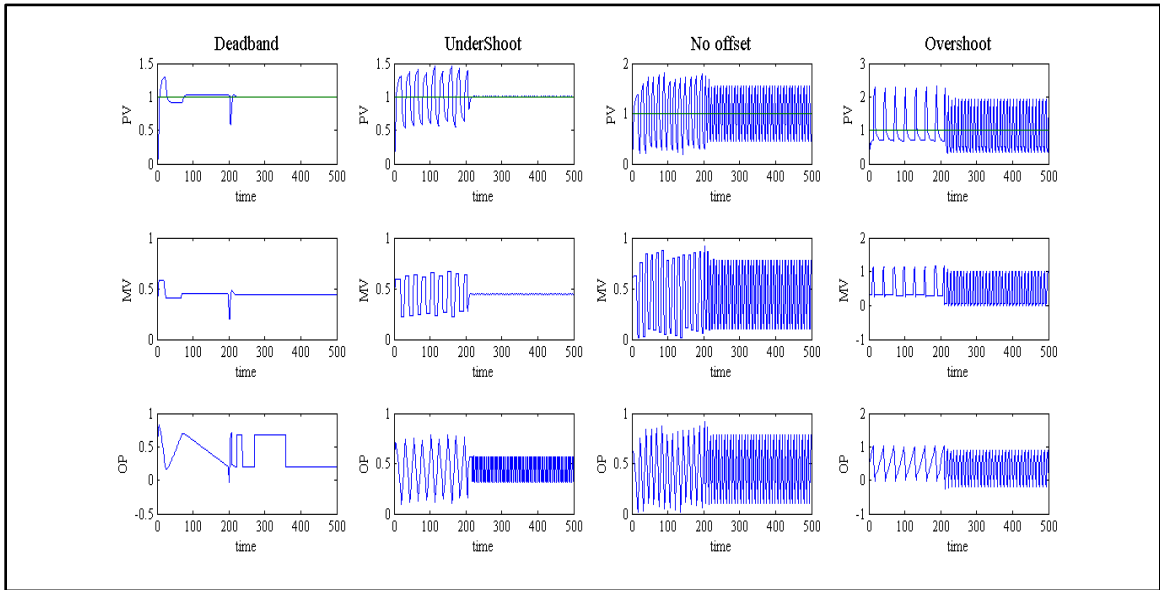


Figure 6.21: Approximate Inverse Compensator with Two Layer Model.

6.4.5. Adaptive Inverse Control Method (LMS-FIR)

A modified version of method introduced by [38] was implemented in this section, the modification on the objective function to be minimize. The loop error ($SP-PV$) has been selected as objective function instead of ($MV-OP$). The new objective function is expected to give better result.

The configuration shown in figure 6.22 was implemented using the normalized least mean square from Simulink signal processing toolbox library. The four length filter was activated at 500 seconds for choudhury model and 200 for the two other models with adaptive LMS tuned with 0.9 leakage factor, 0.01 step size for all cases except the no offset case which used 0.001 instead for convergence purpose.

Figures 6.23, 6.24 and 6.25 showed the PV , OP and MV signals with different models.

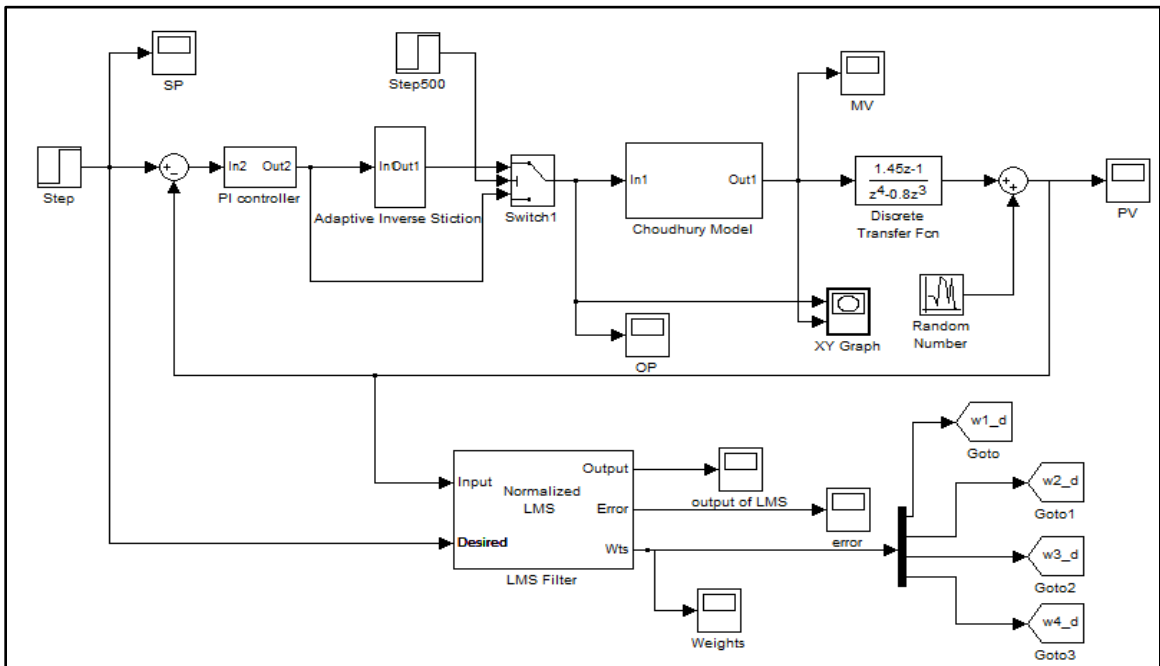


Figure 6.22: Simulink Blocks for LMS-FIR Compensator.

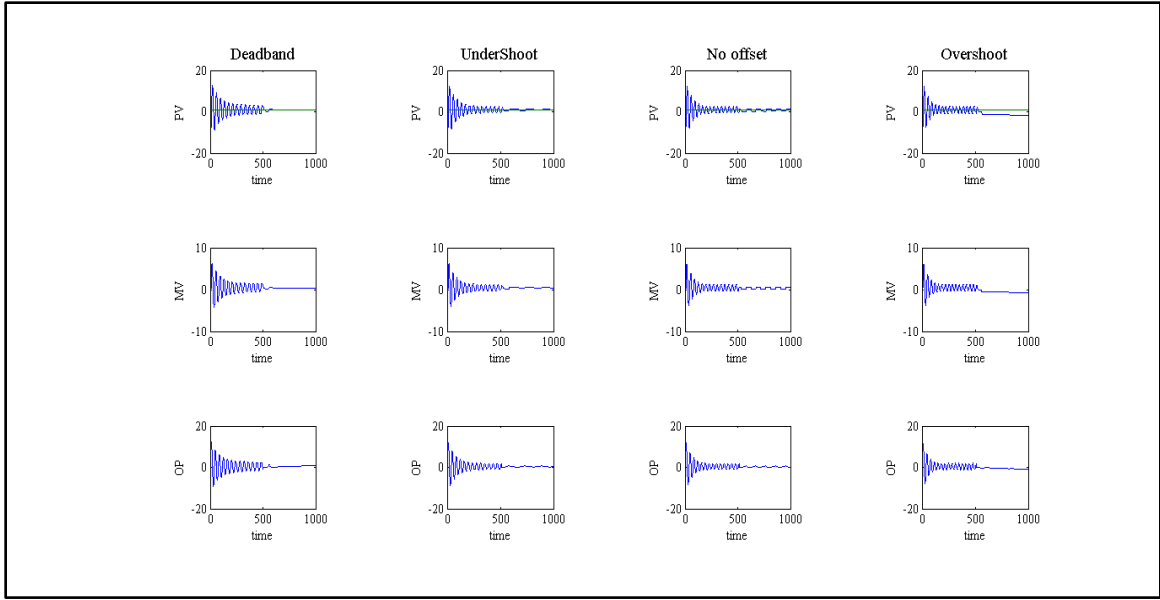


Figure 6.23: LMS-FIR Compensator with Choudhury Model.

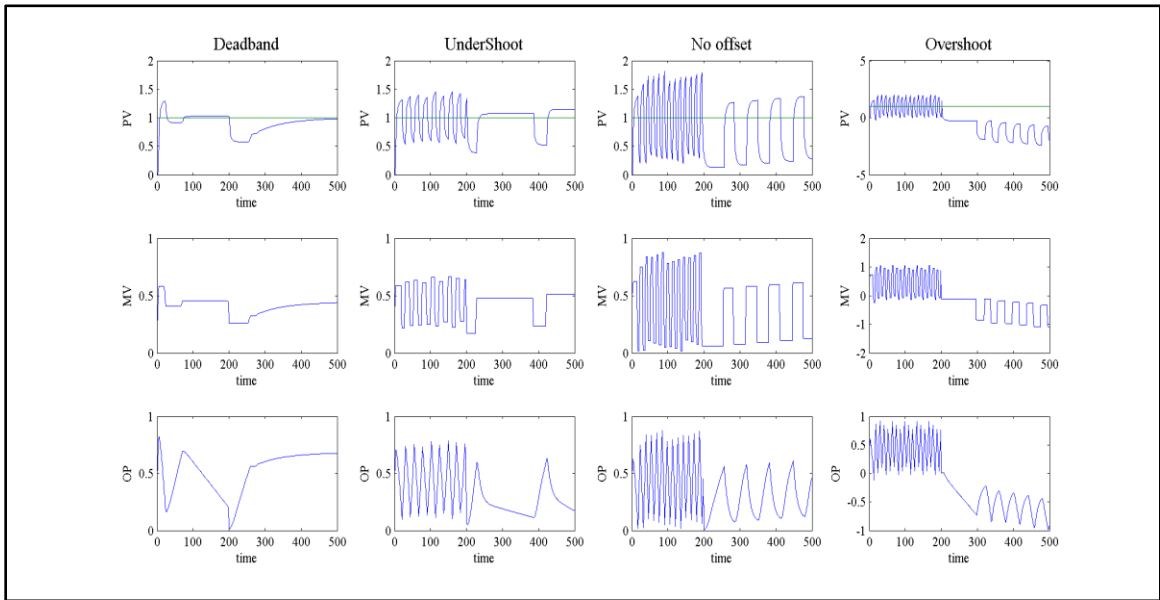


Figure 6.24: LMS-FIR Compensator with Kano Model.

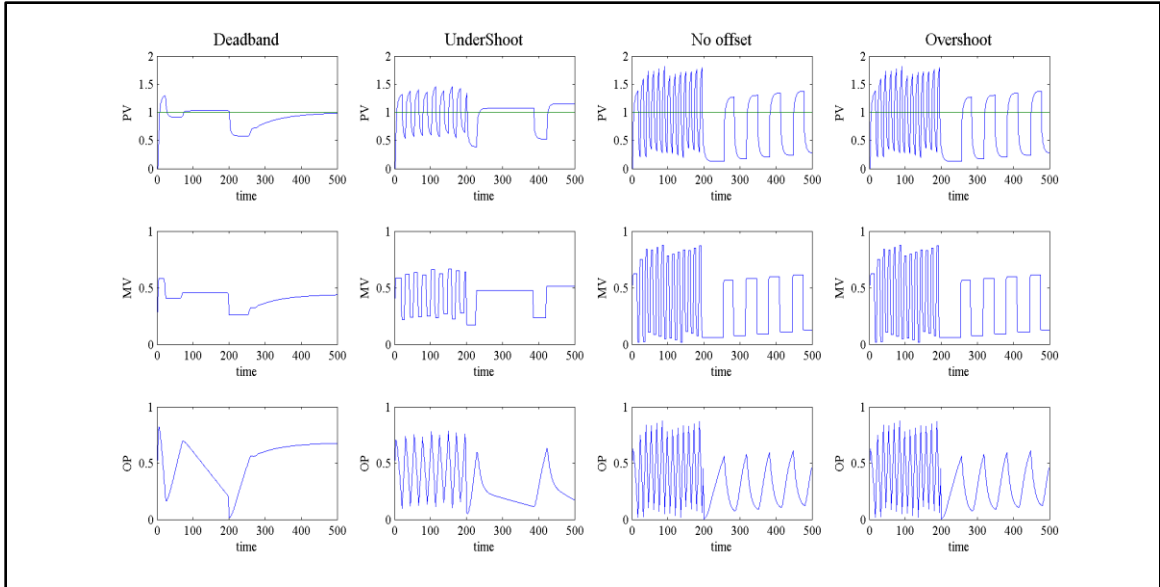


Figure 6.25: LMS-FIR Compensator with Two Layer Model.

The LMS-FIR method failed to compensate the overshoot stiction case in Choudhury and Kano models. However, it disturbed the controller from tracking the set-point and the loop seen as it operated in open loop mode.

The least mean square optimization process was shown in Figures 6.26, 6.27 and 6.28. It is worth mentioning that bad tuning for the LMS algorithm convergence parameters will lead to a situation similar to the pre-mentioned.

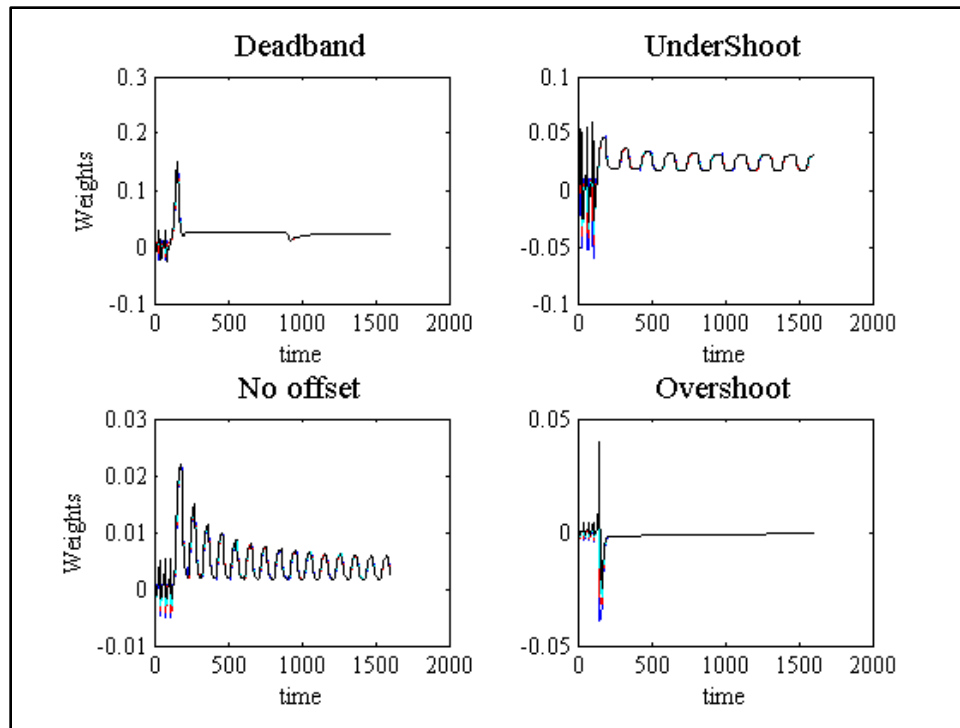


Figure 6.26: LMS-FIR Weights with Choudhury Model.

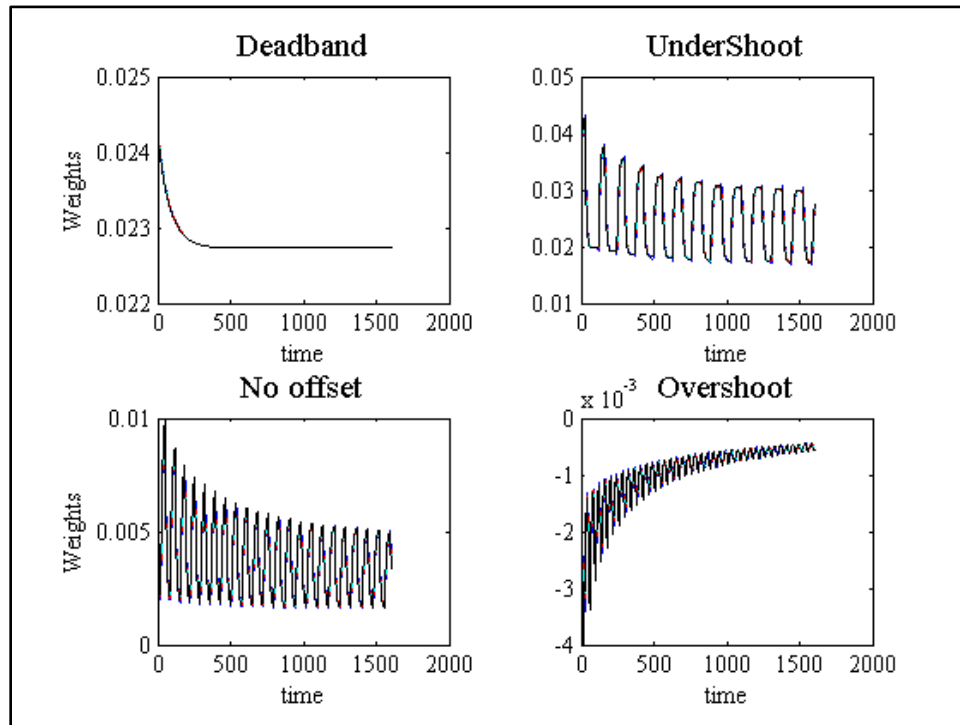


Figure 6.27: LMS-FIR Weights with Kano Model.

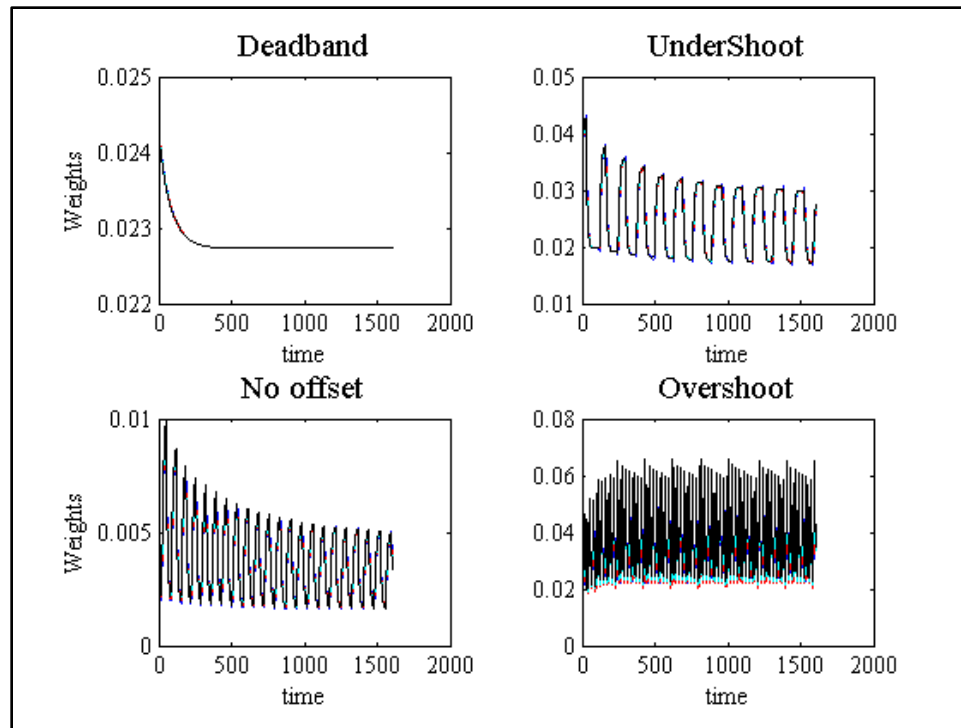


Figure 6.28: LMS-FIR Weights with Two Layer Model.

6.4.6. Adaptive Inverse Control Method (DE-FIR)

The new proposed method was tested using a configuration similar to what implemented for LMS-FIR without the LMS block. The four length weights finite impulse filter was tuned with the DE algorithm in a range between 2 and -2.

The method demonstrated good performance in stiction compensation with less valve stem movements, although there are some abrupt jumps in some cases. However, it is not realistic since the valve stem cannot move that fast in real process.

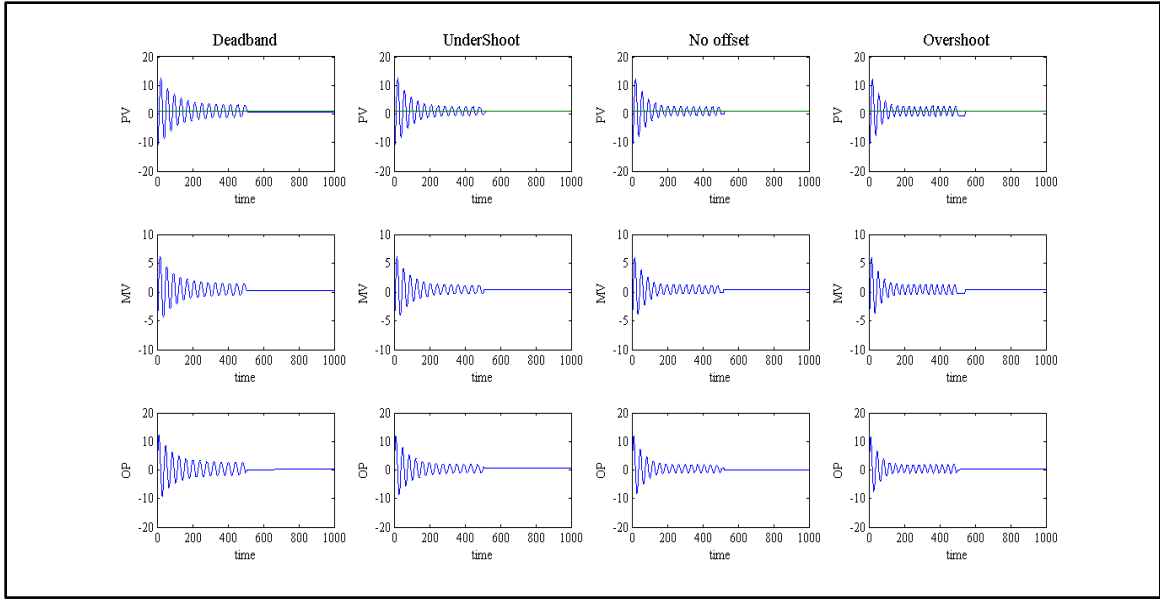


Figure 6.29: DE-FIR Compensator with Choudhury Model.

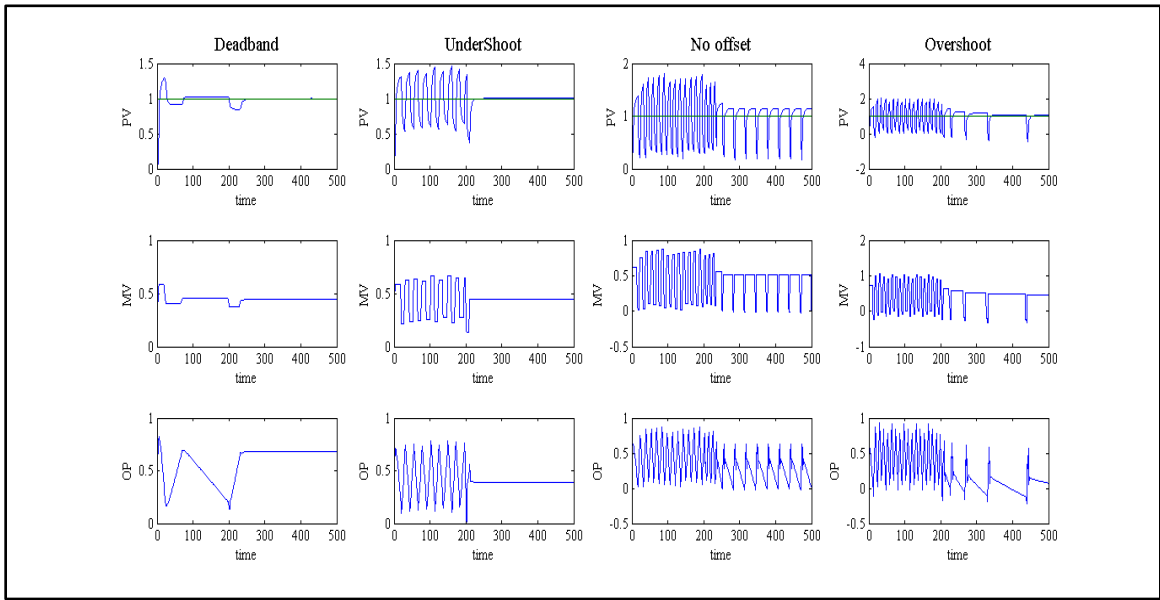


Figure 6.30: DE-FIR Compensator with Kano Model.

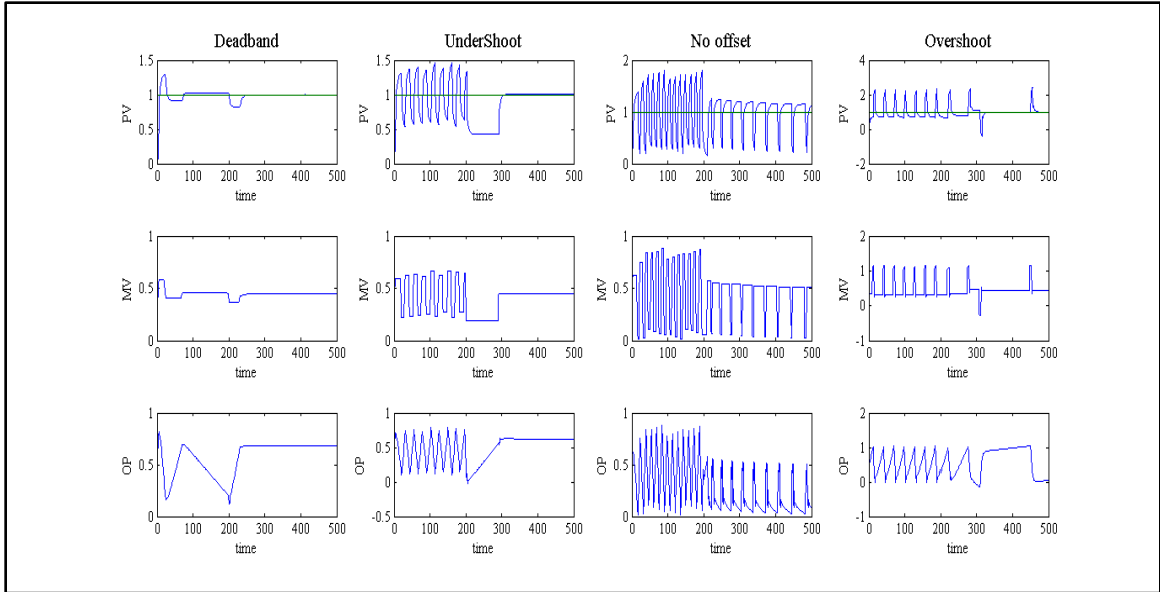


Figure 6.31: DE-FIR Compensator with Two Layer Model.

With the population size set at 20, it has been found that the DE algorithm need 10 iterations or less to reach the optimal solution as depicted in Figures 6.32, 6.33 and 6.34. The filter weights resulted from the optimization process were listed Table 6.13.

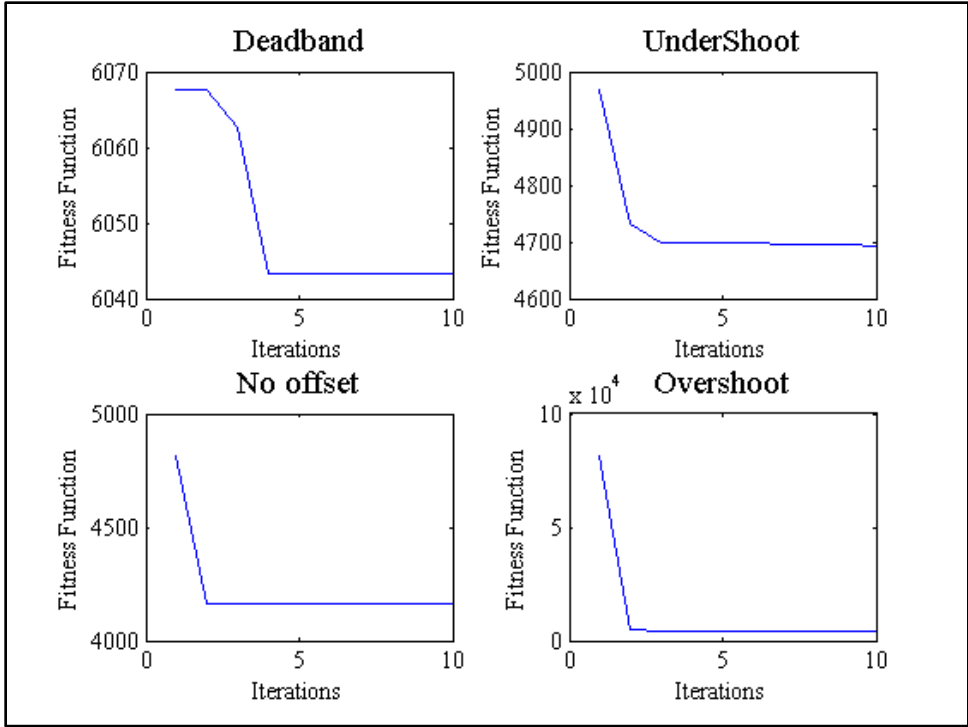


Figure 6.32: Optimization Iterations with Choudhury Model.

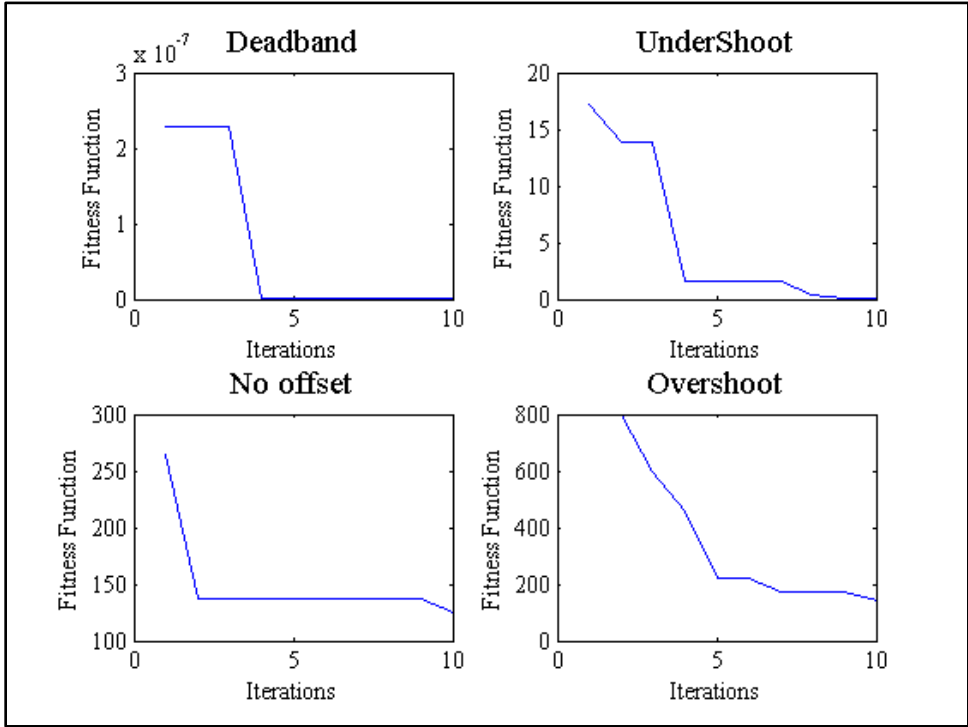


Figure 6.33: Optimization Iterations with Kano Model.

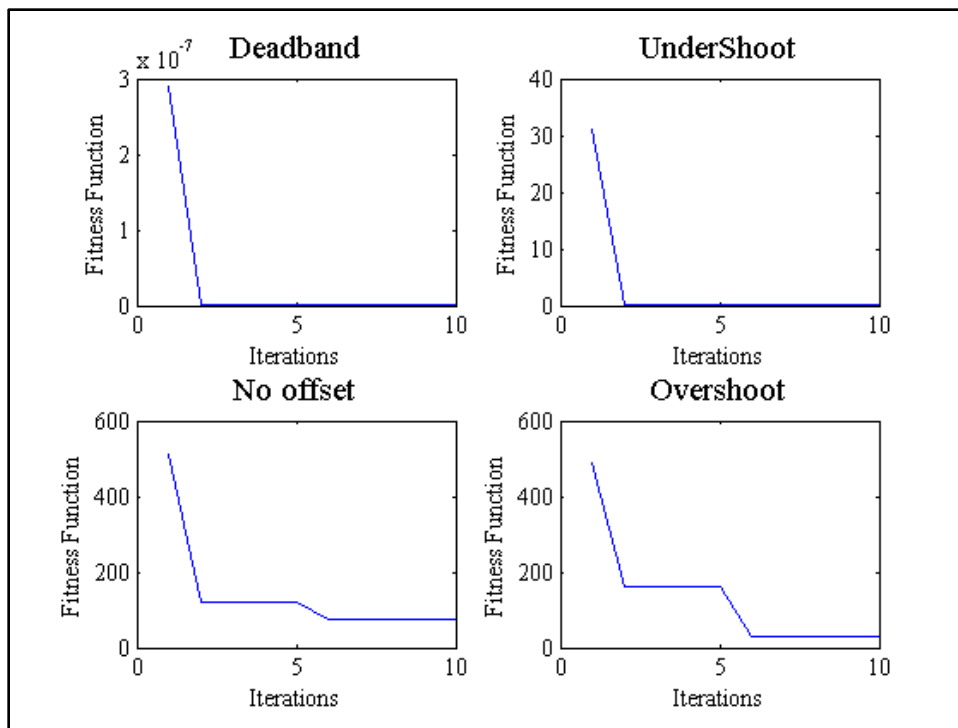


Figure 6.34: Optimization Iterations with Two Layer Model.

Choudhury Model				
	W₁	W₂	W₃	W₄
Dead band	-1.29	1.91	1.25	-2.00
Undershoot	2.00	-0.43	-1.01	-0.29
No offset	0.30	1.68	-1.35	-0.59
Overshoot	0.52	-0.51	-0.35	0.38
Kano Model				
Dead band	0.99	0.61	-0.01	-0.88
Undershoot	1.40	-0.34	-0.63	-0.15
No offset	0.87	1.22	-1.40	0.17
Overshoot	-0.29	1.36	-0.02	-0.83
Two Layer Model				
Dead band	0.48	1.07	-0.09	-0.81
Undershoot	0.26	-0.47	-0.25	0.54
No offset	2.00	-1.75	0.64	-0.77
Overshoot	0.55	0.14	-0.25	0.31

Table 6.13: DE-FIR Filter Weights.

6.4.7. Numerical Analysis and Discussion

For comparison purposes the variance reduction in the process variable was calculated for the four section cases as a percentage, the integral square error, and the variance of the loop error were used as measures for the variability of the process variable. Table 6.14 lists these two performance indicators for all applied compensators as percentage of their associated stiction cases. The proposed method (DE-FIR) was able to achieve the higher reduction rate for process variable, in some cases it reached 100% as seen in cases simulated by Choudhury model. Not applicable value (NA) means that the compensator failed and disturbed the controller from tracking the set-point. Logically, the minus sign that appears in some cases means that the compensator is deteriorating the stiction behavior, it increases the process variable oscillation amplitude. The stiction responses generated by Two layer model is not realistic, specially the overshoot scenario. Thus, the readings based on it are not accurate, and this may explain why some calculated percentage appear with minus.

Knocker Compensation								
TLM Model			Kano Model			Choudhury Model		
	ISE%	Var%		ISE%	Var%		ISE%	Var%
Deadband	81.4815	82.1	Deadband	99.9104	99.8	Deadband	98.5054	98.5048
Undershoot	63.3842	63.442	Undershoot	56.8717	56.9246	Undershoot	92.8054	92.7995
No offset	36.9477	37.0917	No offset	39.9315	40.0773	No offset	73.1534	73.0067
Overshoot	-10.343	-10.328	Overshoot	40.7064	40.6349	Overshoot	65.8799	65.8795
Dither Compensation								
TLM Model			Kano Model			Choudhury Model		
	ISE%	Var%		ISE%	Var%		ISE%	Var%
Deadband	98.3	98.21	Deadband	99.9645	99.75	Deadband	96.7661	96.7742
Undershoot	94.2348	94.1955	Undershoot	58.48	58.554	Undershoot	82.4831	82.5476
No offset	46.8535	46.9968	No offset	44.6574	44.784	No offset	66.9611	66.7787
Overshoot	-122.35	-122.31	Overshoot	39.7418	39.6825	Overshoot	68.6843	68.6825
CR Compensation								
TLM Model			Kano Model			Choudhury Model		
	ISE%	Var%		ISE%	Var%		ISE%	Var%
Deadband	99.8679	99.5	Deadband	99.2516	99.13	Deadband	99.3641	99.3646
Undershoot	99.9873	99.9875	Undershoot	68.7883	68.8391	Undershoot	92.7676	92.7833
No offset	43.444	43.5897	No offset	50.6729	50.7903	No offset	76.5381	76.4169
Overshoot	100	100	Overshoot	41.158	41.1005	Overshoot	71.4787	71.4917
Approximate Inverse Compensation								
TLM Model			Kano Model			Choudhury Model		
	ISE%	Var%		ISE%	Var%		ISE%	Var%
Deadband	99.961	99.74	Deadband	99.9984	99.91	Deadband	99.3832	99.3832
Undershoot	99.9506	99.9507	Undershoot	68.9263	68.9409	Undershoot	91.497	91.5079
No offset	43.102	43.2385	No offset	53.1799	53.3193	No offset	75.6396	75.5123
Overshoot	-58.045	-57.996	Overshoot	40.3627	40.2963	Overshoot	66.54	66.542
LMS-FIR Compensation								
TLM Model			Kano Model			Choudhury Model		
	ISE%	Var%		ISE%	Var%		ISE%	Var%
Deadband	100	100	Deadband	100	100	Deadband	100	100
Undershoot	23.3074	25.7637	Undershoot	23.3074	25.7637	Undershoot	94.0168	94.1395
No offset	13.2339	18.1595	No offset	13.2339	18.1595	No offset	78.3745	78.4982
Overshoot	-101.75	-101.73	Overshoot	NA	NA	Overshoot	NA	NA
DE-FIR Compensation								
TLM Model			Kano Model			Choudhury Model		
	ISE%	Var%		ISE%	Var%		ISE%	Var%
Deadband	100	100	Deadband	100	100	Deadband	99.9872	100
Undershoot	99.9424	99.9588	Undershoot	100	100	Undershoot	99.9977	100
No offset	70.7201	70.8114	No offset	74.2283	74.3238	No offset	99.9244	100
Overshoot	62.5241	62.5434	Overshoot	82.725	82.709	Overshoot	99.6882	100

Table 6.14: ISE and Variance as percentage for all compensators.

CHAPTER 7

Experimental Validation

7.1. Introduction

Similar to the simulation part all the compensators were tested experimentally. He et.al and Kano models were used to generate the stiction in setup introduced in next section. Note that the valve is healthy and does not suffer from stiction. The stiction behavior is generated in the controller by soft elements.

7.2. Experimental Setup

The single tank configuration is shown in Figure 7.1. It has an outlet with on/off valve to keep constant flow and inlet through pneumatic valve to control the tank level. The level is continuously measured via level transmitter and sent to PI controller programmed in NI Compact field point processor using Labview software. The output from the controller is 4-20 mA signal that actuates the pneumatic valve with the help of E/P (electrical to pressure converter). A HMI is developed using Labview software contains many options such as PI adjustment, set-point setting, stiction model selection and its associated parameters setting, compensators selection, graphical plotting for the process variable, control signal and compensation signal if applicable, and finally data recording for offline analysis. Figure 7.1 demonstrates schematic diagram for level control loop, Figures 7.2, 7.3 and 7.4 show the complete components and the human machine interface..

The structure of PI controller used is given in equation 7.1 with $K_c = 4$ and $t_i = 0.2$ minutes to give 2% steady state error at maximum, and the open loop transfer function is given in Equation 7.2.

$$C(S) = K_c \left(1 + \frac{1}{t_i S} \right) \quad (7.1)$$

$$G(S) = \frac{8.9}{5.33S + 1} \quad (7.2)$$

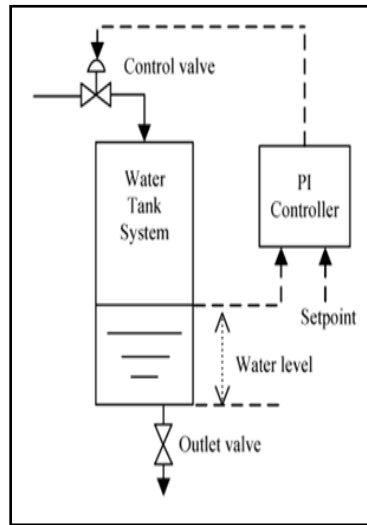


Figure 7.1: Tank Level Control Loop.



Figure 7.2: Experimental Setup (Full picture).



Figure 7.3: Experimental Setup (Components).

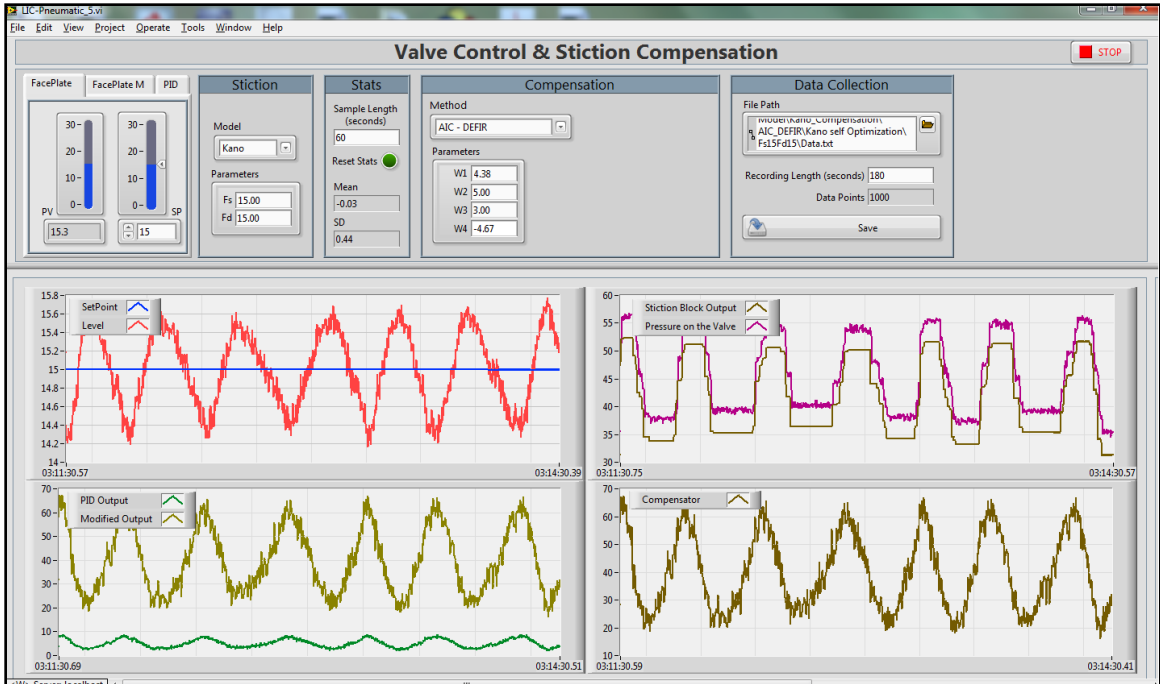


Figure 7.4: Experimental Setup (Human Machine Interface).

7.2.1. Setup Calibration

Calibration was carried out to the level transmitter to give measurements between 0 cm (empty tank) and 30 cm (full tank). For the calibration procedure many readings were recorded starting from full tank ending with near empty tank Table 7.1 and Figure 7.5, then the calibration formula was constructed given in equation 7.3.

$$H = 7.3879I - 114.6 \quad (7.3)$$

Where H and I are respectively the liquid level in centimeters and the current output in Milliampere from transducer.

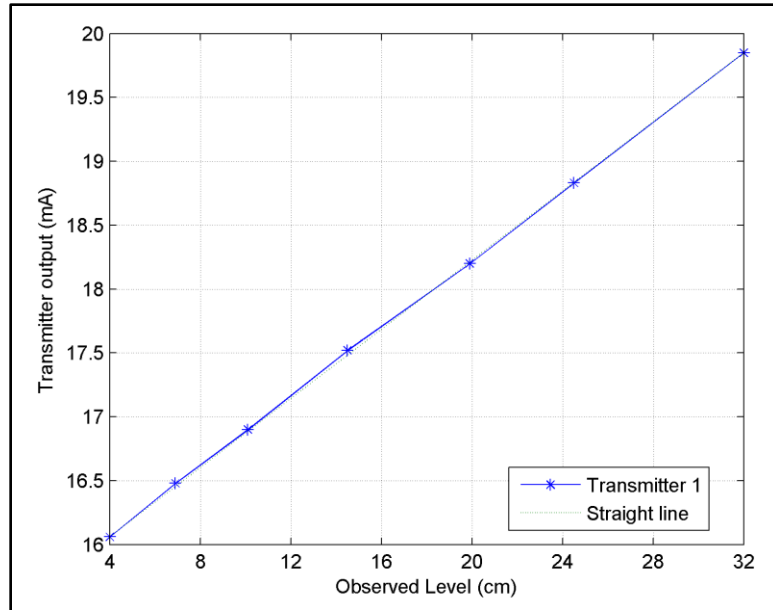


Figure 7.5: Tank Level and Transmitter Current Relation.

Reading No	Tank Level (cm)	Transmitter (mA)
1	32.00	19.85
2	24.50	18.83
3	19.90	18.20
4	14.50	17.52
5	10.10	16.90
6	6.90	16.48
7	4.00	16.06

Table 7.1: Level Transmitter Calibration Measurements.

No need to calibrate the pneumatic control valve and its actuator since they already pre-calibrated.

The stiction or slip jump behavior was generated by a soft element programmed in the NI compact field point controller using Labview software. This soft element was algorithm of either He or Kano models, it can be selected and set from the HMI as experiment parameters with many others such as PID controller gains, compensators type and it is parameters, set-point and data saving option. Table 7.2 lists the four scenario parameters

and the process variable (blue line), set-point (green line) and the control signal were shown in Figures 7.6 and 7.7.

Stiction Scenario	Kano Model		He Model	
	S	J	f_s	f_D
Dead band	30	0	15	15
Undershoot	45	15	30	15
No offset	20	20	20	0
Overshoot	15	45	30	-15

Table 7.2: Equivalent Stiction Scenario's in the TwoModels.

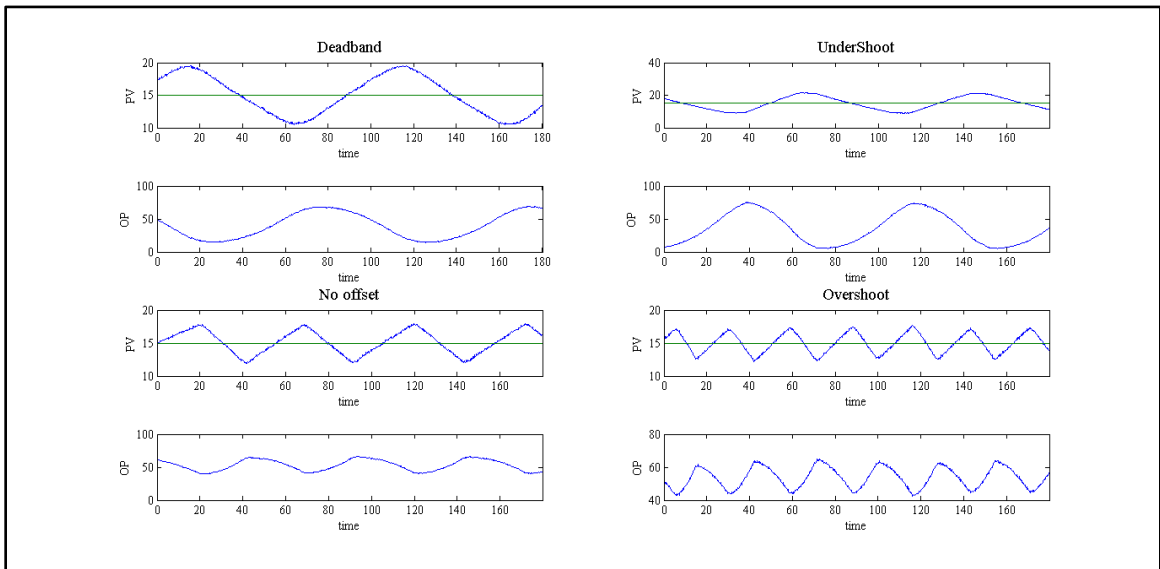


Figure 7.6: The Four Stiction Scenarios with Kano Model.

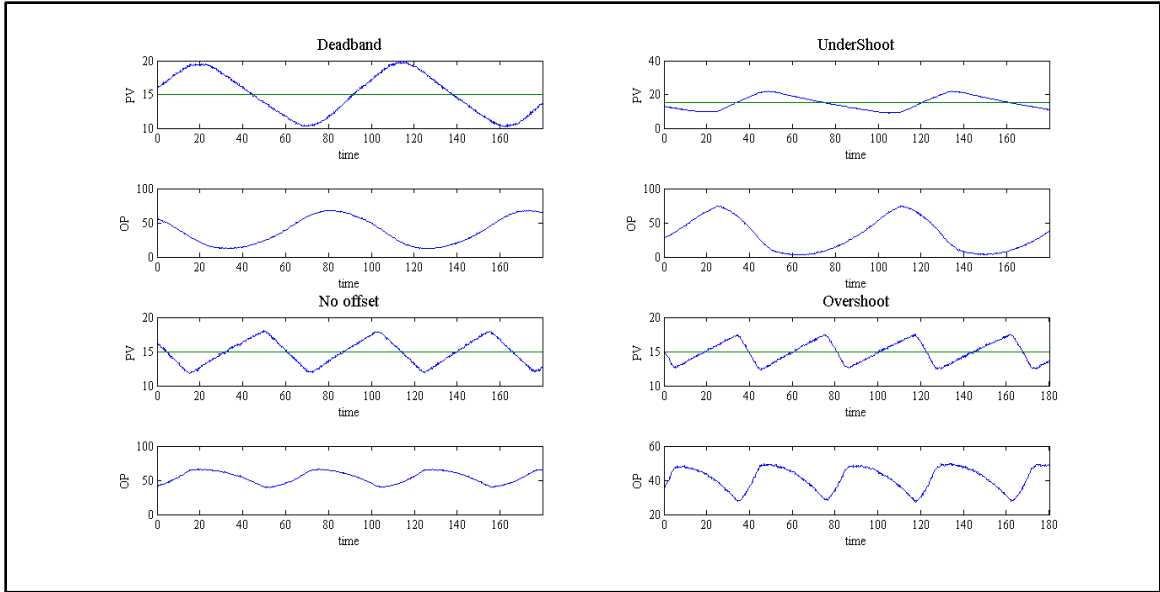


Figure 7.7: The Four Stiction Scenarios with He Model.

The full tank height was selected to be 30 cm and the set-point was set in the middle (15 cm). The control signal was normalized to have a range between 0% to 100%.

7.2.2. Knocker Method

Knocker compensator was tuned manually after several trial and error. The parameters are listed in Table 7.3 and the compensated response is shown in Figures 7.8 and 7.9.

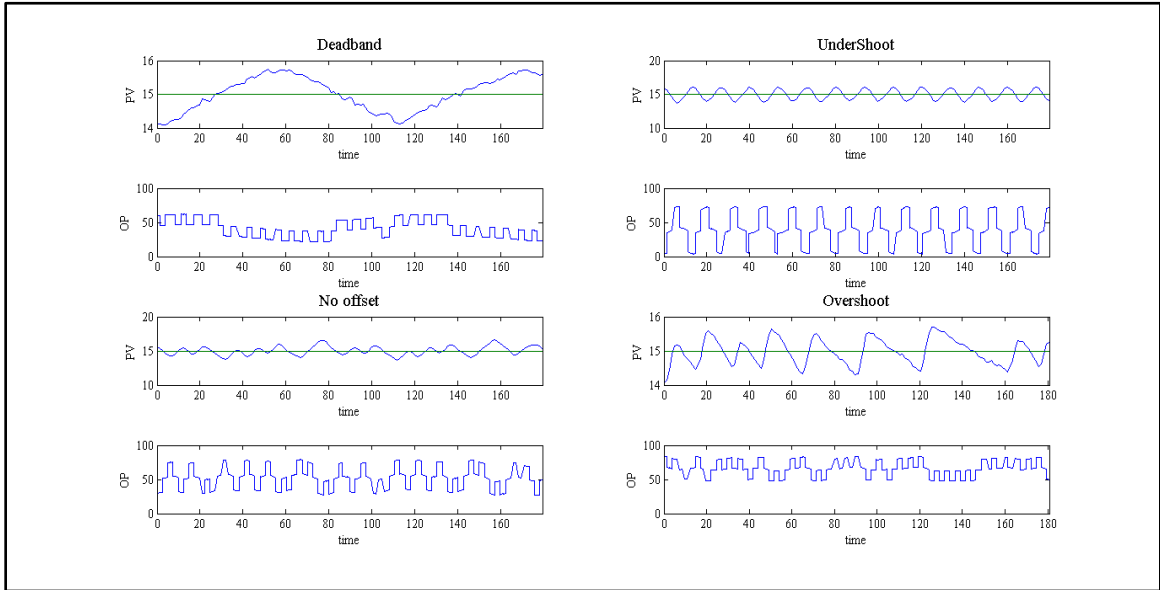


Figure 7.8: Knocker Compensator with Kano Model.

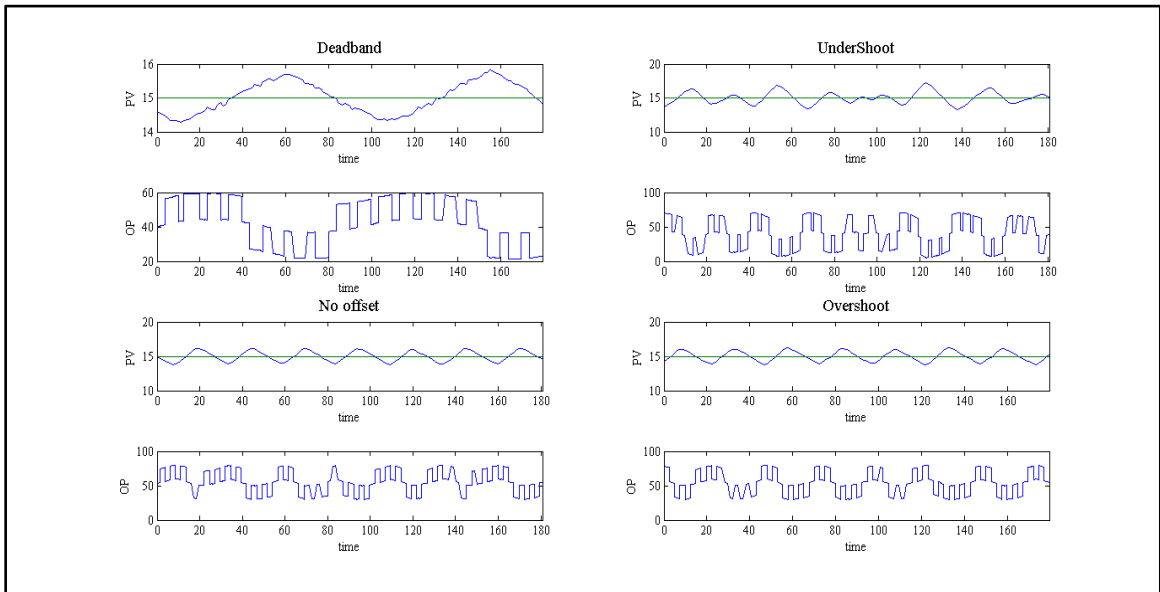


Figure 7.9: Knocker Compensator with He Model.

<i>Knocker Parameters</i>	Kano Model			
	Dead band	Undershoot	No offset	Overshoot
<i>a</i>	15	30	20	15
<i>Tao(sec)</i>	4	3.3	2.5	2.5
<i>h_k(sec)</i>	6.67	6.67	5	5
#	He Model			
<i>a</i>	15	25	20	20
<i>Tao(sec)</i>	6	3.5	2.5	3.5
<i>h_k(sec)</i>	10	5	5	5

Table 7.3: Knocker Compensator Parameters.

7.2.3. Dithering Method

The static force value (f_s) was used as the amplitude for the dithering signal, since the compensator needed to overcome the stiction only without any additional movements that can harm the valve stem, this choice was suitable for all cases except the overshoot case, where manual tuning (trials and error with trends studying) was used instead since it gave better results. Dither parameters and dithered loop response are shown below.

<i>Dither Parameters</i>	Kano & He Models			
	Dead band	Undershoot	No offset	Overshoot
<i>A_m</i>	15	30	20	15
<i>f sec⁻¹</i>	0.15	0.15	0.2	0.2

Table 7.4: Dither Compensator Parameters.

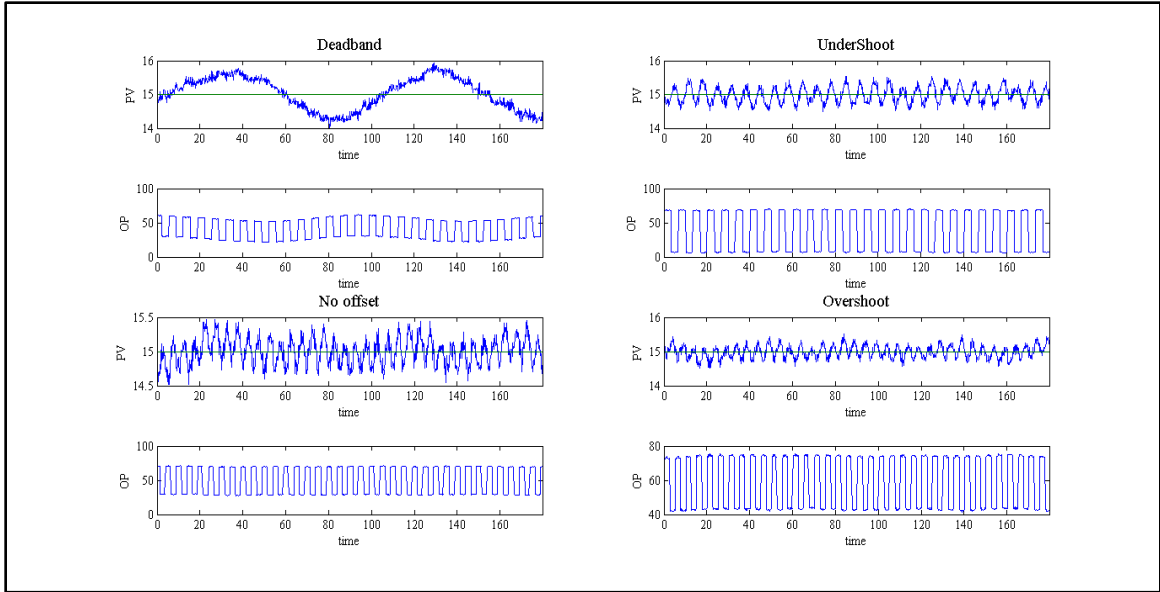


Figure 7.10: Dither Compensator with Kano Model.

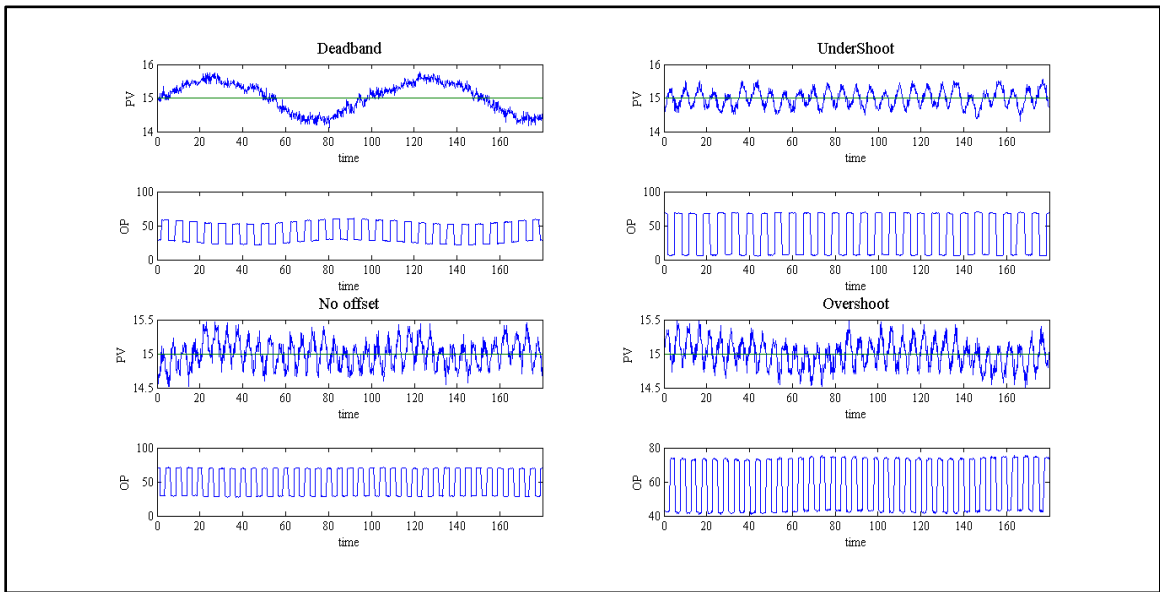


Figure 7.11: Dither Compensator with He Model.

7.2.4. Constant Reinforcement Method (CR)

The same principle applied in dither compensator is applicable here, since there is one parameter to tune it can be directly interfaced with the static force value except for the last case that was tuned manually, the tuning for this CR and approximate inverse compensator was so easy since they have one parameter, starting from low value and increase it in steps the optimum value can be obtained.

The CR compensator is very sensitive to noise, since the process variable reading comes with some noise so will be the loop error and it will be amplified in the controller to generate the control signal, and since the CR compensator depends mainly on the sign of the difference between any two successive instants of the control signal and the amplified noise will lead to wrong sign, then wrong direction for the constant reinforcement to add. The solution is to use smoothing filter or low pass filter to cut out the undesirable noise, more intention should be taken in filter design because too much filtering can damage the signal or can lead to system instability. Tables 7.5 and Figures 7.12 & 7.13 show the results. The good things about the CR compensator that, it avoids any unnecessary movements for valve stem, in other words it compensates the stiction with the minimum stem movements.

<i>CR Parameter</i>	Kano & He Models			
	Dead band	Undershoot	No offset	Overshoot
A_m	15	30	20	25

Table 7.5: CR Compensator Parameters.

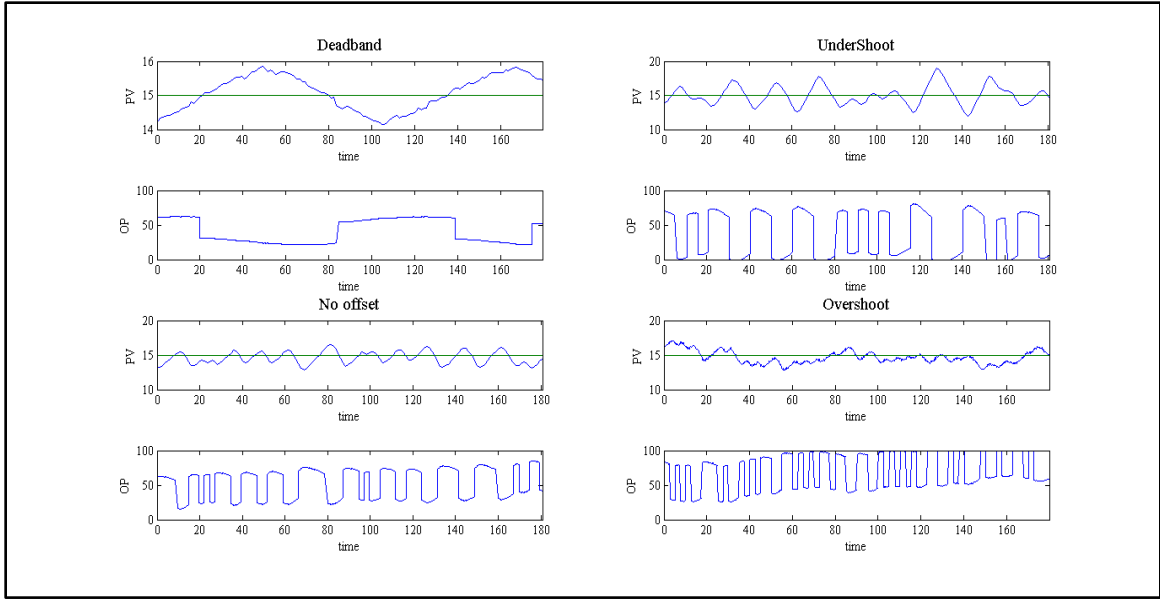


Figure 7.12: CR Compensator with Kano Model.

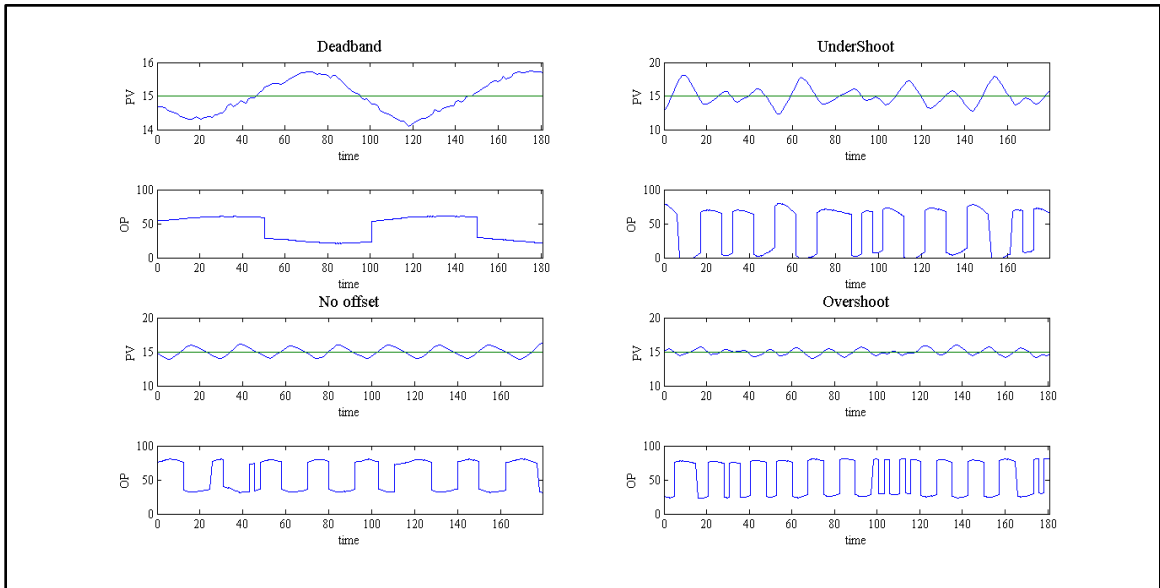


Figure 7.13: CR Compensator with He Model.

7.2.5. Approximate Inverse Method

As explained in section 4.4 the backlash inverse was used as stiction compensator, and as expected the compensator worked well for the cases with small jump value, thus the static force used as the positive and negative crossing edges (dead band and undershoot cases), for the other two cases and manual tuning was applied as explained in CR compensator above.

The backlash inverse assumed symmetric response. Thus, the slope was set to one, and the positive and negative edges were equal. Table 7.6 lists the value of this edge and Figures 7.14 and 7.15 illustrate the associated responses.

<i>Backlash inverse Parameter</i>	Kano & He Models			
	Dead band	Undershoot	No offset	Overshoot
d_+	15	30	30	35

Table 7.6: Approximate Inverse Compensator Parameters.

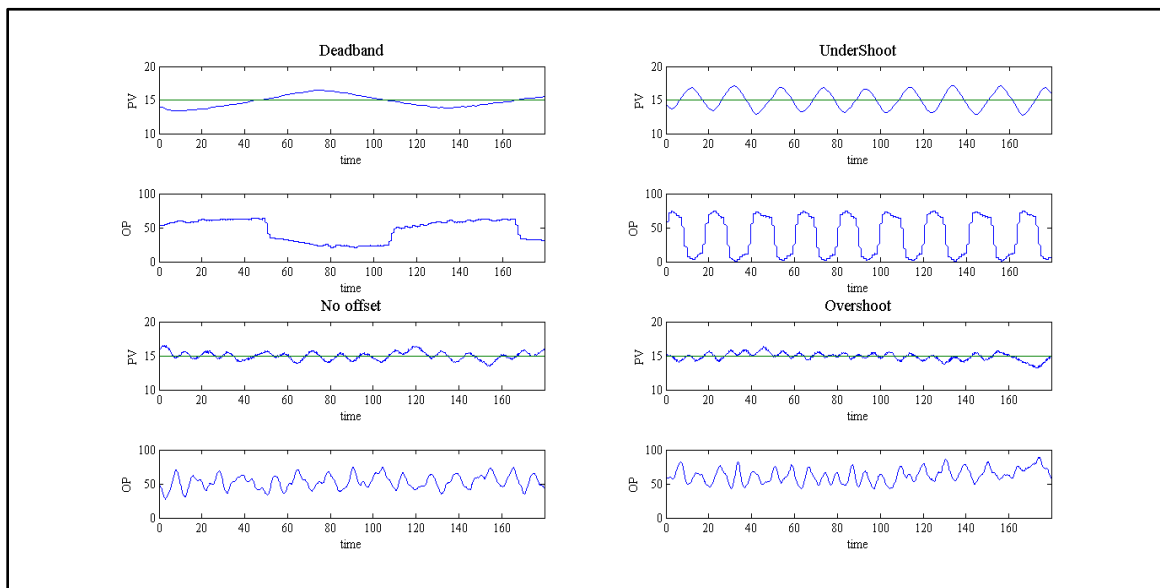


Figure 7.14: Approximate Inverse Compensator with Kano Model.

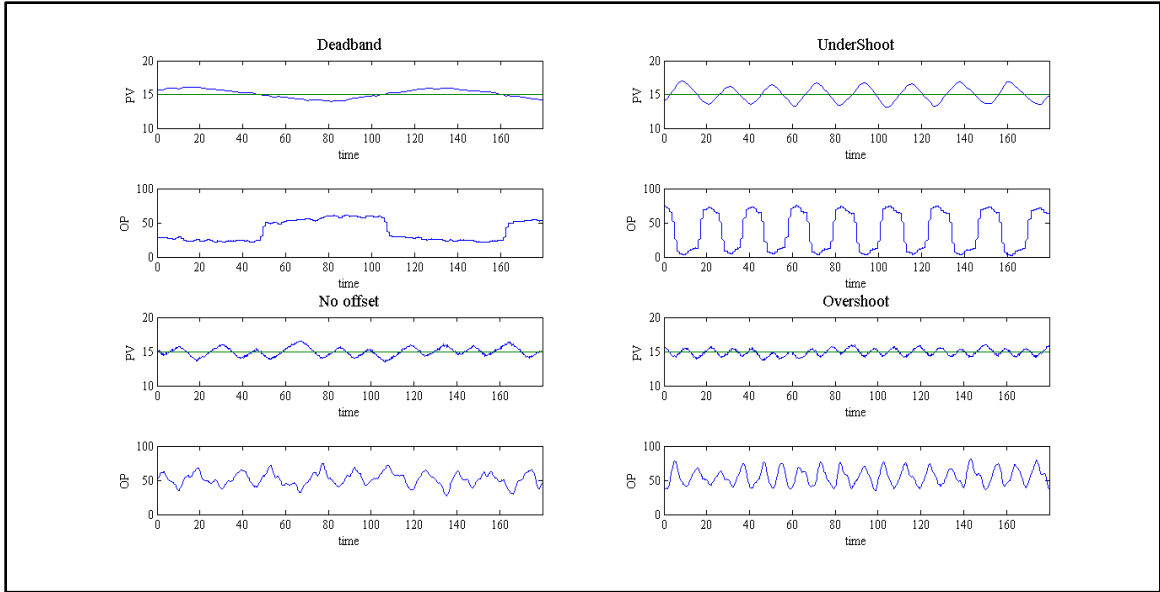


Figure 7.15: Approximate Inverse Compensator with He Model.

7.2.6. Adaptive Inverse Control Method (LMS-FIR)

Already built in blocks for LMS and FIR filter in Labviewsoftware were used to implement the LMS-FIR compensator, the filter length was selected to be four as in simulation part and the step size was adjusted to 0.001 for all stiction scenarios, the loop error ($SP-PV$) was used as fitness function to be minimize.

The LMS-FIR succeeded in stiction compensation but unfortunately the mean of the compensated process variable was biased from the set-point with considerable amount (up to 5% from the set-point in this experiment) as seen from figures 7.16 and 7.17, moreover the compensator sometimes doesnotwork perfectly for the no-offset and overshoot cases, the control signal will oscillate in the whole range from zero to 100% and sometimes can be saturated and it will look like on/off control valve, this explains why the filter weights were getting large in Table 7.7.

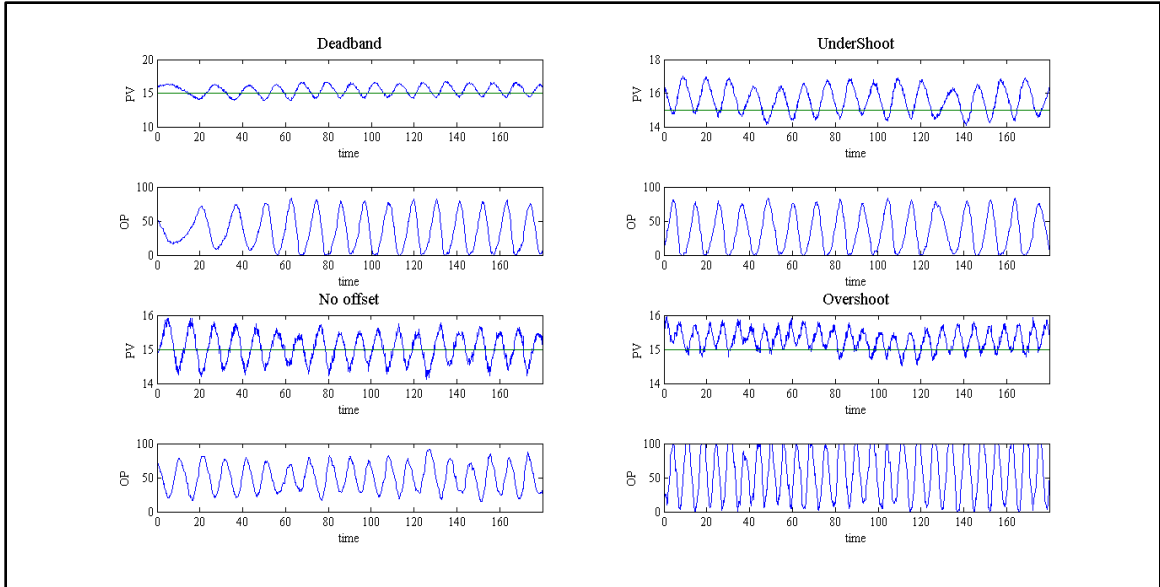


Figure 7.16: LMS-FIR Compensator with Kano Model.

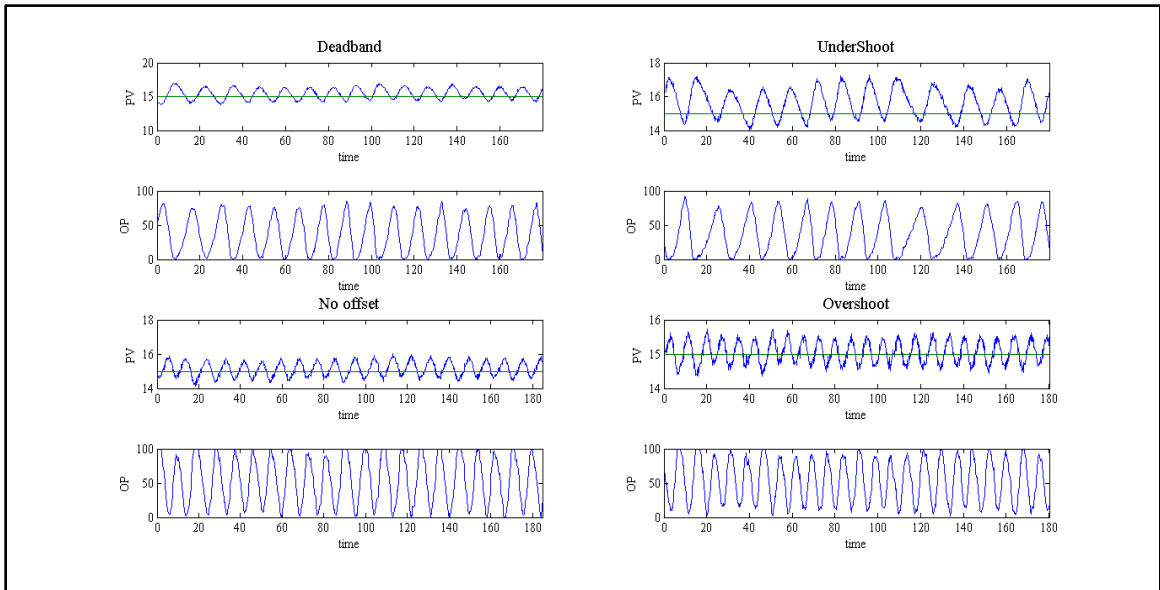


Figure 7.17: LMS-FIR Compensator with He Model.

Kano Model				
	W₁	W₂	W₃	W₄
Dead band	3.71	2.43	2.16	1.85
Undershoot	4.05	2.47	1.95	1.27
No offset	4.57	3.39	3.25	3.08
Overshoot	11.75	9.61	8.53	7.41
He Model				
Dead band	3.53	2.39	2.26	2.1
Undershoot	3.67	2.33	2.03	1.60
No offset	7.44	5.75	5.09	4.38
Overshoot	8.40	6.58	5.87	5.09

Table 7.7:LMS-FIR Filter Weights.

7.2.7. Adaptive Inverse Control Method (DE-FIR)

The FIR block from Labview was used, the DE algorithm was used to tune the filter, the tuning process was carried out online, but not automated, since the DE was implemented in a different computer and the fitness function fed to the algorithm manually every time and the reverse procedure was done with the weights, which optimized in the range between 5 and -5 with Kano model only while He model was used for validation.

The optimization result was not unique that means we could find many possible sets or weight combinations that are able to give the same good results, the validation was done to verify that if the optimization depended on the stiction model used or not. In general the method demonstrated good performance in stiction compensation as seen from Figures 6.18 and 6.19.

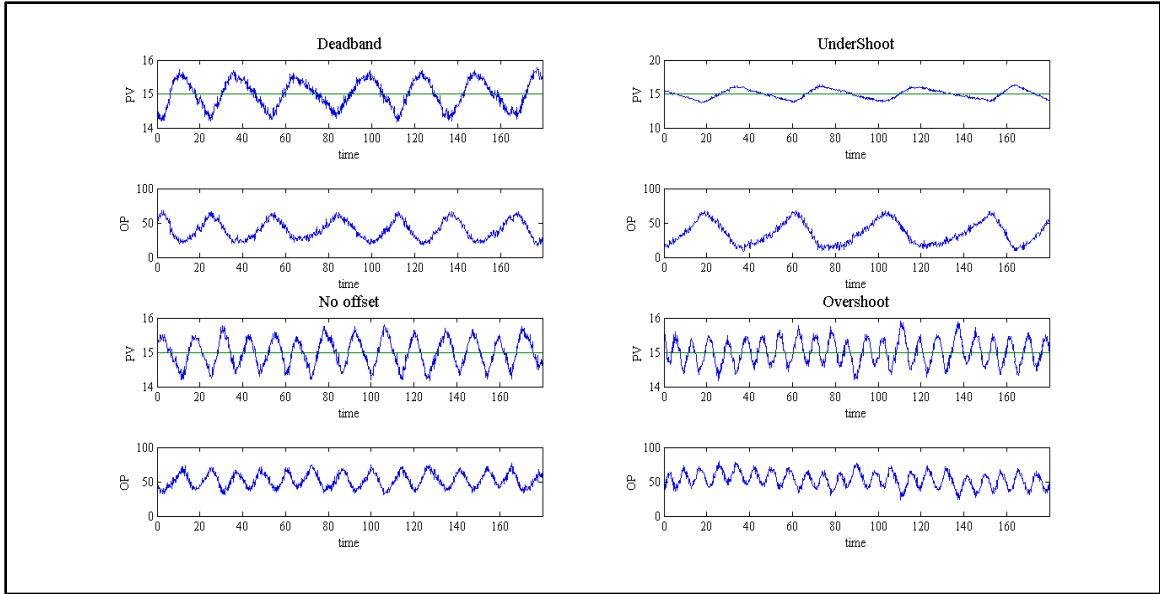


Figure 7.18: DE-FIR Compensator with Kano Model.

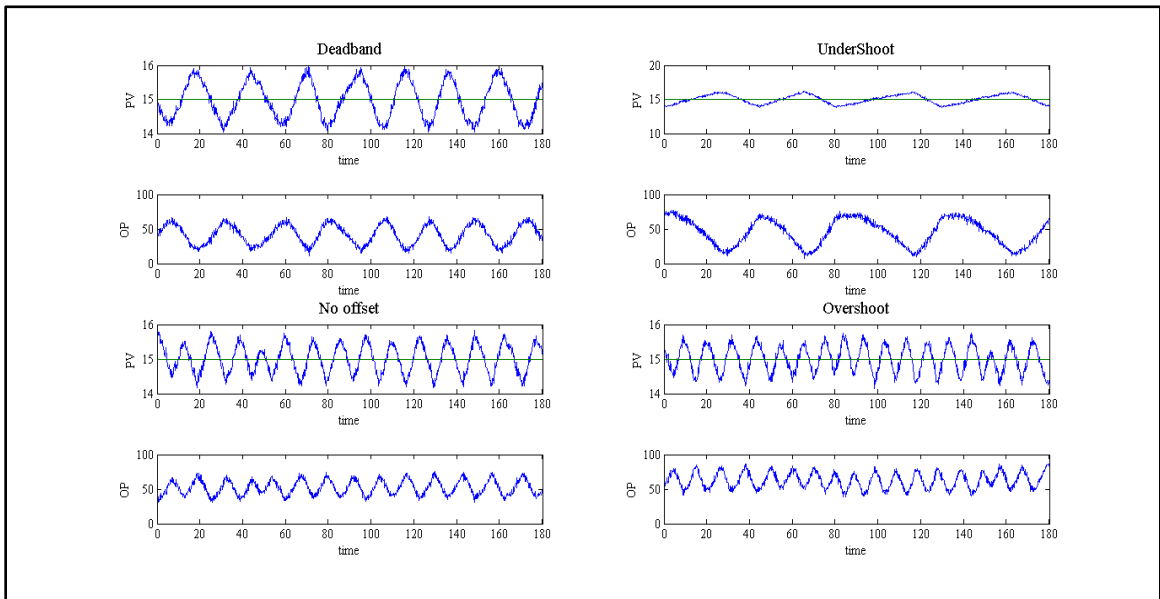


Figure 7.19: DE-FIR Compensator with He Model.

With the population size set at 20, it has been found that the DE algorithm needs six iterations or less to reach the optimal solution as depicted from Figures 7.20. The filter weights resulted from the optimization process were listed in Table 7.8. Due to its

optimization mechanism and the nature of objective function reading, the DE algorithm cannot be automated with the FIR filter in the same computer or controller instead an external computer was used for optimization.

The performance of the DE-FIR compensator was tested against set-point change (disturbance), although the FIR optimized around specific operation point (SP=15) to curb stiction, it has been found that the filter keep the same good performance in others operation points, this were shown by changing the set-point in the two directions up and down to cover the whole operation range, Figures 7.21 and 7.22 illustrating the changing of set-point from 15 to 20 and 15 to 10 with undershoot scenario using Kano stiction model.

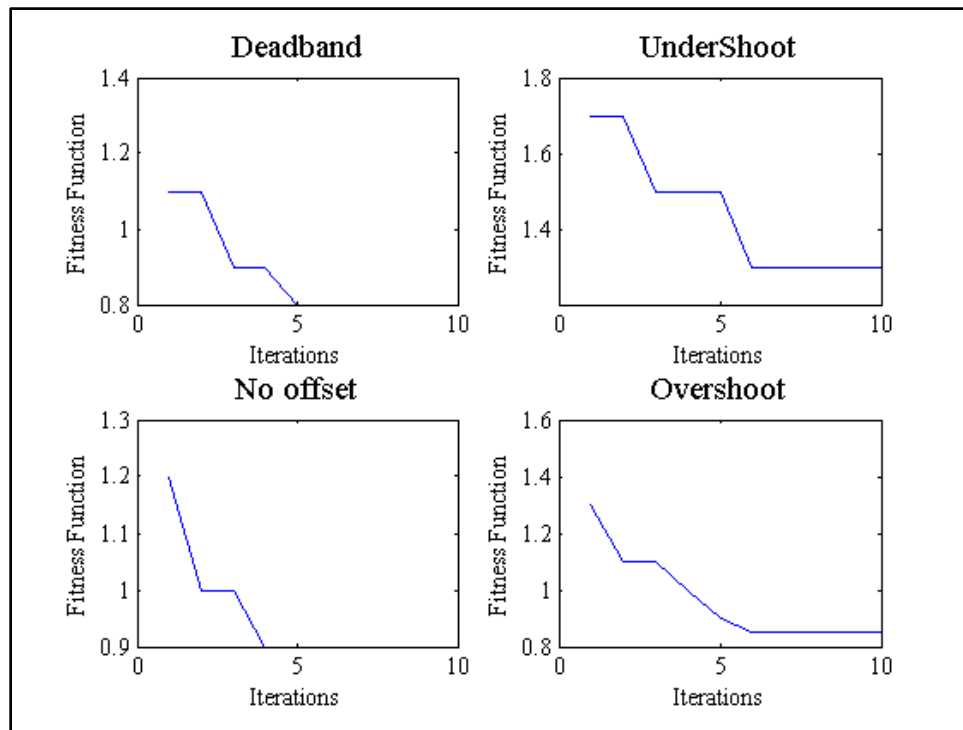


Figure 7.20: Optimization Iterations with Kano Model.

Kano& He Model				
	W₁	W₂	W₃	W₄
Dead band	4.38	5.00	3.00	-4.67
Undershoot	5.00	4.77	-0.76	-3.81
No offset	5.00	5.00	-5.00	1.25
Overshoot	5.00	5.00	-4.3	1.4

Table 7.8: DE-FIR Filter Weights.

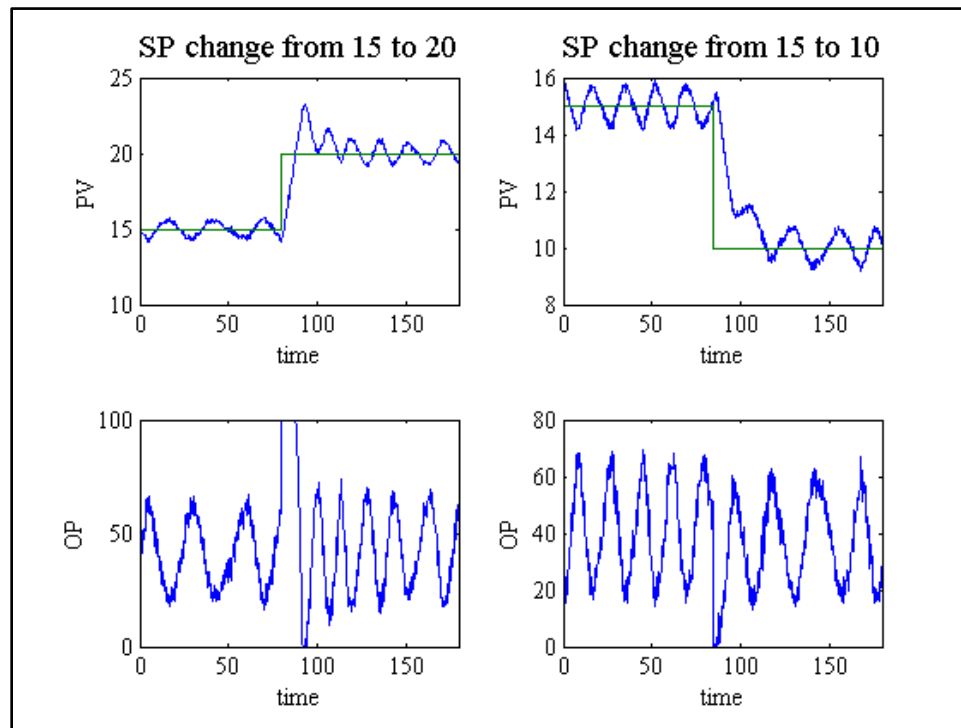


Figure 7.21: SP Change for Dead band of Kano Model with DE-FIR.

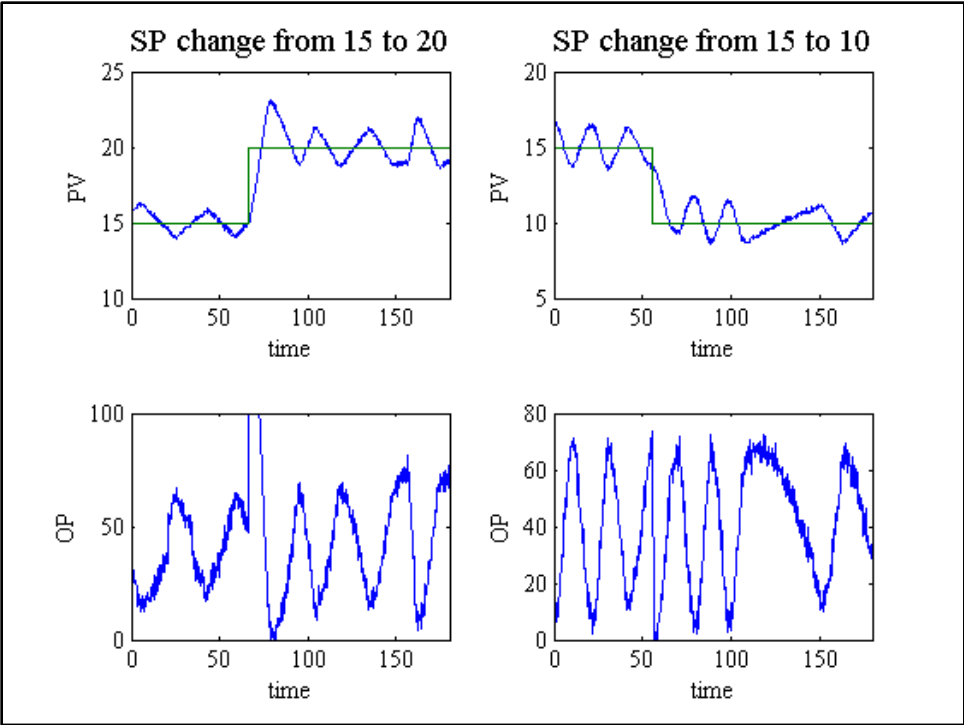


Figure 7.22: SP Change for Undershoot of Kano Model with DEFIR.

7.2.8. Numerical Analysis and Discussion

Srinivasan and Rengaswamy in [6], set the properties of the ideal compensator which is expected to reduce the variability of the process variable, with minimal added energy to the control signal, and with minimum stem movements.

The integral square error (ISE), error variance (Var) and maximum error (max_e) were calculated as a percentage from their associated stiction case for the six compensators, the consumed energy (E%) for the six compensators also was calculated as percentage from the steady state energy for the loop without stiction. For example E=50% that means the specific compensator was consuming additional 50% of the normal control signal energy for normal loop without stiction.

The variability was measured by the statistical variance, although the integral square error and the maximum error can be used instead, but the latter one is not accurate. The energy was calculated by the sum of the square control signal. Since the window size for all measurements was fixed with 1000 points of measurements, it guarantees fair comparison. The energy measured here is the pneumatic energy, since the electrical signal energy is very small compared to the pneumatic energy and can be neglected. Since the control signal and the pneumatic signal has a linear relation, the control signal energy can be used as a measure for the pneumatic signal energy. There is no explicit way or method to measure the valve stem aggressiveness (SA), however, measuring the number of times that the stem moves up and down and the shape of the control signal can be a good indicator, since the triangle and the sinusoidal signal are better than the pulse shape signal for the stem to respond, and the less stem movements lead to less possibility of stem tearing which mean long life for the valve. Table 7.9 listed these results.

Knocker Compensation											
Kano Model						He Model					
	ISE%	max_e%	Var%	E%	SA		ISE%	max_e%	Var%	E%	SA
Deadband	97.14435	79.9825	97.1478	26.1876	47	Deadband	97.8935	83.2545	97.8964	35.3374	32
Undershoot	96.52375	80.1398	96.5237	37.4089	54	Undershoot	95.288	67.9511	95.2914	40.4791	54
No offset	86.20848	45.6621	86.0049	100.196	42	No offset	84.4187	61.963	84.3171	124.879	59
Overshoot	93.37505	65.6968	93.3986	208.664	55	Overshoot	77.8346	54.321	77.7169	109.298	57
Average	93.31291	67.8703	93.2688	93.114	49.5	Average	88.8587	66.8724	88.8055	77.4983	50.5
Dither Compensation											
Kano Model						He Model					
	ISE%	max_e%	Var%	E%	SA		ISE%	max_e%	Var%	E%	SA
Deadband	97.52935	78.1707	97.5524	30.3779	54	Deadband	98.1344	82.1024	98.1444	26.7274	55
Undershoot	99.63026	91.7338	99.6301	60.8435	54	Undershoot	99.591	89.7339	99.5911	59.4467	54
No offset	98.72212	84.3118	98.6999	93.502	71	No offset	98.827	84.9169	98.8188	93.502	72
Overshoot	98.3302	82.0043	98.3332	147.834	72	Overshoot	98.2437	81.8809	98.2337	144.076	73
Average	98.55298	84.0552	98.5539	83.1393	62.75	Average	98.699	84.6585	98.697	80.9379	63.5
CR Compensation											
Kano Model						He Model					
	ISE%	max_e%	Var%	E%	SA		ISE%	max_e%	Var%	E%	SA
Deadband	97.02405	81.1831	97.0971	30.2429	4	Deadband	97.402	81.4441	97.4096	47.6518	3
Undershoot	86.62223	39.8268	86.6245	64.5547	23	Undershoot	89.5589	55.0822	89.5615	86.0594	20
No offset	69.74011	30.1696	74.6	119.109	29	No offset	86.6028	59.2662	86.5296	148.516	17
Overshoot	54.47295	20.0431	59.8597	255.85	48	Overshoot	91.0375	61.8373	91.1076	134.096	31
Average	76.96483	42.8057	79.5453	117.439	26	Average	91.1503	64.4075	91.1521	104.081	17.75
Approximate Inverse Compensation											
Kano Model						He Model					
	ISE%	max_e%	Var%	E%	SA		ISE%	max_e%	Var%	E%	SA
Deadband	91.02187	64.1781	91.5481	61.8016	3	Deadband	95.7084	77.7001	95.8836	10.5331	3
Undershoot	89.0033	65.9322	89.0087	53.0769	17	Undershoot	92.4106	71.2956	92.4166	51.7409	16
No offset	88.66931	49.9348	88.4806	95.1012	29	No offset	87.2578	50.7996	87.2059	85.8772	22
Overshoot	85.30791	35.0934	86.0674	169.676	39	Overshoot	88.4851	54.321	89.0194	116.221	36
Average	88.5006	53.7846	88.7762	94.914	22	Average	90.9655	63.5291	91.1314	66.0931	19.25
LMS-FIR Compensation											
Kano Model						He Model					
	ISE%	max_e%	Var%	E%	SA		ISE%	max_e%	Var%	E%	SA
Deadband	91.63028	61.4058	93.6606	31.5452	28	Deadband	91.7059	57.9922	93.5573	41.2821	32
Undershoot	93.91145	69.336	96.3666	37.058	31	Undershoot	93.0503	66.9478	95.5656	44.7166	26
No offset	94.30517	69.9935	94.2672	94.0148	36	No offset	94.1693	68.4541	94.6571	175.661	41
Overshoot	91.72087	64.4037	95.8706	193.914	50	Overshoot	95.2366	73.3842	95.3624	156.795	47
Average	92.89194	66.2847	95.0413	89.1329	36.25	Average	93.5405	66.6946	94.7856	104.614	36.5
DE-FIR Compensation											
Kano Model						He Model					
	ISE%	max_e%	Var%	E%	SA		ISE%	max_e%	Var%	E%	SA
Deadband	98.10564	81.7289	98.1048	21.1808	12	Deadband	97.0887	79.9835	97.0941	33.7247	15
Undershoot	97.02156	79.5928	97.0249	1.60594	9	Undershoot	97.3261	81.9253	97.3268	64.5074	8
No offset	94.6585	72.7332	94.5704	90.5938	27	No offset	94.8503	71.0568	94.8193	92.139	28
Overshoot	93.93089	67.2055	93.9354	96.3225	44	Overshoot	93.7652	68.7001	93.731	172.746	35
Average	95.92915	75.3151	95.9089	52.4258	23	Average	95.7576	75.4164	95.7428	90.7794	21.5

Table 7.9: ISE,Var,max_e and E as Percentage for All Compensators.

As seen from Table 7.9, by taking Kano model cases for example, we will find that the Dither, DE-FIR and LMS-FIR are the best compensators in terms of PV variability reduction, followed by the knocker, approximate inverse and finally the CR has the worst performance. In terms of energy saving the DE-FIR switched its position with the Dither, the remaining compensators didn't change their positions. As expected the dither and the knocker are the worst compensator in terms of valve stem aggressiveness, since their compensation philosophies are based on continuous pulses with high frequency. On the other hand the approximate inverse and DE-FIR are the best ones, as can be expected from their compensation philosophy.

Table 7.10 summarizes the ranking for the compensators according to Srinivasan and Rengaswamy ideal compensators properties.

- 1) Variability reduction of the process variable.
- 2) Energy saving.
- 3) Less valve stem movements (Stem Aggressiveness).

<i>Compensation Method</i>	<i>Variability Reduction</i>	<i>Energy Saving</i>	<i>Stem Movements</i>
<i>Dither</i>	1 st	2 nd	6 th
<i>Knocker</i>	4 th	4 th	5 th
<i>CR</i>	6 th	6 th	3 rd
<i>ApproximateInverse</i>	5 th	5 th	1 st
<i>LMS-FIR</i>	3 rd	3 rd	4 th
<i>DE-FIR</i>	2 nd	1 st	2 nd

Table 7.10: Compensators Ranking by Kano Model.

CHAPTER 8

Summary and Future Work

8.1. Summary

The body of this thesis, consisting of five chapters focused on compensation of stiction occurred in pneumatic valve. In the third chapter various models used for stiction simulation were reviewed. In the fourth chapter a new compensation method was introduced in spirit of adaptive filtering and intelligent control theory. The method used finite impulse response filter optimized by intelligent method called differential evolution algorithm. The adaptive filtering theory was reviewed in this chapter along with other compensation methods from literature which used in result chapter for comparison purpose. The DE algorithm was reviewed in Chapter Five. Detailed results consisting of figures and tables for different compensation methods, including the proposed method using different section models covering the four scenarios were given in Chapter Six, in Chapter Seven, the obtained results were validated experimentally.

8.2. Contribution of this Thesis

The contributions of this work can be summarized as follows:

- Study of PI controller tuning effects on valve stiction compensation.
- Study of DE algorithm performance on high nonlinear problem optimization.
- Introducing of modified version of Sabih method, which was introduced by Muhamed Sabih in 2009 during his Master thesis.

- A new methodology to compensate stiction in single loop control system, which based on adaptive filtering and intelligence control theory, the proposed method is an evolution of the modified version of Sabih method, the new method was validated by simulation and experimental studies.
- Comparison of existing compensation methods with Sabih modified compensator and the new proposed method, the comparison was carried out in two parts, simulation part using Matlab Simulink and experimental part using water tank level control loop.

8.3. Future Work

Pneumatic valve stiction compensation in control systems will stay a major area of research in the performance assessment field, further research may come with new brilliant ideas or may improve the already existing methods to overcome their flaws toward ideal compensation. The open discussion in this work can be listed as:

- The proposed method was not fully automated, the optimization process was done manually using external computer since the mechanism of the DE algorithm and the nature of the objective function can't allow automated optimization process to be carried on, it is recommended to invent new objective function that allow the automation of optimization process, also it is recommended to investigate the possibility of others intelligent optimization methods that can be fully automated, methods such as particle swarming, Tabu Search, simulated annealing and etc.
- The proposed method was validated for first order process system controlled by PI controller only, further investigation is needed to cover high order systems and nonlinear systems.

- The proposed method was validated experimentally using Kano model to generate stiction behavior, since the valve doesn't suffer from stiction, It can be predicted that there will be more challenges in implementation of this method in real industry valve with real stiction behavior.

References

- [1] Zang, Xiaoyun, and John Howell. "The propagation of whole plant oscillations through a chemical process plant." *Journal of Process Control* 16.9 (2006): 959-970.
- [2] L. Desborough, P. Nordh, R. Miller, "Control system reliability: process out of control." *Industrial Computing* 8 (2001) 52–55.
- [3] Bialkowski, W. L. "Dreams versus reality: a view from both sides of the gap: manufacturing excellence with come only through engineering excellence." *Pulp & Paper Canada* 94.11 (1993): 19-27.
- [4] T. Hägglund, "A friction compensator for pneumatic control valves." *Journal of Process Control*, vol. 12, no. 8, pp. 897–904, 2002.
- [5] Srinivasan, Ranganathan, and Raghunathan Rengaswamy. "Stiction compensation in process control loops: A framework for integrating stiction measure and compensation." *Industrial & engineering chemistry research* 44.24 (2005): 9164-9174.
- [6] Srinivasan, R., and R. Rengaswamy. "Integrating stiction diagnosis and stiction compensation in process control valves." *Computer Aided Chemical Engineering* 21 (2006): 1233-1238.
- [7] Xiang Ivan, Lee Zhi, and S. Lakshminarayanan. "A new unified approach to valve stiction quantification and compensation." *Industrial & Engineering Chemistry Research* 48.7 (2009): 3474-3483.
- [8] Karthiga, D., and S. Kalaivani. "A new stiction compensation method in pneumatic control valves." *Int. J. Electron. Comput. Sci. Eng* 1 (2012): 2604-2612.
- [9] Farenzena, Marcelo, and Jorge Otã Trierweiler. "Modified pi controller for stiction compensation." *Dynamics and Control of Process Systems*. Vol. 9. No. 1. 2010.
- [10] Sivagamasundari, S., and D. Sivakumar. "A New Methodology to Compensate Stiction in Pneumatic Control Valves." *International Journal of Soft Computing and Engineering (IJSCE)* ISSN: 2231-2307.
- [11] Srinivasan, R., and R. Rengaswamy. "Approaches for efficient stiction compensation in process control valves." *Computers & Chemical Engineering* 32.1 (2008): 218-229.

- [12] Cuadros, Marco Antonio de Souza L., Celso J. Munaro, and Saul Munareto. "Improved stiction compensation in pneumatic control valves." *Computers & Chemical Engineering* 38 (2012): 106-114.
- [13] Wang, Jiandong. "Closed-loop compensation method for oscillations caused by control valve stiction." *Industrial & Engineering Chemistry Research* 52.36 (2013): 13006-13019.
- [14] De Wit, C. Canudas, et al. "Adaptive friction compensation in robot manipulators: low velocities." *The International journal of robotics research* 10.3 (1991): 189-199.
- [15] Friedland, Bernard, and Y-J. Park. "On adaptive friction compensation." *Automatic Control, IEEE Transactions on* 37.10 (1992): 1609-1612.
- [16] Keller, H., and R. Isermann. "Model-based nonlinear adaptive control of a pneumatic actuator." *Control engineering practice* 1.3 (1993): 505-511.
- [17] Yazdizadeh, A., and K. Khorasani. "Adaptive friction compensation based on the Lyapunov scheme." *Control Applications, 1996., Proceedings of the 1996 IEEE International Conference on.* IEEE, 1996.
- [18] Huang, S. N., Kok Kiong Tan, and Tong Heng Lee. "Adaptive friction compensation using neural network approximations." *Systems, Man, and Cybernetics, Part C: Applications and Reviews, IEEE Transactions on* 30.4 (2000): 551-557.
- [19] Kayihan, Arkan, and Francis J. Doyle. "Friction compensation for a process control valve." *Control engineering practice* 8.7 (2000): 799-812.
- [20] Alamir, Mazen. "On friction compensation without friction model." *Proceedings of the IFAC World Congress. Barcelona, Spain.* 2002.
- [21] Mei, Zhi-qian, Yun-can Xue, and Ru-qing Yang. "Nonlinear friction compensation in mechatronic servo systems." *The International Journal of Advanced Manufacturing Technology* 30.7-8 (2006): 693-699.
- [22] Selmic, Rastko R., and Frank L. Lewis. "Backlash compensation in nonlinear systems using dynamic inversion by neural networks." *Asian Journal of Control* 2.2 (2000): 76-87.
- [23] Widrow, Bernard "Adaptive Inverse Control." *IFAC Adaptive systems in control and signal processing, Lund, Sweden, 1986.*

- [24] Widrow, Bernard, and Gregory L. Plett. "Adaptive inverse control based on linear and nonlinear adaptive filtering." *Neural Networks for Identification, Control, Robotics, and Signal/Image Processing, 1996. Proceedings., International Workshop on.* IEEE, 1996.
- [25] Tao, G. "Adaptive inverse control using a gradient-projection optimization technique." *Journal of optimization theory and applications* 95.3 (1997): 677-691.
- [26] Thethi, H. Pal, Babita Majhi, and Ganapati Panda. "Development of robust adaptive inverse models using bacterial foraging optimization." *ACEEE International Journal Communication* 1.2 (2011): 18-23.
- [27] Tan, Kok Kiong, et al. "Friction modeling and adaptive compensation using a relay feedback approach." *Industrial Electronics, IEEE Transactions on* 48.1 (2001): 169-176.
- [28] Mohammad, M. Ale, and B. Huang. "Compensation of control valve stiction through controller tuning." *Journal of Process control* 22.9 (2012): 1800-1819.
- [29] Mishra, Puneet, Vineet Kumar, and K. P. S. Rana. "A novel intelligent controller for combating stiction in pneumatic control valves." *Control Engineering Practice* 33 (2014): 94-104.
- [30] Li, Chen, et al. "Frequency analysis and compensation of valve stiction in cascade control loops." *Journal of Process Control* 24.11 (2014): 1747-1760.
- [31] Karnopp, Dean. "Computer simulation of stick-slip friction in mechanical dynamic systems." *Journal of dynamic systems, measurement, and control* 107.1 (1985): 100-103.
- [32] Choudhury, MAA Shoukat, Nina F. Thornhill, and Sirish L. Shah. "Modelling valve stiction." *Control engineering practice* 13.5 (2005): 641-658.
- [33] Kano, Manabu, et al. "Practical model and detection algorithm for valve stiction." *IFAC symposium on dynamics and control of process systems.* 2004.
- [34] He, Q. Peter, et al. "A curve fitting method for detecting valve stiction in oscillating control loops." *Industrial & engineering chemistry research* 46.13 (2007): 4549-4560.
- [35] Chen, Si-Lu, Kok Kiong Tan, and Sunan Huang. "Two-layer binary tree data-driven model for valve stiction." *Industrial & Engineering Chemistry Research* 47.8 (2008): 2842-2848.
- [36] Gang Tao, Petar V. Kokotović. *Adaptive control of systems with actuator and sensor nonlinearities.* John Wiley & Sons, 1996.

- [37] Widrow, Bernard, and Eugene Walach. *Adaptive Inverse Control, Reissue Edition: A Signal Processing Approach*. John Wiley & Sons, 2008.
- [38] Muhammad, Sabih. *DETECTION AND COMPENSATION OF VALVE STICTION IN CONTROL LOOPS*. Diss. King Fahd University of Petroleum and Minerals, 2009.
- [39] Storn, Rainer, and Kenneth Price. *Differential evolution—a simple and efficient adaptive scheme for global optimization over continuous spaces*. Vol. 3. Berkeley: ICSI, 1995.
- [40] Storn, Rainer, and Kenneth V. Price. "Minimizing the Real Functions of the ICEC'96 Contest by Differential Evolution." *International Conference on Evolutionary Computation*. 1996.
- [41] Vesterstrom, Jakob, and Rene Thomsen. "A comparative study of differential evolution, particle swarm optimization, and evolutionary algorithms on numerical benchmark problems." *Evolutionary Computation, 2004. CEC2004. Congress on*. Vol. 2. IEEE, 2004.
- [42] Choudhury, MAA Shoukat, Mridul Jain, and Sirish L. Shah. "Stiction—definition, modelling, detection and quantification." *Journal of Process Control* 18.3 (2008): 232-243.
- [43] Choudhury, Ali Ahammad Shoukat, Sirish L. Shah, and Nina F. Thornhill. *Diagnosis of process nonlinearities and valve stiction: data driven approaches*. Springer Science & Business Media, 2008.
- [44] Romano, Rodrigo A., and Claudio Garcia. "Karnopp friction model identification for a real control valve." *Proceedings of the 17th IFAC World Congress*. Laxenburg, Austria: International Federation of Automatic Control, 2008.
- [45] ISA Subcommittee SP75.05, (1979). Process instrumentation terminology. Technical Report ANSI/ISA-S51.1-1979. Instrument Society of America.

Vitae

Name : Mohamed Abdeen Mohamed Hassan

Nationality : Sudanese

Date of Birth : 11/13/1986

Email : g201202920@kfupm.edu.sa, abdeen009@hotmail.com

Address : Gabra Block 13, Khartoum, Sudan

Academic Background : M.Sc. in System Engineering, Majoring in
Systems and Control Engineering, KFUPM 2015.
B.Sc. in Electrical and Electronic Engineering, Majoring in
Control Systems and Measurements, University of
Khartoum (2008).

Publications and Patents

Sami El Ferik, **Mohamed Hassan**, Muhammed Sabih, Zaid Barghouthi, Mustafa Al-Naser,
" Valve Stiction Compensation In spirit of Adaptive Filtering & Intelligence Control
Theories", in journal of process control (submitted).

Sami El Ferik, **Mohamed Hassan**, Muhammed Sabih, Zaid Barghouthi, Mustafa Al-
Naser, " Valve Stiction Compensation By Dynamic Inversion", in Control Engineering
Practice (submitted).

Sami El Ferik, **Mohamed Hassan**, Zaid Barghouthi, "A Comparative Study of Valve Stiction Compensation: Knocker Based Methods", Industrial & Engineering Chemistry Research (submitted).

Sami El Ferik, **Mohamed Hassan**, Muhammed Sabih, Zaid Barghouthi, " Valve Stiction Compensation using Adaptive Smart Methods", Patent filed (441563US).